INTRINSIC AND EXTRINSIC CONTROLS ON SEDIMENTATION AND THE MORPHOLOGY OF LATE PLEISTOCENE TO MODERN ESTUARIES IN NORTH CAROLINA

Christopher Robin Mattheus

A dissertation submitted to the faculty of the University of North Carolina at Chapel Hill in partial fulfillment of the requirements for the degree of Doctor of Philosophy in the Department of Marine Sciences.

Chapel Hill
2009

Approved by:

Antonio B. Rodriguez

John B. Anderson

Brent A. McKee

Michael F. Piehler

Justin B. Ries

ABSTRACT

CHRISTOPHER ROBIN MATTHEUS: Intrinsic and Extrinsic Controls on Sedimentation and the Morphology of Late Pleistocene to Modern Estuaries in North Carolina
(Under the direction of Dr. Antonio B. Rodriguez)

Coastal morphologies along passive continental margins are the product of complex interactions between erosional and depositional processes that respond to upstream and downstream forcing mechanisms over varying spatial and temporal scales. Upstream controls regulate river-discharge conditions whereby downstream controls govern the distribution of coastal accommodation space and basin hydrodynamics. Understanding how these processes interact over varying timeframes is important for developing accurate models of past and future coastal evolution.

Specifically, three aspects of late Quaternary coastal evolution are investigated, including: 1) controls on late Pleistocene valley incision at the highstand shoreline, 2) connectivity between a coastal-plain watershed and its estuarine depositional basin, and 3) influences of coastal setting and respective land-use modifications on fringe-marsh shoreline evolution.

Research into controls on incised-valley size and shape shows systems at highstand passive-margin shorelines are equilibrated to the size of their respective drainage basins, which reflect long-term discharge. These findings negate widely accepted models that attribute shelf gradient as being the dominant control on valley morphology and offer tools for investigating the data-limited ancient rock record.

The correlation between valley dimension and drainage-basin size degrades for small coastal fluvial systems as slope processes override discharge as the primary mechanism of valley incision. These differences have an effect on resulting highstand river morphology. Large valleys have high accommodation in their low-gradient extensive floodplains and small watersheds on the lower coastal plain have higher fluvial gradients and much less storage space along route. Contrary to large estuaries that are well buffered from changes in sediment load, estuaries associated with small lower coastal plain rivers are directly connected with their watersheds and are more sensitive to climate and land-use changes.

Since riverine landscapes of the lower coastal plain are highly connected to estuaries, land-use changes in the basin quickly facilitate mineral accretion and marsh progradation in upper bay environments. In contrast, marshes distally located to these systems receive little of this sediment and are less likely to maintain a favorable intertidal elevation and stable shoreline position with respect to rising sea level and human impacts.

ACKNOWLEDGEMENTS

Foremost, I would like to thank my advisor Tony Rodriguez. Your enthusiasm for our research has been an inspiration to me all these years and it has been under your tutelage that I found direction to my scholastic endeavors. I will forever be indebted to you for providing me with all the opportunities you have.

I extend my gratitude to my committee members John Anderson, Brent McKee, Mike Piehler, and Justin Ries for providing their expertise and valuable time in helping me throughout the development of my projects and the completion of this manuscript.

Funding for this research was provided by the American Chemical Society's Petroleum Research Fund and the Department of Energy's National Institute for Climate Change Research at Tulane University. Additional funding for ^{210}Pb-dating of marsh cores was provided by Carolyn Currin's lab at the National Oceanic and Atmospheric Administration.

To my friends and family, thank you for your love and support throughout all these years and helping me stay on track to realize my goals.

Lastly, I wish to take this opportunity to acknowledge the members of the IMS surf team for their never-ending stoke. You guys made my time at the coast.

TABLE OF CONTENTS

LIST OF TABLES

Table

LIST OF FIGURES

Figure

LIST OF ABBREVIATIONS

bsl = Below sea level

cm = Centimeter(s)

DEM = Digital elevation model

GPS = Global Positioning System

GIS = Global Information System

km = Kilometer(s)

ka = 1,000 years before present

LGM = Last Glacial Maximum

LIDAR = Light Detection and Ranging

m = Meter(s)

mm = Millimeter(s)

NCDOT = North Carolina Department of Transportation

NPR = Newport River

PKS = Pine Knoll Shores

RTK = Real Time Kinematic

SB2 = Oxygen Isotope Stage 2 sequence boundary

USDA = United States Department of Agriculture

USGS = United States Geological Survey

WP = Walker's Pond

yr = year

Chapter 1

Controls on Late Quaternary Incised-valley Dimension along Passive Margins Evaluated with Empirical Models

1.1. Chapter Summary

Incised valleys are canyon-like features that initially form near the highstand shoreline and evolve over geologic time as rivers erode into coastal plains and continental shelves to maintain equilibrium gradient profiles in response to sea-level fall. These valleys flood during sea-level rise to form estuaries and, as a result, most modern coastal processes are affected by incised-valley morphology. Nonetheless, little is known about what dictates incised-valley size and shape and whether these metrics can be used to explain principle formation processes. The main control on alluvial channel morphology over human timescales is discharge. This is based on numerous empirical studies and is well constrained because all variables are easily measured at this short timescale. Our knowledge of long-term river evolution over a complete glacio-eustatic cycle, on the contrary, remains largely conceptual, experimental, and based on individual systems because variables that are thought to drive morphologic change are not easily quantified. In spite of this, existing models of incised-valley formation suggest that valley evolution is largely driven by downstream forcing mechanisms, highlighting sea level and shelf gradient/morphology as the dominant controls on valley incision. Although valleys are cut by rivers, whose channels are a direct reflection of discharge, an upstream control, little empirical data exists to address the degree to which discharge controls valley evolution. The late Quaternary is the best time

period to examine because it provides the most complete sedimentary record and many variables are accurately constrained. Here, we present information obtained from a comparison study of 36 late Quaternary valleys from two different passive continental margins that suggests valley shape and size are primarily governed by upstream, intrinsic controls. Valley width and depth are found to be predictable at the highstand shoreline, which has important implications for deriving information on ancient river basins from the geologic record.

1.2. Background

Incision occurs when the sediment-transport capacity of the river exceeds its load. At the coast or highstand shoreline, incised valleys are primarily associated with drops in sea level that expose the continental shelf that has a steeper gradient than the river's equilibrium profile (Schumm and Brackenridge, 1987; Schumm, 1993; Schumm and Ethridge, 1994; Wood et al., 1993; Helland-Hansen and Martinsen, 1996; Talling, 1998; Posamentier and Allen, 1999; Blum and Törnqvist, 2000; van Heijst and Postma, 2001; Ardies et al., 2002; Ethridge et al., 2005; Gibling, 2006; Törnqvist et al., 2006). At coastal and shelf settings, incised valleys commonly develop by knickpoint migration and are easily identified by their sedimentary fill sequence, which typically consists of fluvial and estuarine depositional environments that accrete as sea level rises and floods the valley (Dalrymple et al., 1992; Ainsworth and Walker, 1994; Blum, 1994; Clifton, 1994; Foyle and Oertel, 1997; Heap and Nichol, 1997; Dabrio et al., 2000). Incised valleys are widely recognized for: 1) their importance in transporting sediment to deep-sea depositional environments during lowstand periods (Van Wagoner et al., 1988; Van Wagoner et al., 1990; Posamentier, 2001; Törnqvist

et al., 2006); 2) their basal erosional surface being an aid in identifying a sequence boundary; 3) their high accommodation, which makes their sedimentary fill sequence the most complete record of transgression on the continental shelf (Belknap and Kraft, 1981; Belknap et al., 1994; Thomas and Anderson, 1994); and 4) coarse-grained basal deposits, which are commonly overlain by finer-grained and less permeable units, making incised-valley fills important hydrocarbon reservoirs and/or ground-water aquifers (Zaitlin et al., 1994). Incised valleys which are underfilled (i.e. associated with estuaries) located on coastal plains along passive continental margins are the subject of this study.

Alluvial river-channel size and shape generally reflect discharge and substrate lithology, whereas incised-valley geometry is influenced not only by these controls, but also by extrinsic forces that are not easily quantified and operate over longer time scales. Alluvial channels exist in steady-state equilibrium and adjust their form rapidly to accommodate changes in sediment load and water discharge. The width and depth of alluvial channels increase with discharge, which increases in a downstream direction, as simple power functions (Figure 1.1; Leopold and Maddock, 1953; Schumm, 1977; Knighton, 1998). Changes in width/depth ratios commonly reflect changes in substrate lithology (Schumm, 1960; 1968; Couper, 2003; Finnegan et al., 2005). Unlike alluvial channels, incised valleys are the product of long-term river incision coupled with the effects of large-scale subaerial exposure and weathering (Schumm, 1993) in addition to the subsequent inundation and reworking by coastal and marine processes, which makes it difficult to identify the controls on valley morphology using empirical methods.

The dominant controls on incised-valley geometry are base-level fall, gradient profiles, climate, lithology, tectonics, and inherent fluvial processes. At the coast, vertical

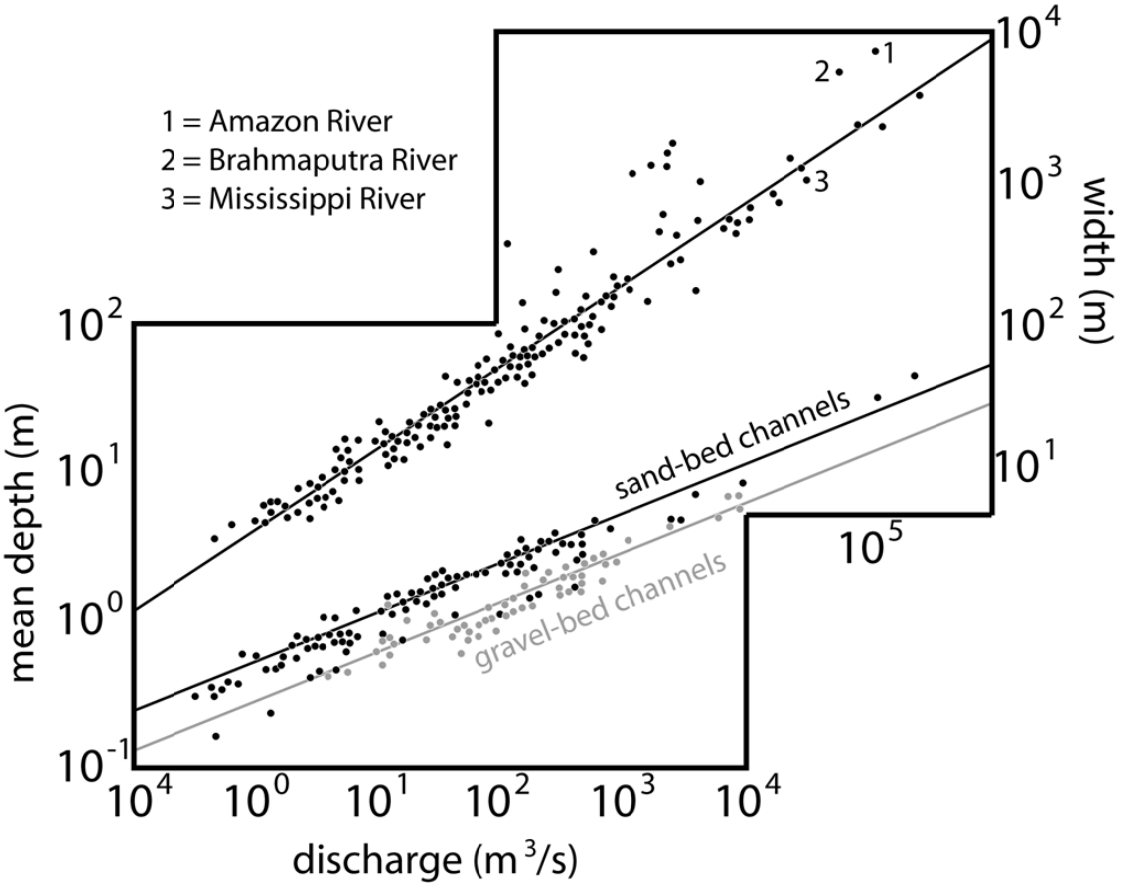

Figure 1.1 - Plot of mean channel depth (primary y-axis) and width (secondary y-axis) against discharge. Figure modified from Knighton (1998).

incision commonly initiates when base-level fall exposes a surface with a steeper gradient than the fluvial equilibrium profile, which is common at the depositional shoreline break (apex of the coastal prism; Helland-Hansen, 1996; Talling, 1998; Törnqvist et al., 2000) and the shelf break (Schumm and Ethridge, 1994; Wood et al., 1994; Posamentier and Allen, 1999; Törnqvist et al., 2006). River systems equilibrate to a new gradient by the process of landward knickpoint migration (Schumm et al., 1984; Schumm and Brackenridge, 1987; Koss et al., 1994; Schumm and Ethridge, 1994; Wood et al., 1994; Hassan and Klein, 2002; Ethridge et al., 2005). The knickpoint moves upstream only several kms for small, high-gradient fluvial systems, whereas large, low-gradient fluvial systems adjust their profiles 100s of km upstream (Blum and Törnqvist, 2000). The degree of vertical incision is primarily attributed to the magnitude and duration of base-level fall (Schumm, 1993; van Heijst and Postma, 2001), the substrate lithology (Tooth et al., 2004; Wohl and Achyuthan, 2002), and the angle of the exposed break-in-slope (Figure 1.2; Wood et al., 1994).

Valley width is primarily linked to the rate of base-level fall and climate. At slow rates of sea-level fall, channel migration and associated slope-adjustment processes operate over longer time spans, which results in wider valleys (Schumm and Ethridge, 1994). The role of climate in incised-valley development is complex because river and slope processes are affected by variations in temperature, precipitation, and flood frequency and/or magnitude and their effects on vegetation and subsoil/surface runoff characteristics change over varying timescales (Blum et al., 1994; Vandenberghe et al., 1995; Blum and Törnqvist, 2000; Leigh and Feeney, 1995; Leigh et al., 2004). These parameters are difficult to constrain throughout the long time period of incised-valley evolution, but all contribute to valley incision/excavation and accretionary processes. For example, drier climates are

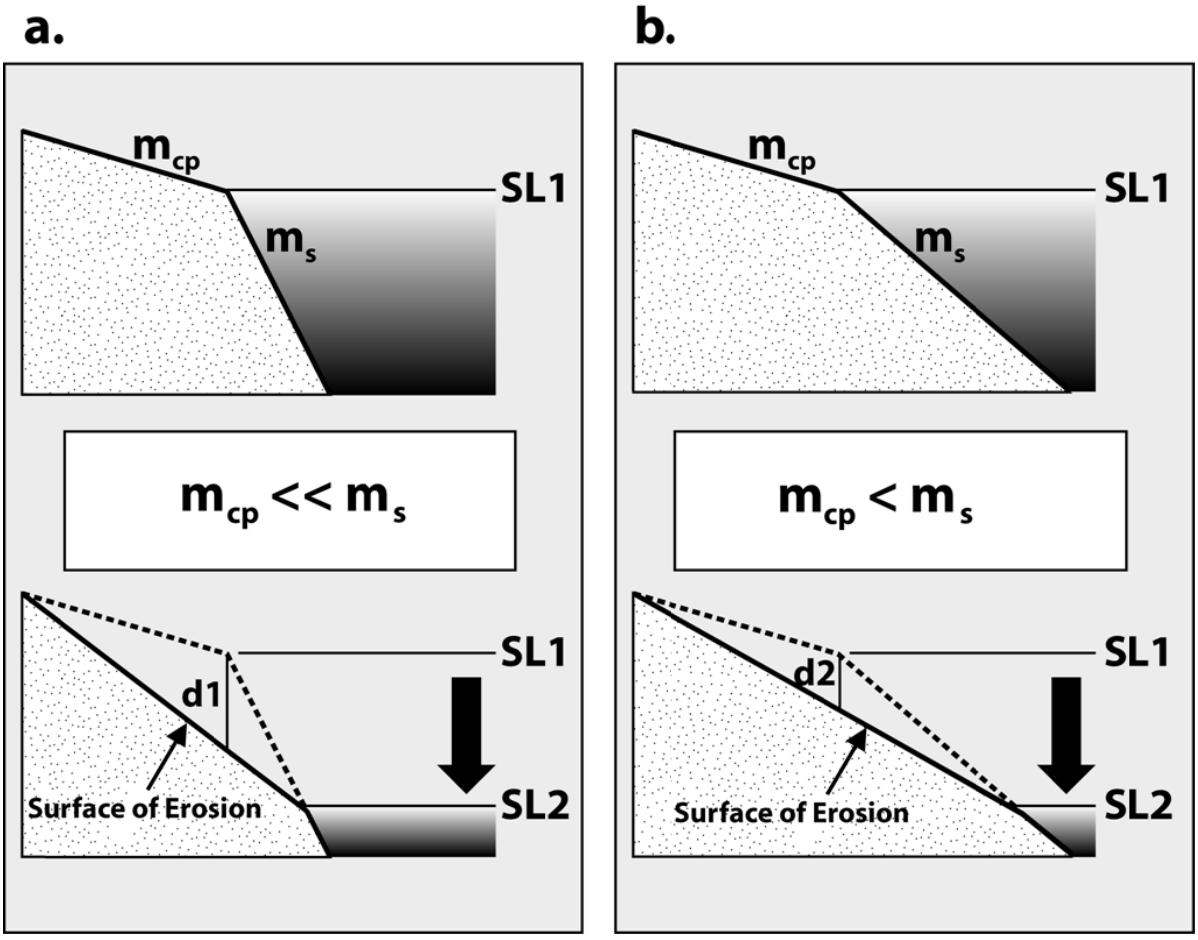

Figure 1.2 - Conceptual diagram showing hypothesized vertical river adjustment for a system in equilibrium following a base-level fall from SL1 to SL2 as a function of margin convexity; In scenario a, the coastal-plain gradient (m_{cp}) was much shallower than the shelf gradient (m_s) and subsequent incision through the coastal prism (d1) is greater than in scenario b (d2), where coastal-plain and shelf gradients were more similar.

characterized by variable discharge and low amounts of channel-margin vegetation, which decreases bank stability and promotes valley widening (Schumm and Brackenridge, 1987). Valley dimension also varies along dip in bends, at tributary junctions, and as a result of changes in substrate and/or tectonic influence (Schumm and Ethridge, 1994; Ardies et al., 2002, Plint and Wadswoth, 2003).

The empirically-derived relationships from flume experiments and observational studies that explain variations in channel morphology may not apply to incised valleys due to temporal and spatial-scale differences (van Heijst et al., 2001). This issue is particularly difficult to reconcile since calculations of river-response to forcing mechanisms and subsequent equilibrium times, which are easily measured for flume models, require values of paleodischarge and relief for natural systems (van Heijst et al., 2001). These and other parameters such as drainage-basin size, relative sea level, and climate are generally poorly constrained for ancient systems, making meaningful comparisons between them exceptionally difficult (Davidson and North, 2009). Late Quaternary incised valleys present the most complete record of fluvial response to sea-level fluctuations and many of the variables responsible for their evolution can be constrained, such as sea level, climate, drainage-basin size, gradients, substrate lithology, and tectonics.

Investigating late Pleistocene systems, Mattheus et al. (2007) found that valley width and cross-sectional area correlate with drainage-basin size and valley depth does not correlate with downstream parameters (magnitude of base-level fall, coastal-plain and shelf morphologies) along the northern Gulf of Mexico margin, suggesting that valley evolution is strongly dictated by upstream controls (i.e. discharge) at the highstand shoreline. Because of the low degree of geologic variability along the northern Gulf of Mexico margin, the

applicability of that study elsewhere is uncertain, but if discharge is found to be the dominant control on valley dimension along other passive continental margins, then it would suggest that comparing the dimensions of ancient incised valleys across any passive margin will provide important information about the size of their associated drainage basins and deep-water depositional systems. To achieve this, we compare data from the US mid-Atlantic margin to the existing Gulf database because this margin differs from the northern Gulf of Mexico in terms of lithology as well as coastal-prism and shelf morphology; it also contains fluvial systems of various sizes.

1.3. Geologic Setting

The northern Gulf of Mexico margin study area extends from western Georgia (around 85° W) to south Texas (around 100° W) and falls between 25° to 35° in northern latitude (Figure 1.3). Major Gulf-bound rivers, excepting the Mississippi and Rio Grande, have drainage basins that are almost entirely confined to the coastal plain. The Gulf coastal plain generally consists of unconsolidated Cretaceous to Holocene sedimentary units that parallel the modern shoreline (Figure 1.3) and decrease in age seaward. Coastal-plain width varies from 500 to 700 km west of the Mississippi to around 250 km in eastern Alabama, where the NE-trending Appalachian range terminates. The surficial extent of Quaternary deposits is variable across the northern Gulf of Mexico, ranging in width (updip contact to the shoreline) from about 200 km in eastern Texas to <1.0 km along coastal Alabama. Sediment supply to the northern Gulf of Mexico margin was high throughout the Cenozoic (Galloway et al., 2000) and during the last sea-level cycle, rivers incised exclusively into unconsolidated Quaternary mud and sand deposits across the continental shelf (Anderson et

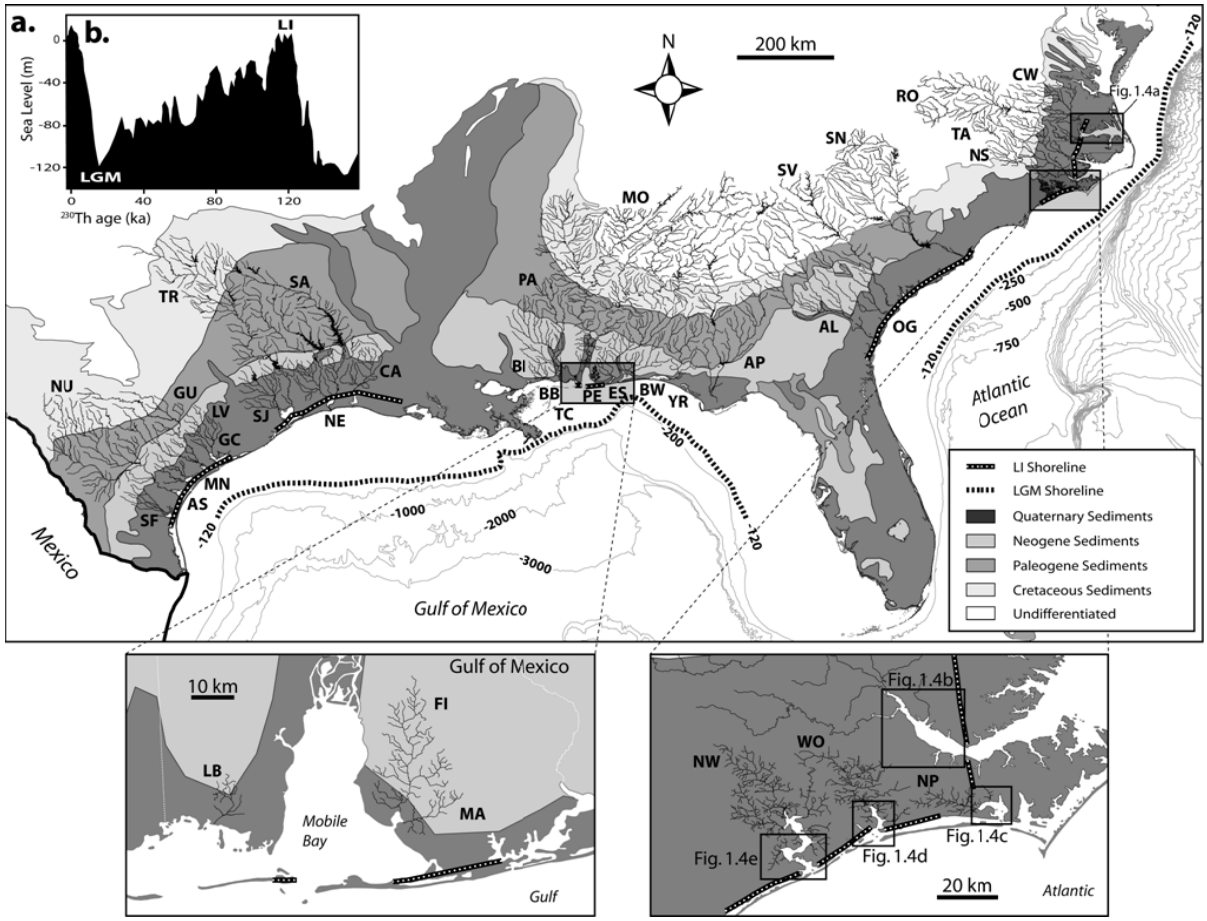

Figure 1.3 - Map of the northern Gulf of Mexico and U.S. mid-Atlantic margins (a) showing variability in geology, margin physiography, and the distribution of river basins included in this study (refer to Table 1.2 for legend to river abbreviations). The eustatic sea-level curve (b) after Chappell and Shackleton (1986). LGM = last glacial maximum; LI = last interglacial.

al., 2004).

The U.S. mid-Atlantic margin study area stretches from northeastern North Carolina (around 37° N) to south Georgia (around 31° N) and between -75° and -85° in western longitude (Figure 1.3). The mid-Atlantic coastal plain is consistently narrow along strike and is flanked to the northwest by igneous and metamorphic rocks of the piedmont that extend seaward beneath the coastal-plain sedimentary wedge (LeGrand, 1961). Unlike the northern Gulf of Mexico margin, where dip-oriented profiles show the same predictable succession of sediments by age (Figure 1.3), the mid-Atlantic margin is characterized by along-strike changes in coastal-plain stratigraphy. For example, Quaternary surface deposits in South Carolina border Paleogene-aged strata, whereas to the north, along the southern North Carolina coast, Quaternary surface deposits border outcropping Cretaceous strata (Figure 1.3). Although surface deposits of the mid-Atlantic coastal plain are generally unconsolidated, slight differences in the degree of consolidation are observed and linked to sediment composition, age, and the degree of calcification. The Eocene Castle Hayne Formation in the southwestern North Carolina coastal plain, for example, is described by Richards (1967) as a very fossiliferous limestone that is locally cemented and consolidated. Relative to the northern Gulf of Mexico, the North Carolina Atlantic margin is sediment-starved. During the last sea-level cycle, rivers incised mostly into Tertiary rock on the continental shelf south of Cape Lookout where thin (typically <10 m) unconsolidated Quaternary sediments are perched on top of hardgrounds (Hine and Snyder, 1985; Riggs et al., 1995; Riggs et al., 1996). North of Cape Lookout, rivers incised mostly into unconsolidated Quaternary deposits during the last sea-level cycle on the continental shelf which are approximately 60 m thick (Mallinson et al., 2005).

1.4. Materials and Methods

1.4.1. Measuring Incised-valley Dimension

Since incised-valley dimension varies along dip and Strong and Paola (2006 and 2008) emphasize that valley sides are highly diachronous, it is important to compare systems at the same respective location. This will ensure the valleys have an equal duration of subaerial exposure and adjustment to fluvial and mass-wasting processes. Using the methodology of Mattheus et al. (2007), valley geometries of six fluvial systems on the U.S. mid-Atlantic margin (Figure 1.4) were derived at or in close proximity to the Sangamon (last interglacial) highstand shoreline that parallels the modern shoreline at the Suffolk Scarp (Figure 1.3; Winker and Howard, 1977; Wells and Kim, 1989; Brill, 1996; York et al., 2000). For most systems, the position of the Sangamon shoreline is in very close proximity (<40 km) to the modern bay-head deltas. An additional 19 incised valleys, which we did not acquire subsurface data from, were evaluated for width using 250k USGS digital elevation models and aerial photographs at the bay-head delta. It is important to measure incised-valley dimension close to the Sangamon shoreline, because this is the approximate location where coastal-plain and shelf gradients intersected during the last interglacial period and where a knickpoint was created when the inner shelf initially became exposed as sea-level fell. This common location reduces the effects of wave and tidal ravinement on valley dimension. Drainage-basin areas are also more accurately quantified landward of this location than any other location further seaward.

It is vital to compare incised valleys of the same sequence, i.e. incised valleys that formed during the same sea-level cycle, to minimize glacio-eustatic variations between fluvial systems. Incised valleys that formed in response to the fall in base level associated

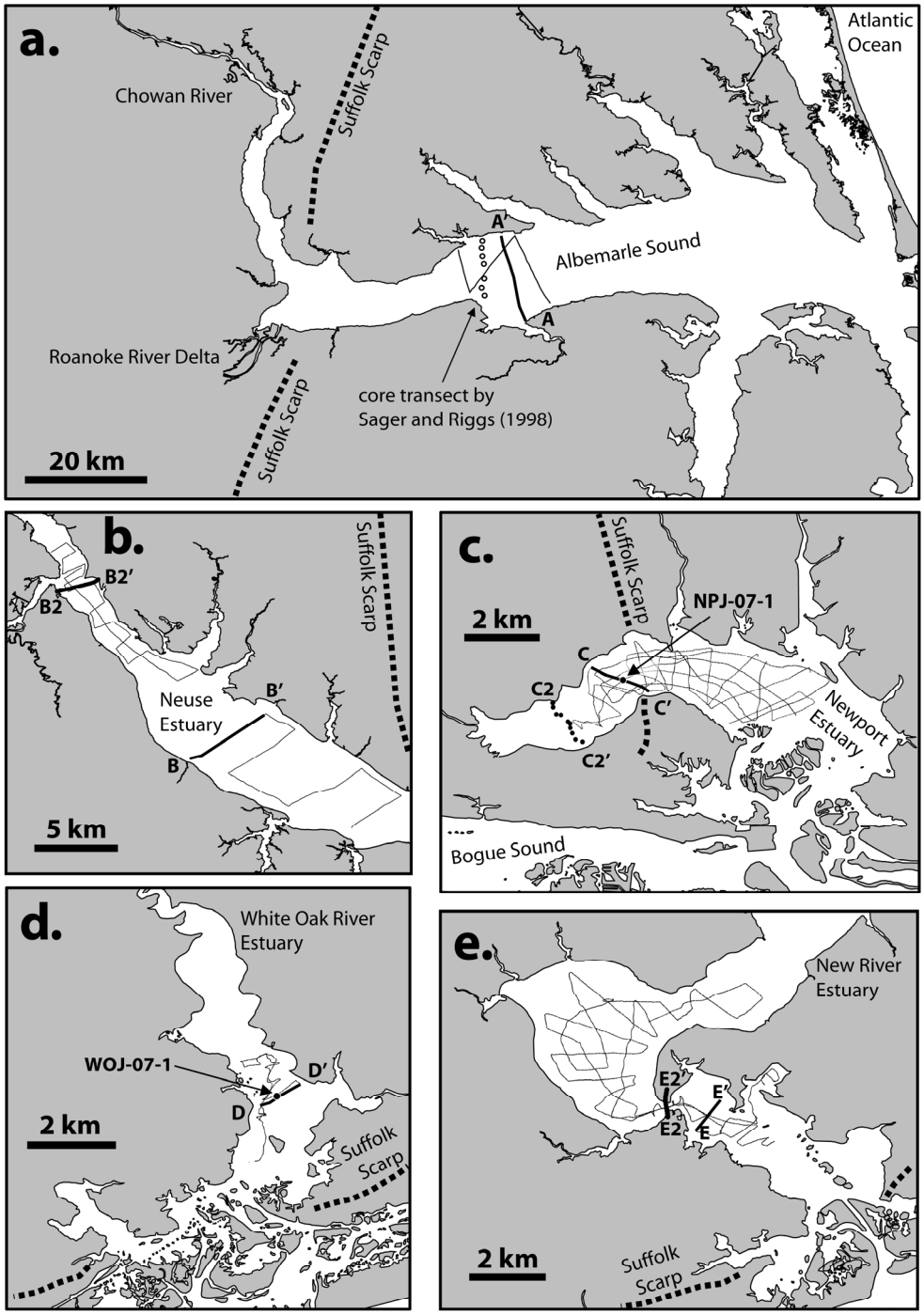

Figure 1.4 - Maps of the estuaries in North Carolina (Figure 1.1) showing locations of core (circles) and seismic data (solid thin lines). Core locations are listed in Table 1.1. Core descriptions are shown in Appendix A. The position of the Sangamon shoreline (Suffolk Scarp) is represented as a dashed black line.

with the last glacial maximum (LGM) are compared here. These valleys are all bounded below by the same erosional surface thought to be the sequence boundary associated with the last sea-level cycle (SB2). The locations of underfilled valleys, the subjects of this study, coincide with their modern estuaries, which is not always the case with overfilled systems. Given their high sediment supply, overfilled systems like the Colorado and Brazos Rivers shifted their position numerous times during the last glacio-eustatic cycle as they filled their valley accommodation, avulsed, and re-incised (Simms et al., 2006). However, underfilled valleys, which are most common along passive margins, remained in the same location over this timespan.

Incised-valley dimension was measured from high-resolution seismic data and cores oriented perpendicular to the valley axis. Approximately 275 km of seismic data were collected from 5 estuarine systems in North Carolina with an Edgetech SB216 "chirp" sub-bottom profiler (Figure 1.4). Seismic data were interpreted using Chesapeake Technology Inc. SonarWiz map plus SBP software. These data were supplemented with 132 platform boring descriptions from the North Carolina Department of Transportation (NCDOT), 9 vibracores, and 2 cores collected with the aid of a jackhammer (Table 1.1). Platform borings from the NCDOT were collected prior to bridge construction across the estuaries. Jackhammer cores from the Newport and White Oak (Table 1.1; Figure 1.4) estuaries were obtained using Geoprobe™ tools through a moon well located in the middle of the R/V Jenny. Jackhammer cores were collected in intervals of 152.0 cm and this method provided nearly continuous (90% recovery) and pristine core. Vibracores (85% recovery) were collected in shallow-water areas of the Newport River Estuary across the modern bay-head delta front (Table 1.1; Figure 1.4).

Site	Core Name	Latitude	Longitude	Environment	Penetration Depth (m)	Coring Method
Newport	NPJ-07-1	34.766117	-76.740050	central bay	-6.99	Jack-Hammer
Newport	NP-07-1	34.759400	-76.760460	delta front	-3.46	Vibracore
Newport	NR-07-1	34.758217	-76.760350	delta front	-2.50	Vibracore
Newport	NR-07-2	34.756183	-76.759383	delta front	-4.53	Vibracore
Newport	NR-07-3	34.754017	-76.755967	delta front	-3.68	Vibracore
Newport	NR-07-4	34.752083	-76.755300	delta front	-4.50	Vibracore
Newport	NR-07-5	34.750550	-76.754700	delta front	-2.62	Vibracore
Newport	NR-07-6	34.748700	-76.753750	delta front	-2.28	Vibracore
Newport	NR-07-7	34.748000	-76.751717	delta front	-2.05	Vibracore
Newport	NR-07-8	34.755967	-76.758017	delta front	-7.30	Vibracore
Newport	NR-07-9	34.753333	-76.755400	delta front	-5.47	Vibracore
White Oak	WOJ-07-1	34.711396	-77.105130	lower bay	-7.19	Jack-Hammer

Table 1.1 - Listing of core information including name, location, coring method, and penetration depth. Core locations are plotted in Figure 1.4. Core descriptions are shown in Appendix A.

To ensure measurement consistency between fluvial systems, we adhered to strictly-defined incised-valley dimensions. Cross-sectional area is calculated to the nearest 10 m^2 between SB2 (the exposure surface) and sea level. Incised-valley depth is measured at the deepest part of the valley transect to the nearest 1.0 m relative to sea level. Valley width is measured at a perpendicular to the valley axis and is the linear distance between each side of the valley, defined as the prominent break in slope separating the interfluve from the valley flank. Shallow-water areas at bay margins that were inaccessible for coring and seismic data collection made it necessary to project incised-valley flanks linearly to the modern floodplain.

Incised-valley depth is sometimes difficult to measure accurately because of its variability along both strike and dip and due to data quality and resolution. Gas is a common occurrence within valley thalwegs and attenuates seismic energy. The depth of the active lowstand channel is the component of the valley that would be equilibrated to the base-level fall and is what should be measured. The active lowstand channel may not coincide with what is mapped as the base of the valley floor or thalweg, because its size could be below the resolution of the data.

1.4.2. Measuring Drainage-basin Size and Gradient Profiles

Studied fluvial basins are separated by well-defined drainage divides that have likely remained unchanged over Quaternary timescales. In this study, drainage basins are defined as catchment area landward of the modern bay-head delta locations. Small drainage networks (<1,000 km²) were delineated using 250k USGS digital elevation models while large fluvial basins were delineated utilizing hydrologic data files (hydro-shapefiles) obtained from the USGS GIS database. Graded-stream profiles were constructed from river origin to

river mouth with the same USGS digital elevation data used to delineate their basins. River origins are defined as the highest tributary reach within a system's respective drainage basin. Coastal-plain fluvial gradients were measured from the bay-head delta to the first prominent change in slope. Shelf gradients were measured across the margins, from the Sangamon shoreline to the shelf break, using digital bathymetric data from the National Geophysical Data Center. The computer programs used to display and evaluate the data are the software packages Surfer® 8 and ArcGIS 9.1.

1.5. Results

1.5.1. Drainage Basins

Studied drainage basins along the northern Gulf of Mexico margin vary in area by over three orders of magnitude (Table 1.2), ranging from systems confined to the coastal plain that drain < 100 km^2 (e.g. La Batre) to systems that originate in piedmont regions that drain > 100,000 km^2 (e.g. Mobile). Selected drainage basins along the U.S. mid-Atlantic margin vary by almost two orders of magnitude (Table 1.2). The Newport, White Oak, and New Rivers in North Carolina represent small coastal drainage systems < 1,500 km^2 in size. These systems originate at elevations on the order of 10s of meters (Table 1.2), drain lower coastal-plain Quaternary deposits, and do not exceed 50 km in length. Piedmont systems, such as the Tar, Chowan, Neuse, and Roanoke Rivers, have longitudinal profiles that extend into piedmont regions of the southern Appalachian Mountains, originate at elevations ranging from 152 m (Chowan River) to 616 m (Roanoke River), and are characterized by drainage basins on the order of several 10,000 km^2 in area (Table 1.2).

System	Margin	DBS (km^2)	L (km)	L5e (km)	h (m)	cpg (m/km)	sw (m)	sbd (m)
Albemarle (RO+CH)	Atlantic	35906	561	645	797	0.10	149	42
Altamaha (AL)	Atlantic	34608	-	-	-	-	-	-
Chowan (CW)	Atlantic	11502	-	-	-	-	-	-
Neuse (NS)	Atlantic	12793	331	377	170	0.07	126	43
New (NW)	Atlantic	1032	38	77	28	0.42	118	45
Newport (NP)	Atlantic	214	30	30	11	0.25	105	43
Ogeechee (OG)	Atlantic	10370	-	-	-	-	-	-
Roanoke (RO)	Atlantic	24404	-	-	-	-	-	-
Santee (SN)	Atlantic	35116	-	-	-	-	-	-
Savannah (SV)	Atlantic	25863	-	-	-	-	-	-
Tar (TA)	Atlantic	8019	255	297	153	0.11	162	41
White Oak (WO)	Atlantic	604	29	45	12	0.26	111	42
Appalachicola (AP)	Gulf	43370	-	-	-	-	-	-
Aransas (AS)	Gulf	1531	-	-	-	-	-	-
Bernard (BB)	Gulf	144	-	-	-	-	-	-
Biloxi (BI)	Gulf	656	-	-	-	-	-	-
Blackwater (BW)	Gulf	2015	-	-	-	-	-	-
Calcasieu (CA)	Gulf	8110	190	190	105	0.25	232	64
Choctawhatchee (CH)	Gulf	10588	-	-	-	-	-	-
Escambia (ES)	Gulf	10003	-	-	-	-	-	-
Fish (FI)	Gulf	372	45	65	67	1.49	74	43
Garcitas (GC)	Gulf	745	-	-	-	-	-	-
Guadalupe (GU)	Gulf	23812	-	-	-	-	-	-
Jacinto (SJ)	Gulf	9970	156	158	106	0.42	210	61
La Batre (LB)	Gulf	73	17	27	40	2.35	74	43
Lavaca (LV)	Gulf	5707	137	195	121	0.54	94	65
Magnolia (MG)	Gulf	87	19	39	31	1.63	74	43
Mission (MN)	Gulf	2044	-	-	-	-	-	-
Mobile (MO)	Gulf	107704	525	594	143	0.13	74	43
Neches (NE)	Gulf	23697	428	443	182	0.15	214	74
Nueces (NU)	Gulf	39092	592	629	711	0.24	99	104
Pascagoula (PA)	Gulf	20223	-	-	-	-	-	-
Perdido (PE)	Gulf	1940	-	-	-	-	-	-
Sabine (SA)	Gulf	23610	604	604	198	0.18	214	74
San Fernando (SF)	Gulf	4165	-	-	-	-	-	-
Tchoutacabouffa (TC)	Gulf	369	-	-	-	-	-	-
Trinity (TR)	Gulf	44302	769	769	368	0.20	210	61
Yellow (YR)	Gulf	3199	-	-	-	-	-	-

Table 1.2 - Metrics of studied river systems (DBS = drainage-basin size, L = length, L5e = fluvial length to Sangamon (Stage 5e) shoreline, h = elevation of origin, cpg = coastal-plain gradient, sw = shelf width, sbd = shelf-break depth).

1.5.2. Fluvial Profiles

Mid-Atlantic fluvial systems exhibit coastal-plain gradients that range from 0.06 m/km (Cape Fear River) to 0.26 m/km (White Oak River), while along the northern Gulf of Mexico margin, coastal-plain gradients range from 0.21 m/km (Mobile-Tensaw River) to 0.48 m/km (Lavaca River). Small systems (<1500 km² in size and < 50 km in length) have nearly constant down-stream gradients and are not characterized by well-defined, concave upward longitudinal profiles. River profiles of large systems (>1500 km^2) increase significantly as they extend into the higher elevation upper coastal plain (Paleogene and Cretaceous sedimentary belts, etc.). These high-relief upper coastal plain topographies are many hundreds of km removed from the Sangamon shoreline and gradients here should have little effect on erosional processes associated with eustatic cyclicity at that shoreline. To be consistent with coastal-plain gradient measurements of the small river systems, gradients of the large river systems were calculated in the coastal plain seaward of the first significant break in relief along the profiles (Figure 1.5). Fluvial gradients in the Gulf coastal plain are generally steeper than those of size-equivalent Atlantic margin systems (Table 1.2; Figure 1.5b). For example, the Trinity (Gulf margin) and Chowan-Roanoke (Atlantic margin) river systems are similar in size, but the coastal-plain gradient of the Trinity (0.20 m/km) is twice as steep as the Chowan-Roanoke's (0.10 m/km; Table 1.2; Figure 1.5). This trend is noticeable for most other systems as well (Figure 1.5).

1.5.3. Continental Shelf Profiles

Shelf morphology along the Gulf margin is variable as evident from gradient profiles that can be described as ranging from ramp-style, along the southern Texas margin (Figure

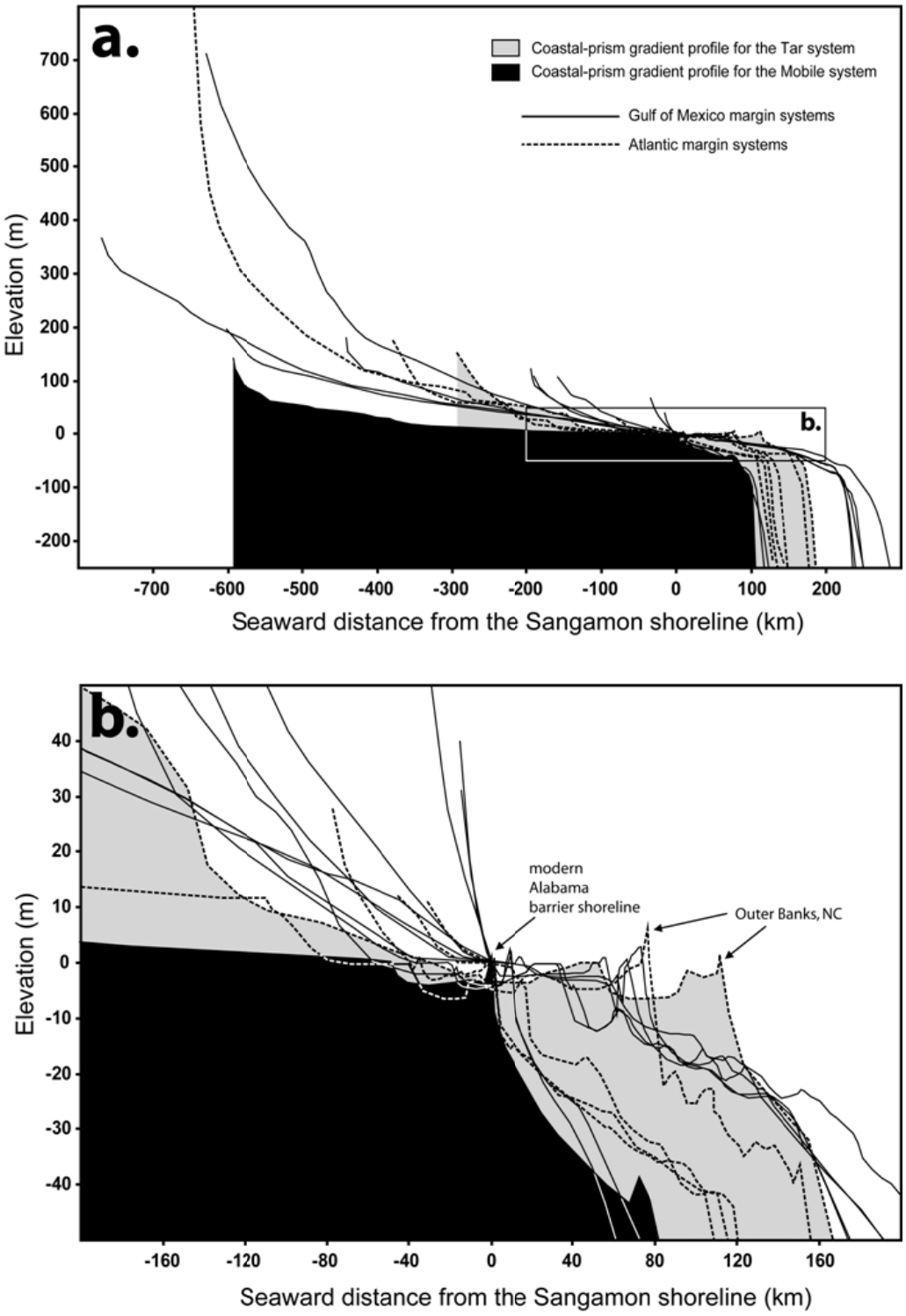

Figure 1.5 - Gradient profiles hinged at the Sangamon shoreline for the rivers included in this study. Variability in coastal-prism morphology is shown from river origin to the shelf slope (a) and from the lower coastal plain to the inner shelf (b). The profiles of the Tar and Mobile end-member type systems are highlighted by light gray and black fill, respectively.

1.3) to profiles that show a well-defined shelf break at depths ranging from 61 to 104 m along eastern Texas, western Louisiana, and Alabama margins. In addition, the shelf itself is not always a planar surface; the eastern Texas and western Louisiana shelf profiles show localized bathymetric highs on the outer shelf that correspond to tectonic features (salt domes; Figure 1.5). The location of the modern barrier shoreline is generally close to the position of the Sangamon shoreline along most of the northern Gulf of Mexico margin (Figure 1.5). Northern Gulf of Mexico shelf gradients and widths vary across the margin from 0.40 m/km for the 200-km wide eastern Texas shelf to 0.63 m/km for the 80-km wide Alabama shelf (Table 1.2; Figure 1.3).

The shelf break along the mid-Atlantic margin is well defined. It's depth of 43 m deviates little along strike (Table 1.2). The location of the modern barrier shoreline generally coincides with the position of the Sangamon shoreline in the south, but the shorelines diverge to the north, where they are separated by up to 120 km (Figures 1.3 and 1.5). The bathymetry of North Carolina's inner shelf, defined as extending from the Sangamon shoreline to the shelf break, is modified by the presence of the large Pamlico-Albemarle estuarine basin, which is separated from the Atlantic by the Outer Banks (Figures 1.3 and 1.5). Shelf gradients along the North Carolina margin range from 0.25–0.41 m/km while shelf widths range from 105 – 162 km (Table 1.2).

1.5.4. Incised-valley Size and Shape

1.5.4.1.Chowan and Roanoke Rivers

The Chowan and Roanoke rivers merge landward of the Sangamon shoreline; therefore, valley dimensions measured in Albemarle Sound are a result of the combined

discharge. A high-amplitude and high-relief seismic reflector is recognized and traced between 12 and 15 km seaward of the Suffolk Scarp. The reflector is a maximum of 11 m below sea level (bsl) along the central portion of the estuarine system, shallows towards the modern shoreline, and is interpreted as SB2 (transect A-A'; Figure 1.6). Data quality in portions of the middle estuary is poor because of seismic attenuation, which is likely caused by shallow gas (Figure 1.6). Vibracores collected by Sager and Riggs (1998) about 5 km west of transect A-A' (Figure 1.4), sampled SB2 as a subaerial exposure surface along the margins of the estuary at the same depth as the high-amplitude seismic reflector imaged here. In the center of the estuary Sager and Riggs (1998) interpret SB2 to be ~5 meters below where we interpret it from seismic data. The close proximity of the vibracore transect to 2 tributary junctions likely accounts for the discrepancy.

1.5.4.2.Neuse River

A high-amplitude seismic reflector was mapped regionally in the upper Neuse River estuary between 5 and 30 km landward of the Suffolk Scarp (Figure 1.6). The reflector is between 5 and 10 m bsl in the middle of the estuary and shallows towards the estuarine margin where it amalgamates with the shoreline. A lithologic contact, which correlates with the high-amplitude seismic reflector, is identified in 62 NCDOT borings as dense fine to coarse sand below organic-rich soft clay, silt and fine sand (Figure 1.7). This surface is interpreted as SB2, separating alluvial from overlying estuarine deposits, and was mapped towards the southeast at the measurement location near the Suffolk Scarp (Figure 1.6). The Neuse River Estuary widens seaward from 2 km around core transect B2-B2' to about 5 km at seismic cross-section B-B' (Figure 1.4). The widening is associated with a decrease in

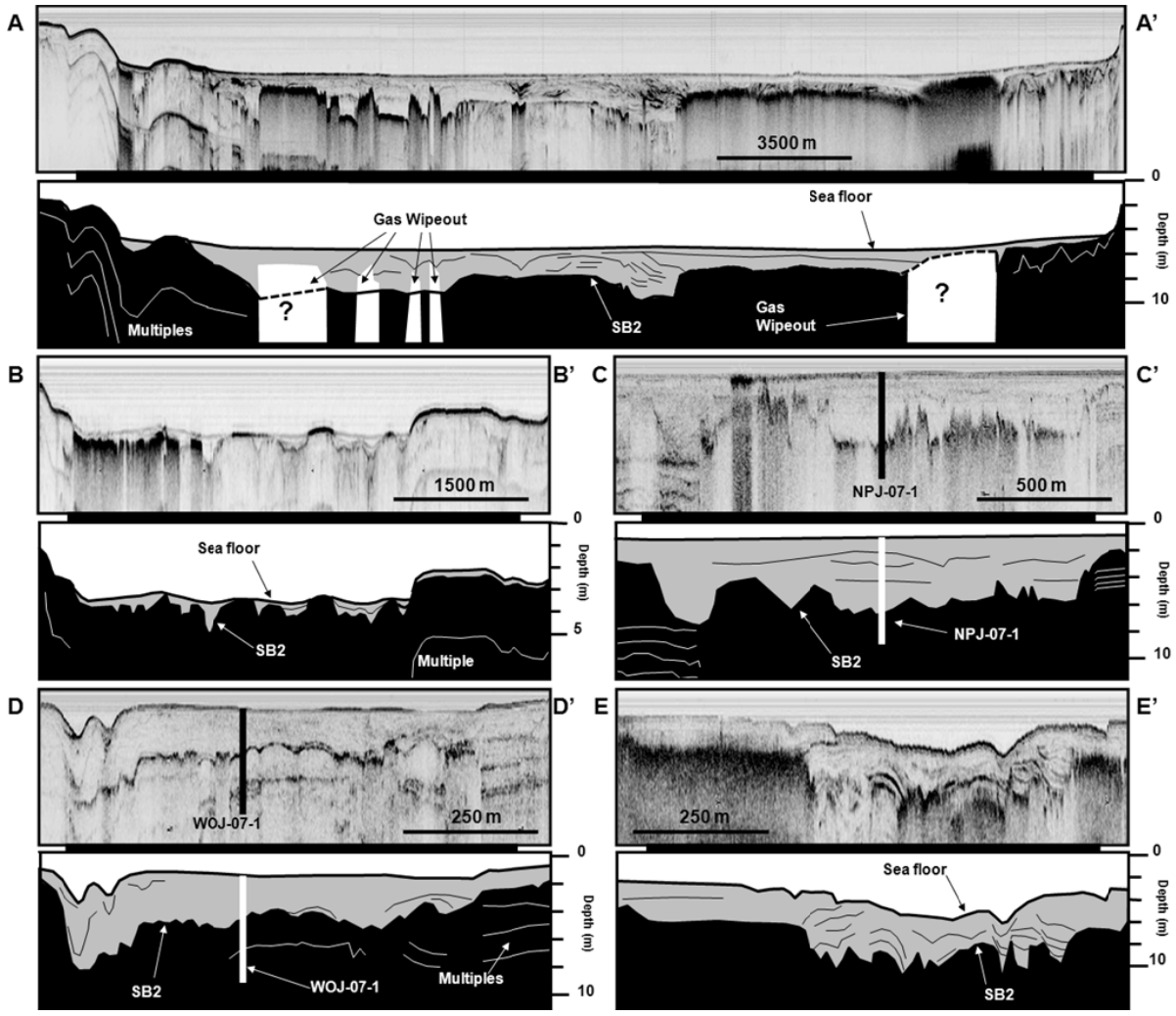

Figure 1.6 - Representative seismic lines, highlighted in Figure 1.4. Sediments below the sequence boundary are colored black; valley-fill sediments are shaded gray. The sequence boundary (SB2) is interpolated through areas of complete seismic attenuation (gas wipe-out; white), but usually marks the SB because peat normally forms on the SB along the valley flanks as sea-level rises. Core descriptions for NPJ-07-1 and WOJ-07-1 are shown in Appendix A.

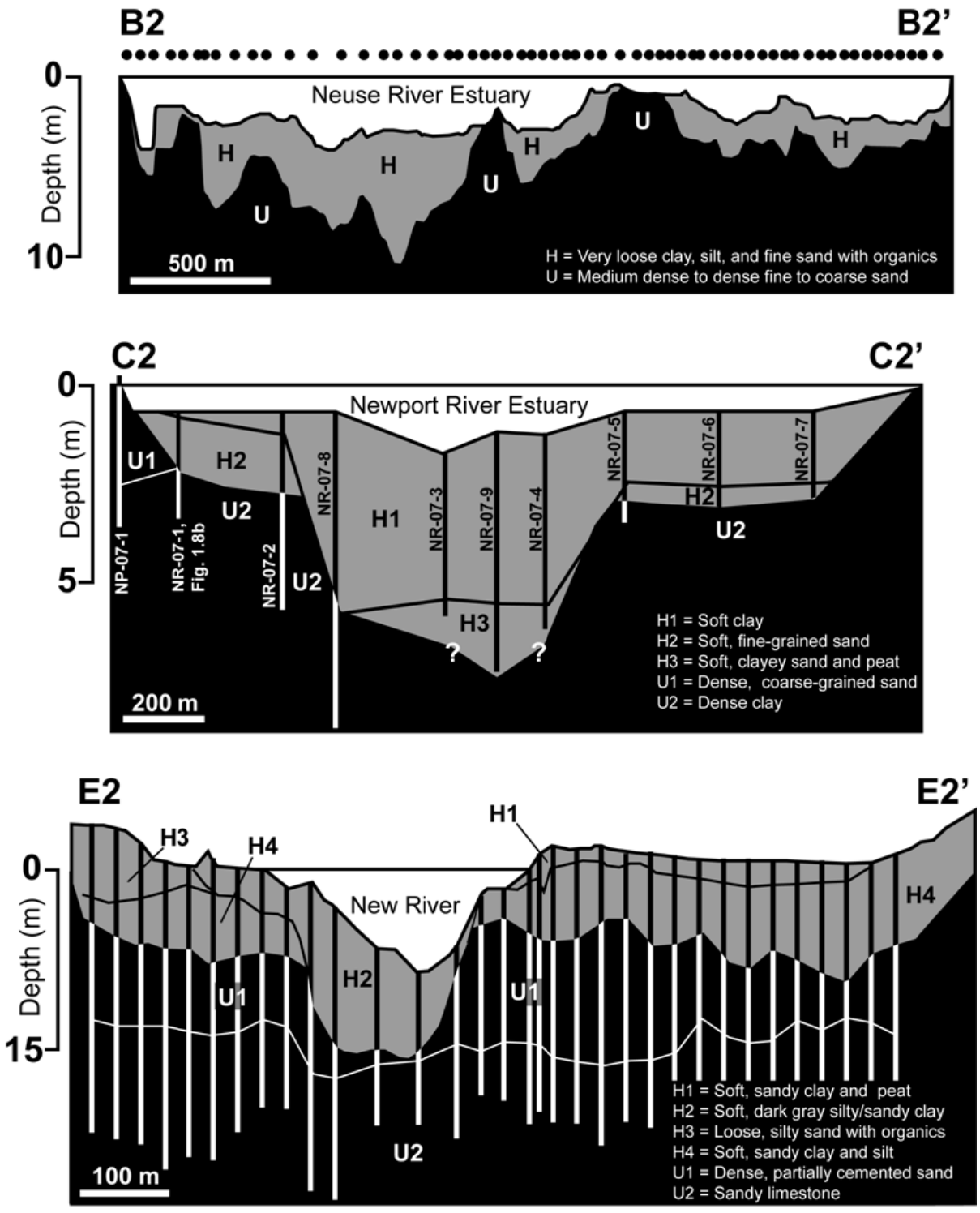

Figure 1.7 - Cross sections based on cores from the Neuse (B2-B2'), Newport (C2-C2'), and New (E2-E2') River estuaries. Transect locations shown in Figure 1.4. Valley-fill sediments are shaded gray and sediments below SB2 are black. Core descriptions for transect C2-C2' are shown in Appendix A.

mean depth of the valley from around 10 m along the core transect to approximately 5 m along seismic transect B-B' (Figures 1.4, 1.6, and 1.7).

1.5.4.3.Newport River

A high-relief, high-amplitude reflector was mapped regionally in the Newport estuary (Figure 1.6). Core NPJ-07-1 samples the reflector as a lithologic contact separating gravely sand from underlying oxidized stiff and homogeneous clay (Figures 1.6 and 1.8a). Cores collected near the shoreline in a strike-oriented transect across the modern Newport bay-head delta also samples the seismic reflector (Figures 1.7 and 1.8b). Depending on location along this transect, the contact separates dense sand (at the bay shoreline) or clay (from the subtidal area of the estuary), which commonly shows signs of oxidation, from overlying soft, organic-rich fine-grained sand or clay (Figure 1.7). The surface is interpreted as SB2 and extends below thick estuarine clay in the center of the bay where interpreted pre-Holocene sediments are overlain by peat deposits (Figure 1.8). The depth of the thalweg, near the measurement location at the Suffolk Scarp (Figure 1.6) and in the upper estuary (Figure 1.7), is measured to be around 6 m bsl, and based on the seismic data set does not change significantly. There is, however, a down-dip increase in width from 1.5 km to 3 km as the estuary bends and widens towards the inlet area (Figure 1.4). Correspondingly, the depth of the thalweg becomes more variable, reaching depths >10 m, seaward of the Suffolk Scarp.

1.5.4.4.White Oak River

Seismic transect D-D', through the White Oak River estuary, shows a high-relief and high-amplitude seismic reflector (Figure 1.6). The reflector is at a maximum depth of ~8 m

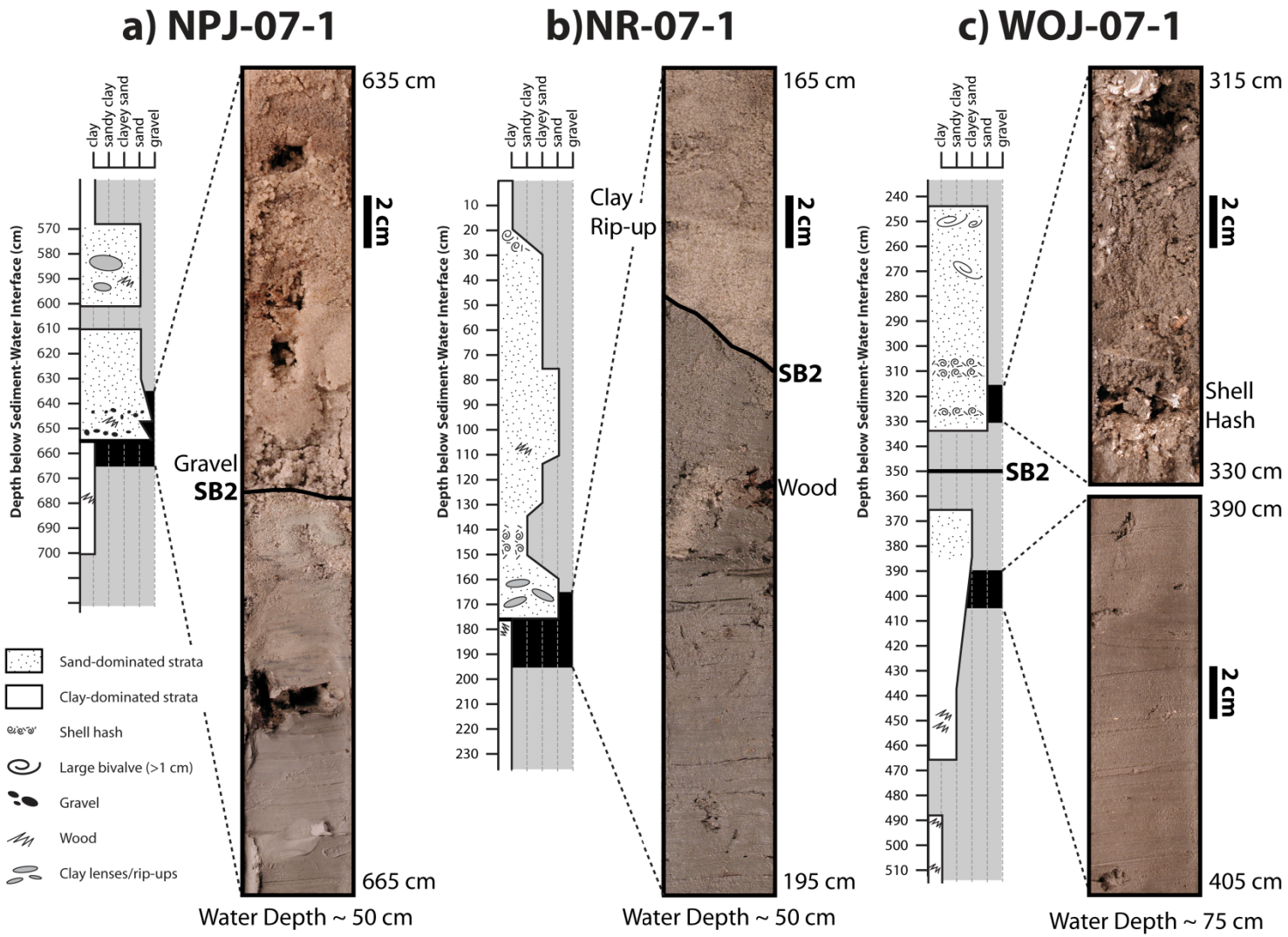

Figure 1.8 - Core photos of SB2 in the Newport (a and b) and lithologic units above and below SB2 in the White Oak (c). See Figures 1.4, 1.6, and 1.7 for locations. Core descriptions are shown in Appendix A.

bsl along the west side of the estuary, the reflector shallows gradually toward the eastern estuarine shoreline, and the overlying reflectors onlap onto it (Figure 1.6). Core WOJ-07-1, collected adjacent to the valley thalweg, samples the reflector at around 4.25 m bsl as a lithologic contact separating dense sandy clay from overlying soft clayey-silty sand with abundant shell material (Figures 1.6 and 1.8c). The lithologic contact and reflector is interpreted as SB2. The width of the paleovalley is ~1.5 km near the Suffolk Scarp and is not highly variable along dip (Figure 1.4).

1.5.4.5.New River

A high-amplitude, high-relief seismic reflector, which overlying strata onlaps, was mapped regionally throughout the lower New River estuary (Figures 1.4 and 1.6). Boring descriptions by the NCDOT from the lower New River show a lithologic contact separating dense, partially cemented sand and clay from overlying soft organic-rich silts and clays (Figure 1.7). This lithologic contact correlates with the high-amplitude seismic reflector and is mapped at a maximum depth of 16 m bsl within the middle of the estuary at the core transect. The surface shows high relief, shallows towards the estuarine shoreline, and is interpreted as SB2 (Figures 1.6 and 1.7). The dimensions of the paleovalley are variable along dip; it widens from 0.2 km to 1.4 km and SB2 shallows from 16 m to 9 m from core transect E2-E2' to seismic transect E-E' (Figures 1.4 and 1.6).

1.6. Discussion

1.6.1. Incised-valley depth

Researchers have shown that incised-valley depth is predominately a function of the magnitude of base-level fall (Schumm, 1993; van Heijst and Postma, 2001), substrate erodibility (Tooth et al., 2004; Wohl and Achyuthan, 2002), the gradient of the newly exposed seafloor (Figure 1.1; Schumm and Ethridge, 1994; Wood et al., 1994; Helland-Hansen, 1996; Talling, 1998; Hassan and Klein, 2002; Ethridge et al., 2005; and Törnqvist et al., 2006), and the time available for equilibration (Schumm, 1993; van Heijst et al., 2001; Doyle and Harbor, 2003). The equilibrium time to regrade a surface (T_{eq}) depends on the basin length (L), the duration of the sea-level cycle (T), and the sediment-transport diffusivity (k), which is defined by relief, substrate characteristics, and discharge (van Heijst et al., 2001). Paola et al. (1992) approximates this equilibrium time as $T_{eq} = L^2/k$ (Equation 1). Systems studied here, evolved under similar eustatic conditions. In addition, variations in total subsidence over the last 120 ka are likely to be negligible across the study areas where incised-valley dimensions were measured, as evidenced by the near constant elevation of the Sangamon shoreline across the northern Gulf (1.0-2.5 m) and mid-Atlantic (2.0-4.0 m) margins. In this study, changes in valley depth should primarily be governed by substrate lithology, gradient (Figure 1.1), and discharge.

1.6.1.1. Substrate lithology at the Sangamon Shoreline

Although substrate lithology is an important control on the rate of incision and degree of fluvial profile equilibration in response to base-level lowering, almost all of the studied valleys incised into unconsolidated late Tertiary and Quaternary coastal deposits at the

Sangamon shoreline (Figure 1.3). In contrast to this general lithology, the Belgrade Formation, an Oligocene sandy limestone, is only ~2 m below the surface close to the Sangamon shoreline at the margins of the lower New River estuary and is ~15 m bsl at the E2-E2' cross section (Figure 1.7). The New River valley incised into this formation and is the only incised valley examined that is characterized by sharp fluctuations in shape (i.e. width/depth ratios) and size (i.e. cross-sectional area) over short distances along dip. These changes are generally associated with high-sinuosity valley meanders reflected in the morphology of the estuarine shoreline (Figure 1.4). Core transect E2-E2', across a narrow stretch of the New River incised valley, shows late Pleistocene incision reached depths of 16 m bsl (Figure 1.7), whereas this surface shallows to approximately 8 m bsl only 2 km seaward (Figure 1.6). These pronounced changes in valley shape over short distances are unique to the New River and suggest a strong control of substrate lithology on river incision. An incision depth of 8 m was used for the New River in statistical analyses since this depth uniformly defines straight segments of the valley, not constricted valley reaches which are bedrock-influenced.

1.6.1.2.Coastal-prism convexity

Conceptual models and flume studies suggest that incision cannot occur if the gradient of the coastal plain is steeper than the shelf (Wood et al., 1993; Posamentier and Allen, 1999; van Heijst and Postma, 2001; Törnqvist et al., 2006). The fluvial profiles of the Magnolia, La Batre, and Fish valleys, which flank Mobile Bay, AL (Figure 1.3), are only 10's of km in length and extend into relatively high coastal elevations (31-67 m; Table 1.2), yielding high (> 1) coastal-plain to shelf gradient ratios. Although these gradient ratios are

unsuitable for promoting fluvial incision in response to sea-level fall, the Magnolia, La Batre, and Fish rivers incised valleys that are 7, 11, and 12 m- deep, respectively (Table 1.3; Figure 1.9a). Greene et al. (2007) mapped the valleys as merging with the larger Mobile incised valley around 20 km seaward from where their modern bay-head deltas are located. Incision and knick-point migration of the large Mobile valley likely influenced incision of these and other smaller tributary rivers. Similarly, the San Jacinto valley merges with the much larger Trinity valley in the middle of Galveston Bay (Rodriguez et al., 2005). Although the San Jacinto River is substantially larger than any of the Mobile tributaries, it is still characterized by a relatively high coastal-plain to shelf gradient ratio (~1.45; Table 1.2; Figure 1.9a) and incision was likely promoted by the confluence with the Trinity system. Small lower coastal-plain systems with gradient ratios >1 would likely not have incised if not for merging with systems that did, which promoted rejuvenation of their drainage networks.

Excluding tributary systems and despite a broad range of coastal convexities included in our study, no correlation is resolved between coastal-plain/shelf gradient and incision depth at the Sangamon shoreline (i.e. apex of the coastal prism; Figure 1.9a). This could be because there is an insufficient degree of variability in gradients along the two passive margins for a distinct trend to emerge. Talling (1998) does demonstrate that if the magnitude and duration of base-level fall is constant, then incision depth at the highstand shoreline increases with increasing coastal-prism convexity; however, that study includes coastal-prism profiles in different tectonic settings (foreland basin and passive margin) and coastal convexities that differ by much more than what exists along the northern Gulf of Mexico and U.S. mid Atlantic passive margins. Although the degree of coastal-prism convexity is a control on valley depth (Figure 1.1), the high scatter shown in Figure 1.9a suggests that

System	Margin	VW (m)	VD (m)	VA (km²)	Data Type and Origin	VW at BHD (m)
Albemarle (RO+CH)	Atlantic	14912	11	98000	seismic	6783
Altamaha (AL)	Atlantic	-	-	-	-	6610
Chowan (CW)	Atlantic	-	-	-	-	4313
Neuse (NS)	Atlantic	3019	10	12500	DOT borings	5045
New (NW)	Atlantic	1570	8	6700	seismic	2683
Newport (NP)	Atlantic	1733	6	5100	seismic	1705
Ogeechee (OG)	Atlantic	-	-	-	-	4623
Roanoke (RO)	Atlantic	-	-	-	-	5355
Santee (SN)	Atlantic	-	-	-	-	5388
Savannah (SV)	Atlantic	-	-	-	-	6063
Tar (TA)	Atlantic	4241	11	11200	DOT borings	3358
White Oak (WO)	Atlantic	1789	9	9300	seismic	2030
Appalachicola (AP)	Gulf	-	-	-	-	6930
Aransas (AS)	Gulf	-	-	-	-	1348
Bernard (BB)	Gulf	-	-	-	-	445
Biloxi (BI)	Gulf	-	-	-	-	1580
Blackwater (BW)	Gulf	-	-	-	-	895
Calcasieu (CA)	Gulf	2781	24	32000	Nichol et al. (1996)	2998
Choctawhatchee (CH)	Gulf	-	-	-	-	4595
Escambia (ES)	Gulf	-	-	-	-	4730
Fish (FI)	Gulf	862	12	5750	Mattheus et al. (2007)	1048
Garcitas (GC)	Gulf	-	-	-	-	1253
Guadalupe (GU)	Gulf	-	-	-	-	5480
Jacinto (SJ)	Gulf	3083	17	19600	Morton et al. (1996)	2908
La Batre (LB)	Gulf	1065	11	6000	Mattheus et al. (2007)	665
Lavaca (LV)	Gulf	5813	18	37800	Wilkinson and Byrne (1977)	3028
Magnolia (MG)	Gulf	522	7	2200	Mattheus et al. (2007)	723
Mission (MN)	Gulf	-	-	-	-	2615
Mobile (MO)	Gulf	14304	19	201000	DOT borings	13533
Neches (NE)	Gulf	7750	18	76000	Morton et al. (1996)	3555
Nueces (NU)	Gulf	4483	22	46200	seismic	5540
Pascagoula (PA)	Gulf	-	-	-	-	5688
Perdido (PE)	Gulf	-	-	-	-	1085
Sabine (SA)	Gulf	4235	13	44400	Morton et al. (1996)	5905
San Fernando (SF)	Gulf	-	-	-	-	2535
Tchoutacabouffa (TC)	Gulf	-	-	-	-	1095
Trinity (TR)	Gulf	16594	22	97500	Smyth (1991)	8195
Yellow (YR)	Gulf	-	-	-	-	1458

Table 1.3 - Metrics of studied valleys (VW = valley width, VD = valley depth, VA = valley cross-sectional area, VW at BHD = valley width at the bay-head delta).

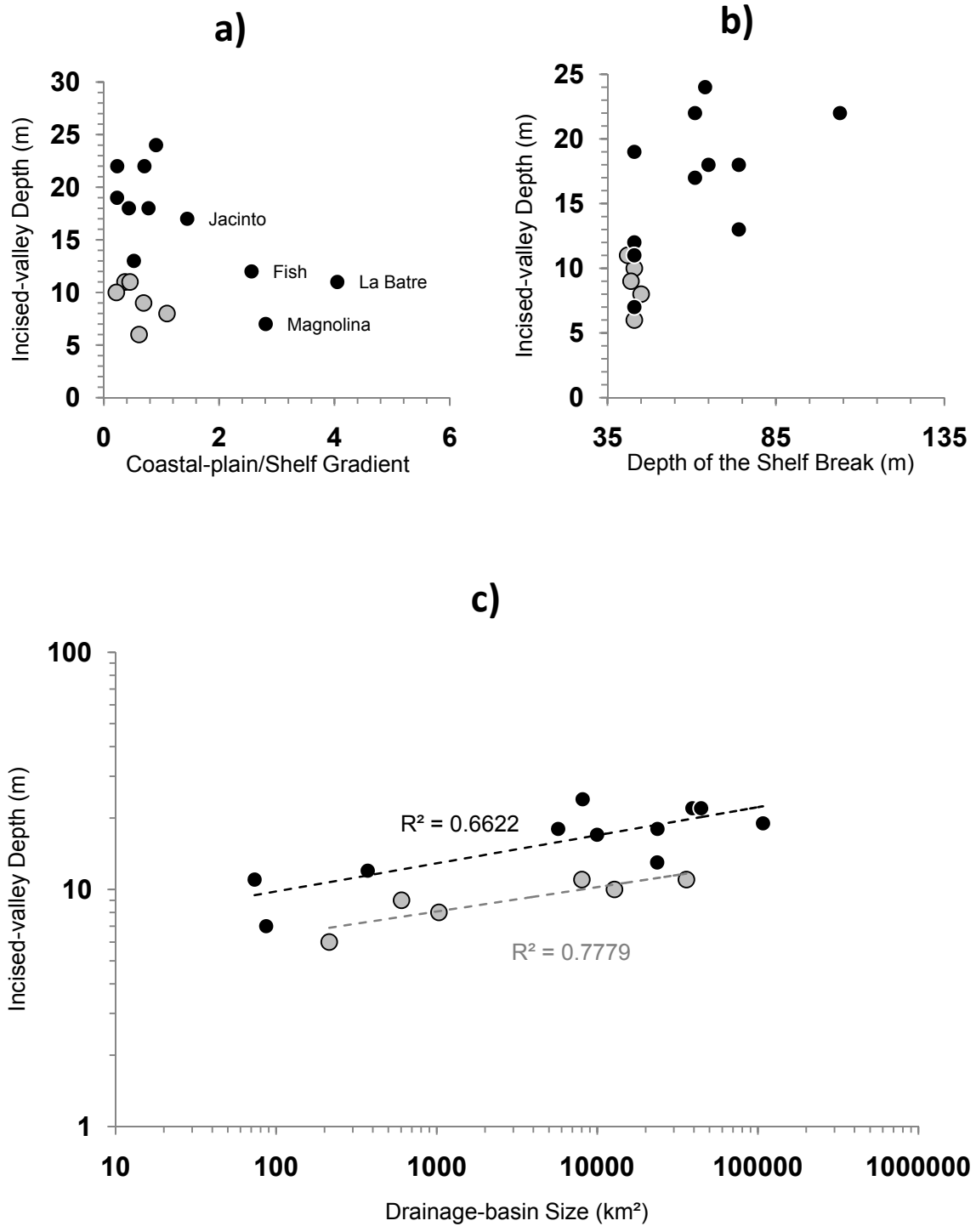

Figure 1.9 - Plots of a) coastal-plain/shelf gradient, b) depth of the shelf break, and c) drainage-basin size versus incised-valley depth (at a log-log scale). Gulf of Mexico valleys are black circles; gray circles are North Carolina valleys. Tributary valleys are labeled. See Tables 1.2 and 1.3 for additional information.

across a margin where gradients vary by less than an order of magnitude, which is typical for passive continental margins, other factors are primarily influencing incision depth at the studied locations. This is evident when systems with similar gradient profiles are compared like the Trinity and Sabine valleys that differ in depth by 9 m even though they share very similar coastal-plain gradient profiles, shelf morphologies, and drainage-basin lithologies (Mattheus et al., 2007; Table 1.2). The rivers do have different drainage-basin sizes with the Trinity draining over 44,000 km² and the Sabine draining less than 24,000 km² (Table 1.2; Figure 1.3). From Equation 1, the higher the discharge the lower the equilibration time (T_{eq}) is, indicating that the Trinity progressed more towards reaching an equilibrium profile than the Sabine, which likely explains its greater depth. Since differences in valley depth between respective systems cannot be explained solely by variations in coastal convexity across the margins, variables linked to river discharge and the timing and duration of incision need to be considered.

1.6.1.3.Depth of the Shelf Break

The two areas where fluvial incision in response to base-level lowering should be greatest are at the depositional shoreline break and at the shelf break. Incision at the depositional shoreline break initiated at similar times across the margins as sea-level fell exposing the inner shelf; however, given the large differences in shelf morphology across the margins, particularly with regards to the depth of the shelf break, incision here should have initiated at different times. In addition, the transition from continental shelf to slope is a larger gradient increase than the transition from coastal plain to continental shelf (Figure 1.5) and the more shallower the depth of the shelf break, the greater the magnitude of river profile

adjustment should be, which, in combination with discharge, influences the upstream distance of knickpoint migration from that location.

The magnitude of the fall in eustatic sea level associated with the LGM is around -120 m (Fairbanks, 1989; Bard et al., 1990), well below the measured shelf-break depths along the mid-Atlantic margin. Simms et al. (2007) presents evidence that sea-level was up to 35 m shallower during the LGM in the Gulf of Mexico than lower latitudes (Table 1.2; Figure 1.5). Despite this, in the Gulf of Mexico there exists a large degree of variability in shelf morphology along strike, in contrast to the North Carolina Atlantic margin (Table 1.2; Figure 1.5). Correspondingly, the depths of incision, close to the Sangamon shoreline, are more similar along the North Carolina Atlantic margin than the Gulf (Table 1.3; Figure 1.9b). Although the data set as a whole shows no direct correlation between the depth of the shelf break and incised-valley depth (Figure 1.9b), the overall shallower valley depths along the Atlantic margin (range of 8-11 m) than Gulf margin (range of 7-24 m) may be explained by differential influence from the shelf-break knickpoint.

From Equation 1, the narrow continental shelf offshore North Carolina ,or small basin length (L), indicates a small equilibration time (T_{eq}), suggesting that North Carolina valleys should be closer to equilibrium with respect to depth. In addition, the shallow shelf break along the Atlantic margin implies that valley incision there should be deeper than along the Gulf, which contrasts with our results. Lithologic differences between the shelves explain the discrepancy. Rivers along the Gulf incised into thick unconsolidated sediments (Galloway et al., 2000; Anderson et al., 2004) whereas Atlantic rivers met lithified strata at very shallow depths on the shelf (Hine and Snyder, 1985; Riggs et al., 1995; Riggs et al., 1996). The more robust lithified sediments on the North Carolina shelf likely slowed shelf-

break knickpoint migration, minimizing its influence on valley depth at our measurement location (i.e. the highstand shoreline). This explains why incision depths are much shallower and more consistent there than along the Gulf and approximate the thickness of the highstand coastal prism. The high degree of variance in incision depth for Gulf valleys is likely influenced by the broad spectrum of shelf morphologies (particularly regarding shelf-break depths; Table 1.2; Figures 1.5 and 1.9) coupled with easily erodible substrates on the shelf (Anderson et al., 2004), promoting different shelf-break knickpoint-migration rates and degrees of influence on valley depth at our measurement locations across the margin.

1.6.1.4.Discharge

Gully-erosion research highlights that rates of knickpoint migration are heavily dependent on discharge (Schumm et al., 1984), suggesting that drainage-basin size, which serves as a proxy for (i.e. is scaled with) discharge, should play a significant role in determining incision depth at the Sangamon shoreline. Since most of the valleys included in this study incised into comparable substrates, equilibrium timescales for these rivers to regrade their surfaces should depend heavily on discharge (Paola et al., 1992). Variances in incision depth could be explained if our studied valleys are in different stages of vertical adjustment at the Sangamon shoreline on account of varying discharge. Equation 1 states that if other factors are constant then the higher the river discharge, the lower the equilibrium time (T_{eq}). Discharge varies greatly between the studied systems, much more so than any other factor in Equation 1. This would imply that some of the river systems did not incise to equilibrium depth with respect to their graded profile, but were limited by discharge to varying degrees.

Figure 1.9c illustrates that large fluvial basins along the northern Gulf and mid-Atlantic margins are generally associated with greater incision depths than their smaller counterparts. On the Atlantic margin, for example, the lower coastal plain Newport and White Oak rivers incised to depths of 7 and 8 m, respectively while the Tar and Roanoke rivers, characterized by drainage basins an order of magnitude larger, both incised to a depth of 11 m (Table 1.3; Figures 1.6 and 1.7). Together with 11 data points from the northern Gulf of Mexico margin, a general trend is resolved that explains incised-valley depth as a power function of drainage-basin size, which has an R^2-value of 0.50 (Figure 1.9c). If the Gulf and Atlantic margin valleys are evaluated individually, this value improves significantly to 0.66 and 0.78, respectively (Figure 1.9c). These relationships are similar to the correlation between discharge and channel depth (Leopold and Maddock, 1953) and suggest that the upstream parameters that factor into discharge (drainage-basin size, gradient, and climate) play the primary role in determining to what degree river systems are able to adjust vertically in response to sea-level fall. Although at the coastline, base-level fall is responsible for incision and gradient influences fluvial response to that forcing, coastal-prism convexity and the depth of the shelf break do not correlate to measured incision depths. The separation of Gulf- and Atlantic-margin valleys is likely influenced by variations in substrate lithology in addition to the differences in respective shelf morphologies, which also dictate the equilibrium profile and influence equilibrium timescales. Incised-valley depth is controlled by a combination of the aforementioned parameters outlined in Equation 1, but at the highstand shoreline of the previous sequence along passive margins, discharge is the main factor limiting the degree of vertical equilibration.

1.6.2. Incised-valley width and cross-sectional area

Researchers have shown that incised-valley width is primarily controlled by the rate of base-level fall, the angle of the newly exposed shelf, climate, and the duration of subaerial exposure (Schumm, 1993; Schumm and Ethridge, 1994; Ardies, 2002; Ethridge et al., 2005). The rate of base-level fall and convexity of the highstand coastal-prism apex should determine the degree of lateral fluvial adjustment prior to entrenchment. Once the active river channel incises to a level where it is unable to overtop its banks, the morphology of the valley flanks are principally modified by processes related to subaerial weathering and mass wasting. These processes are closely linked to vegetation and its controls on bank stability, which are ultimately related to climate (Schumm, 1993; Schumm and Ethridge, 1994; Ardies, 2002). The duration of subaerial exposure determines the degree to which slope-adjustment processes can operate and modify the morphology of interfluve areas and valley flanks. Flume studies also suggest that fluvial activity (meandering, etc.) associated with the transgressive stage of incised-valley infilling modifies valley flanks substantially, which results in valley sides being highly diachronous along strike (Strong and Paola, 2006; 2008).

Given that valley sides are modified throughout the entire sea-level cycle by processes related to river incision, river aggradation, and mass wasting, valley widths might be highly variable and not correlate distinctly to upstream controls. Nonetheless, Figure 1.10 shows correlations between incised-valley width, cross-sectional area and drainage-basin size along the Gulf of Mexico- and Atlantic-margin systems as simple power functions. Incised-valley size is proportional with drainage-basin area, which is a proxy for long-term discharge, the sum of upstream control mechanisms (climate, gradient, drainage basin size, etc.). The New River Valley is the only system that shows dramatic morphologic changes

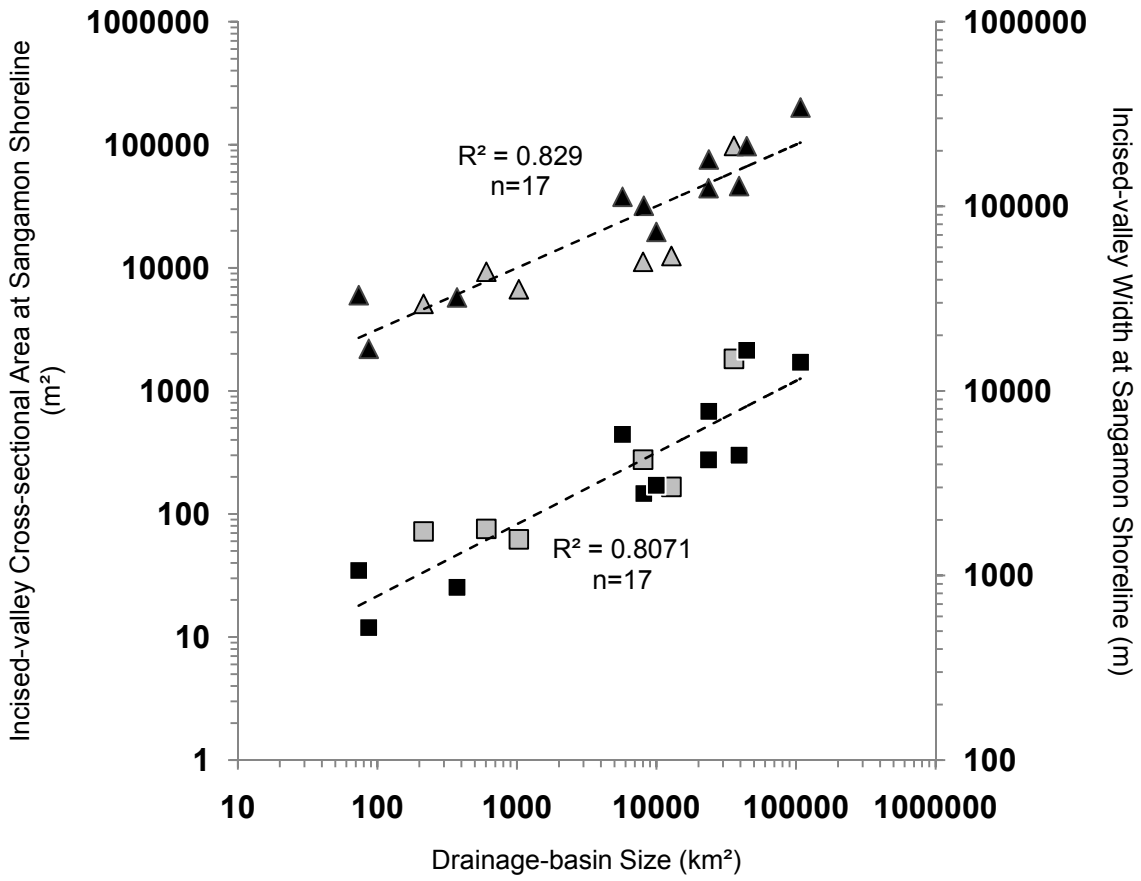

Figure 1.10 - Plots of drainage basin size versus incised-valley cross-sectional area (triangles) and incised-valley width (squares) at seismic and core-transect locations (log-log scale) for 17 systems from the northern Gulf of Mexico (black) and U.S. mid-Atlantic (gray) margins. See Tables 1.2 and 1.3 for additional information.

along dip (Figure 1.4) due to the well-cemented Belgrade Formation, found at shallow depths, which also influenced the aforementioned changes in valley depth. All other systems examined incised through unconsolidated substrates and do not exhibit a high degree of along-dip variability in valley shape.

1.6.2.1.Climate

Climate is a control on river evolution because it regulates precipitation and vegetation, which in turn helps dictate discharge of sediment and water as well as influence bank stability (Schumm and Brackenridge, 1987; Blum and Törnqvist, 2000; Cecil, 2003). At modern times, there exists a steep climate gradient across the northern Gulf of Mexico Figure 1.10 – width and cross-sectional area margin, defined by a westward increase in aridity (Thornthwaite, 1948). Comparatively, North Carolina does not exhibit much spatial variation in precipitation (Boyles and Raman, 2003). The response of vegetation to late Quaternary environmental change in North America is thought to be complex over a wide range of spatial, temporal, and ecological scales (Delcourt, 1981; Williams et al., 2004). Researchers rely on vegetation records and other proxies to infer past climate conditions on land; however, with few exceptions (Delcourt, 1981), detailed vegetation studies focus almost exclusively on the LGM and transition to the Holocene (Prentice et al., 1991; Adams and Faure, 1997; Webb et al., 1998; Jackson et al., 2000; Ray and Adams, 2001; Williams, 2002; Williams et al., 2004), while the duration of valley formation/modification spans the last ~120 ka (since the last interglacial). Tundra and boreal forests in North America extended 100s of km south of the ice sheets and temperate forests of the East expanded into the Texas Coastal Plain during the LGM (Delcourt, 1981; Prentice et al., 1991). At this time,

the northern Gulf of Mexico coastal plain was overall warmer and drier than the mid-Atlantic, but the intra-marginal variance in vegetation cover across both margins was relatively low (Delcourt, 1981; Prentice et al., 1991; Adams and Faure, 1997; Jackson et al., 2000; Ray and Adams, 2001; Williams, 2002; Williams et al., 2004). Incised-valley width at the highstand shoreline being equilibrated to drainage-basin size suggests that either climate change is not a dominant modifier of valley width over >10,000-year timescales or, more likely, that climate conditions and vegetation patterns were similar enough across the southern and southeastern United States to promote similar precipitation conditions and bank stability.

1.6.2.2.Bay Ravinement

Incised valleys widen seaward (Schumm, 1993); but at our inundated measurement location, bay-ravinement processes also contribute to the widening. Bay ravinement is controlled by the imposing energy regime (waves and tides), which is strongly linked to the fetch and depth of the estuarine body. Bay ravinement is observed today as estuarine shoreline erosion (Riggs and Ames, 2003) and modifies incised-valley flanks throughout inundation. Valleys that have similar drainage-basin sizes are wider along the North Carolina Atlantic margin than the Gulf. The presence of the extensive Pamlico-Albemarle estuarine system and large separation of the Sangamon shoreline from the modern barrier shoreline in North Carolina reflects this margin's relatively low sediment supply and/or large accommodation during the Holocene sea-level rise as compared to the Gulf (Riggs et al., 1995; Riggs et al., 1996; Mallinson et al., 2005). Differences in sedimentation, estuarine energy regime, and fetch could have contributed to spatial and temporal differences in bay ravinement at the Sangamon shoreline location between the two margins.

To reduce the contribution of bay ravinement in the measure of valley width and to increase the sample size, we measured the width of 36 valleys across both margins at the modern bay-head delta using aerial photographs (Table 1.3; Figure 1.3). Measurement locations are not influenced by tributary junctions or bends and are located no further than 50 km landward from the Sangamon shoreline (for large systems). Increasing the sample size resulted in the addition of numerous small fluvial systems (drainage-basin size < ~5000 km^2) to the data set. Similar to the plot in Figure 1.10, created from width measurements taken in the estuaries, Figure 1.11 also shows a power relationship between drainage-basin size and incised-valley width. A higher R^2-value (0.86) is explained by an increase in the number of systems included and the data location, which minimizes the contribution of bay-ravinement processes to valley widening. This model also shows a high degree of variability among smaller systems (< ~5000 km^2), with drainage basins that do not extend far from the Sangamon shoreline. River discharge of these small fluvial systems likely had minimal influence on erosion at the coastal-prism apex, which was exposed as base-level fell, in comparison to mass wasting/slope processes. Some of these small rivers likely didn't exist prior to the exposure of the inner continental shelf. Figure 1.12 shows four small coastal North Carolina systems that have similar valley widths, but variable drainage-basin sizes. The North River system does not have a fluvial basin and is considered to have formed exclusively by gully formation (i.e. slope erosion); however, the resulting estuarine body is very comparable in width (~1900 m) to that of the Newport, White Oak, and New (1705, 2030, and 2683 m, respectively; Table 1.3; Figure 1.12). These examples highlight the variability in valley widths on the small end of the drainage-basin size spectrum, which is explained by non-fluvial erosion dominating incision. Well-developed and large drainage

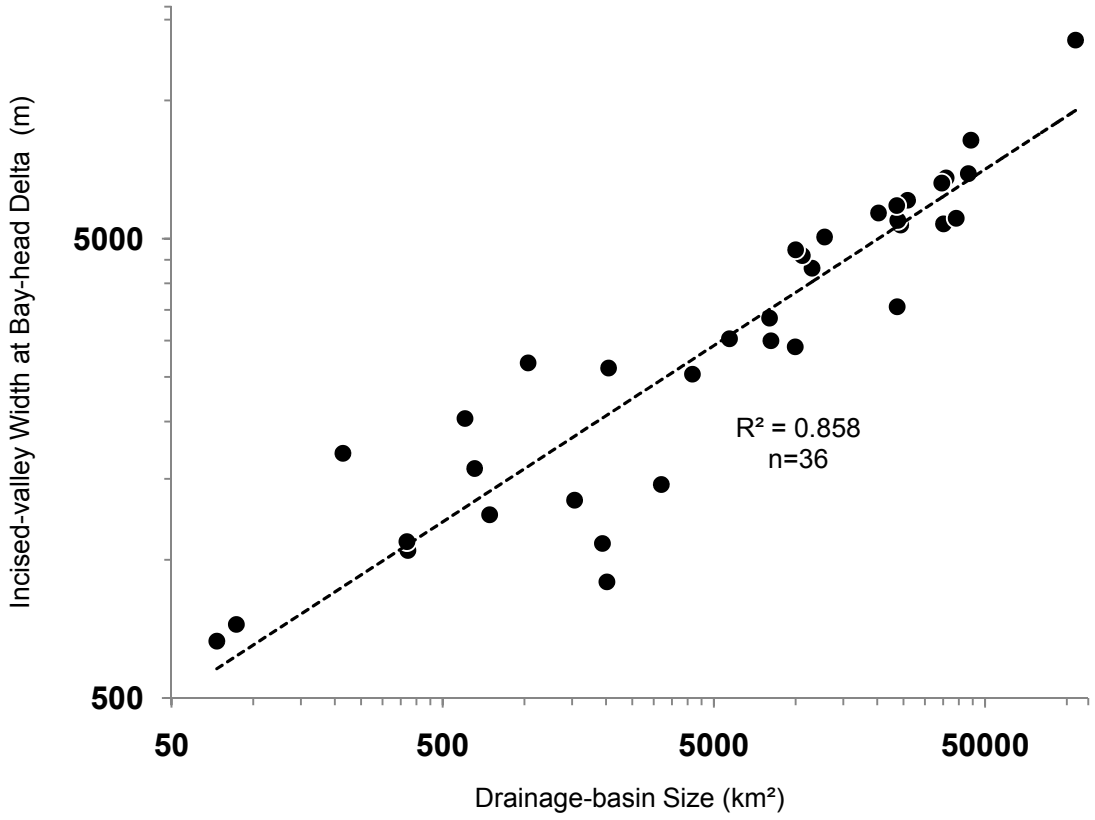

Figure 1.11 - Plot of drainage-basin size versus incised-valley width (log-log scale) at the bay-head delta for 36 systems from the North Carolina and northern Gulf of Mexico continental margins. See Tables 1.2 and 1.3 for additional information.

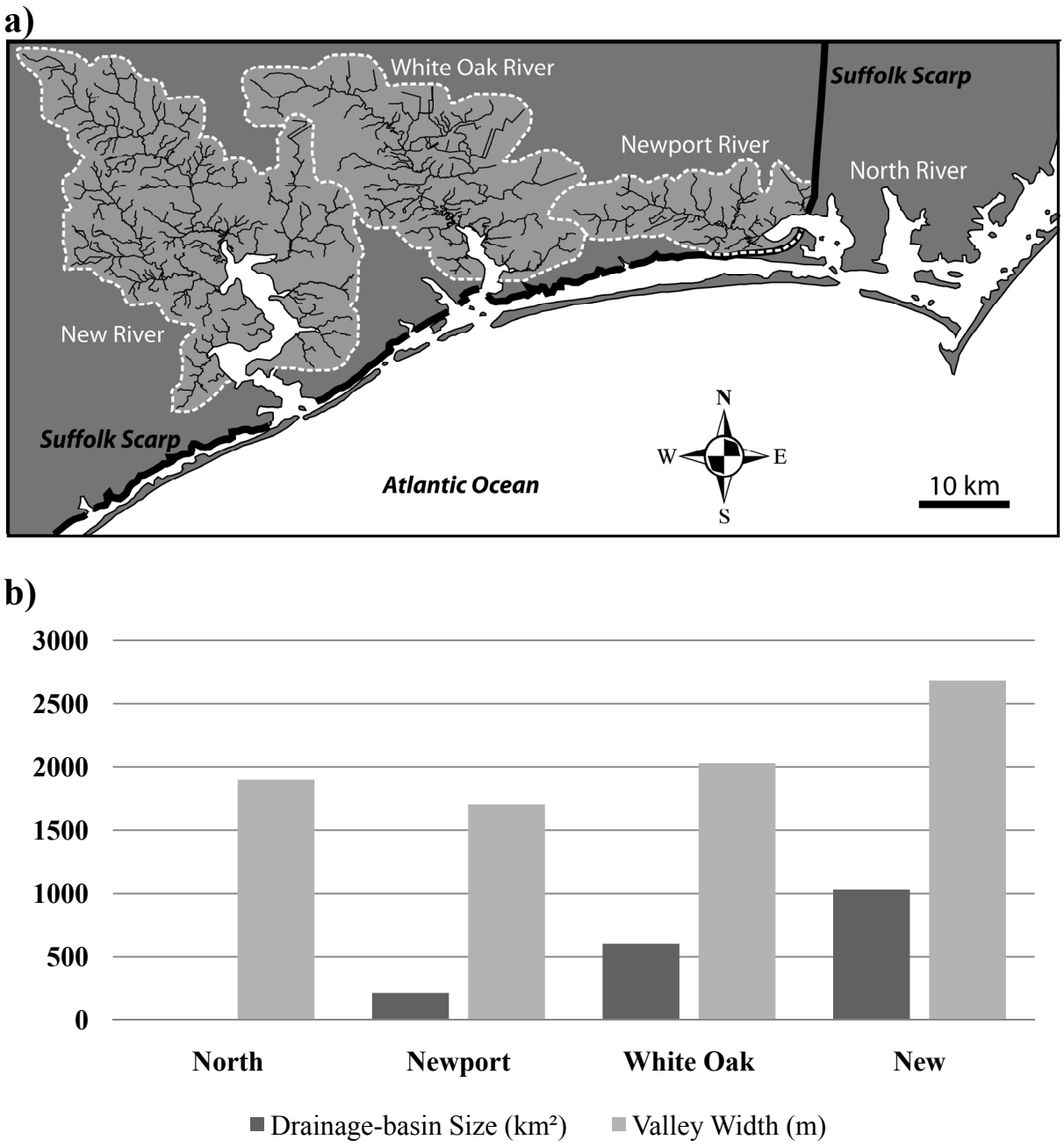

Figure 1.12 – Map of coastal Carteret County, NC (a), showing the drainage basins for the New, White Oak, Newport, and North Rivers; part b plots drainage-basin sizes against valley widths for these systems.

networks, on the contrary, ensure more steady discharge conditions than the smaller rivers that formed as a result of the base-level fall and gravity-driven processes. Mass wasting is a secondary control on valley width for large rivers.

1.7. Conclusions

Relationships between fluvial drainage-basin size and incised-valley width, depth, and cross-sectional area suggest that valley dimension at the highstand shoreline is driven primarily by upstream parameters along both the U.S. mid-Atlantic and northern Gulf of Mexico margins. An exception to the correlation is given by systems that are bounded by bedrock. Incised valleys that are partially rock-bound exhibit significant variances in width, depth, and cross-sectional area along dip over relatively short distances. The morphology of valleys associated with small rivers (~ <5000 km^2) that do not extend far landward of the previous highstand shoreline is influenced more by mass-wasting processes, which initiate as the coastal-plain apex is exposed during base-level fall, and an event-dominated discharge regime than larger rivers. Well-developed larger drainage networks ensure more steady discharge conditions at the highstand depositional shoreline break and mass wasting is a secondary control on valley width.

The relationships between valley dimensions and drainage-basin size, presented here, are largely the product of including a broad range of drainage-basin sizes, which vary by over three orders of magnitude, and a low respective variance in margin-gradient profiles in the study; however, the values incorporated in the study is what exists across the two margins. The level of variability in drainage-basin size and gradient profiles is not unique to the Gulf of Mexico or U.S. mid-Atlantic margins, which suggest applicability of our empirically-

derived models to any passive margin, provided underfilled systems are compared. This is especially important for studies of the data-limited ancient rock record, because our findings show that larger valleys are connected to larger drainage networks, which impacts estimates of sediment discharge to continental shelf and deepwater environments during periods of low sea level. Underfilled valleys are distinguished from overfilled by their fill sequence, as the latter lack estuarine facies (Simms et al., 2006). Models that assume valley size at the highstand depositional shoreline break only reflects variations in the degree of coastal convexity significantly underestimate sediment supply to basin margins.

Chapter 2

Direct Connectivity between Upstream and Downstream Promotes Rapid Response of Lower Coastal-plain Rivers to Land-use Change

2.1. Chapter Summary

Low-relief fluvial systems that originate in the lower coastal plain and discharge into estuaries are common along passive margins. These watersheds are thought to be disconnected from their termini by floodplains, which buffer the sediment-routing system by sequestration. Here, we present a detailed study of the Newport River, a typical lower coastal-plain system, which reveals high connectivity between watershed and delta. Connectivity is measured as the time lag between initiation of a silviculture operation (i.e. tree farm), which increased landscape erosion by extensive clear-cutting, and when the sediment appeared at the bay-head delta. The time lag, measured from aerial photographs and sedimentation rates calculated from ^{210}Pb- and ^{137}Cs-activities in cores from the watershed and delta, is <3 years. Most lower coastal-plain rivers are steeper and have less floodplain accommodation available for storage than their larger counterparts that originate landward of the fall line, which promotes higher connectivity between upstream and downstream.

2.2. Introduction and Background

Rivers are the primary means by which terrestrial sediments are transferred from non-glaciated continental interiors to coastal and marine basins (Ritter et al., 1978); however,

depending on the time frame of interest, the sediment-transport pathway is not always direct (Harvey, 2002). At millennial and longer time scales the sediment-delivery ratio (downstream deposition/upstream erosion; Walling, 1983) is theorized to approximate unity (Schumm, 1977; Allen, 2008). At centennial and shorter time scales it is more difficult to predict the sediment-delivery ratio and the impacts of a large-scale watershed modification and/or climate change on sediment discharge at a river's terminus because fluvial systems have a natural buffering capacity to change (Trimble, 1983; Fryirs et al., 2007).

The buffering capacity of a fluvial system is associated with its drainage-basin size (Figure 2.1; Walling, 1983; deVente et al., 2007) and gradient (Figure 2.1; Milliman and Syvitski, 1992; Swiechovicz, 2002). Connectivity between upstream and downstream sections of a fluvial system generally decreases as the catchment area increases due to sediment storage in alluvial plains, which are typically extensive for large rivers (Yeager et al., 2005; Brierley et al., 2006). Overall, landscape-to-channel and upstream-to-downstream connectivity increases as the fluvial gradient increases (Fryirs et al., 2007).

Although all coastal-plain river profiles on passive margins are considered to be low gradient, rivers that originate landward of the fall line (the transition between piedmont and coastal plain) have much lower gradients than smaller rivers that originate near the coastline (lower coastal-plain rivers). For example, in North Carolina the Neuse and Tar rivers originate ~100 km landward of the fall line and have longitudinal gradients on the coastal plain of 0.15 and 0.19 m/km, respectively, while lower coastal-plain rivers in North Carolina are between 0.27-0.74 m/km. Phillips (1992) and Noe and Hupp (2009) suggest a decoupling exists between the upstream and downstream components of coastal-plain rivers that originate near the fall line, due to extensive alluvial storage in the low-gradient and

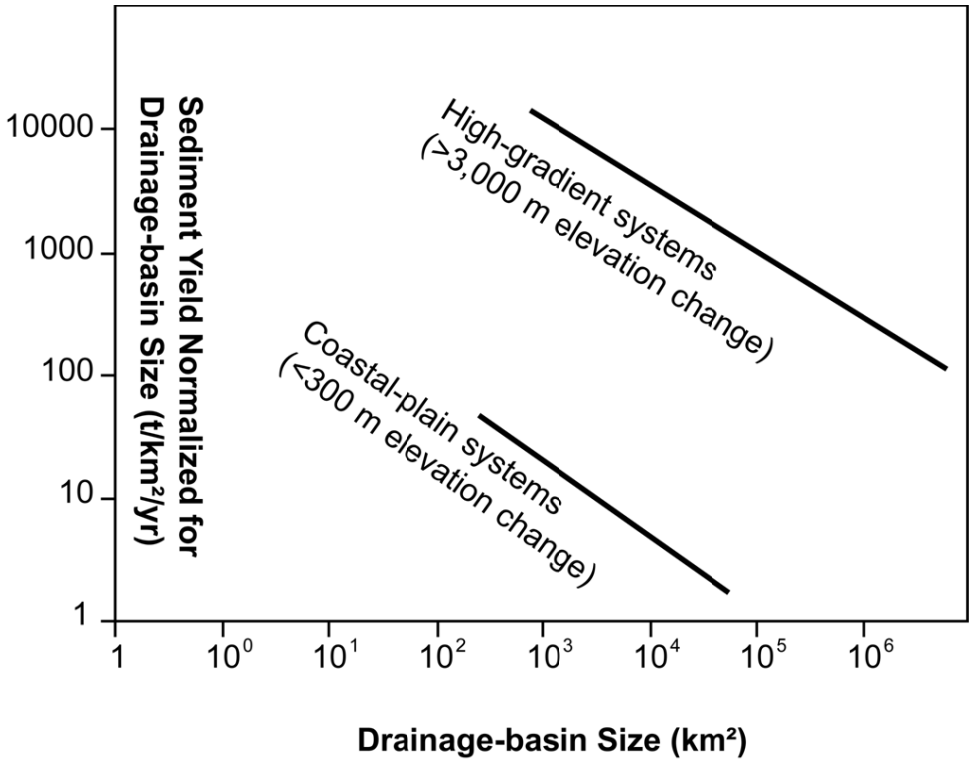

Figure 2.1 - Plot of area-specific sediment yield (i.e. normalized for drainage-basin size) versus drainage-basin size for high-gradient and coastal-plain river systems as regression lines; after deVente et al. (2007). This graph shows that high-gradient systems yield more sediment than size-equivalent systems on the coastal plain and that the buffering capacity of a system increases with the size of the fluvial catchment (as indicated by the negative slope on the regression lines).

broad floodplain. Not much is known about the efficacy of sediment transport through lower coastal-plain river systems. These lower-relief but higher-gradient (relative to rivers that originate near the fall line) watersheds are important because they are very common to passive margin settings, making up ~75% of the counties in North Carolina with estuarine shorelines (Figure 2.2), and are frequently being altered as a result of rapidly increasing coastal populations (Small and Cohen, 2004; McGranahan et al., 2007). Additionally, land-use change in watersheds is often associated with an increase in suspended-sediment concentration in the river, which commonly presents a water-quality problem (Binkley and Brown, 1993; Nelson and Booth, 2002) and degrades the benthic environment of coastal estuarine systems (Wolanski and Spagnol, 2000).

Researchers suggest that, over human timescales, agriculturally-derived sediment in lower coastal-plain watersheds has little chance of exiting the basin because it is sequestered within localized sinks (e.g. drainage ditches and dams) and the floodplain (Belk and Phillips, 1993; Slattery et al., 2002, 2006; Lecce et al., 2006a, 2006b). We infer, however, that relative to larger passive-margin river systems, lower coastal-plain river systems should have lower buffering capacities (higher upstream to downstream connectivity) because of their smaller and narrower floodplains (lower accommodation) and higher fluvial gradients. Fluvial connectivity is related to the time lag between when a change occurs in the watershed and its manifestation at the river's terminus. Larger time lags indicate lower connectivity due to higher buffering. Here, we measure the time lag between when a change in land-use of a small coastal-plain watershed occurred and when the change appears at its bay-head delta. The study area is the Newport River, NC because this small (210 km^2) and low-elevation (originates at 4 m elevation) coastal-plain watershed has been heavily modified

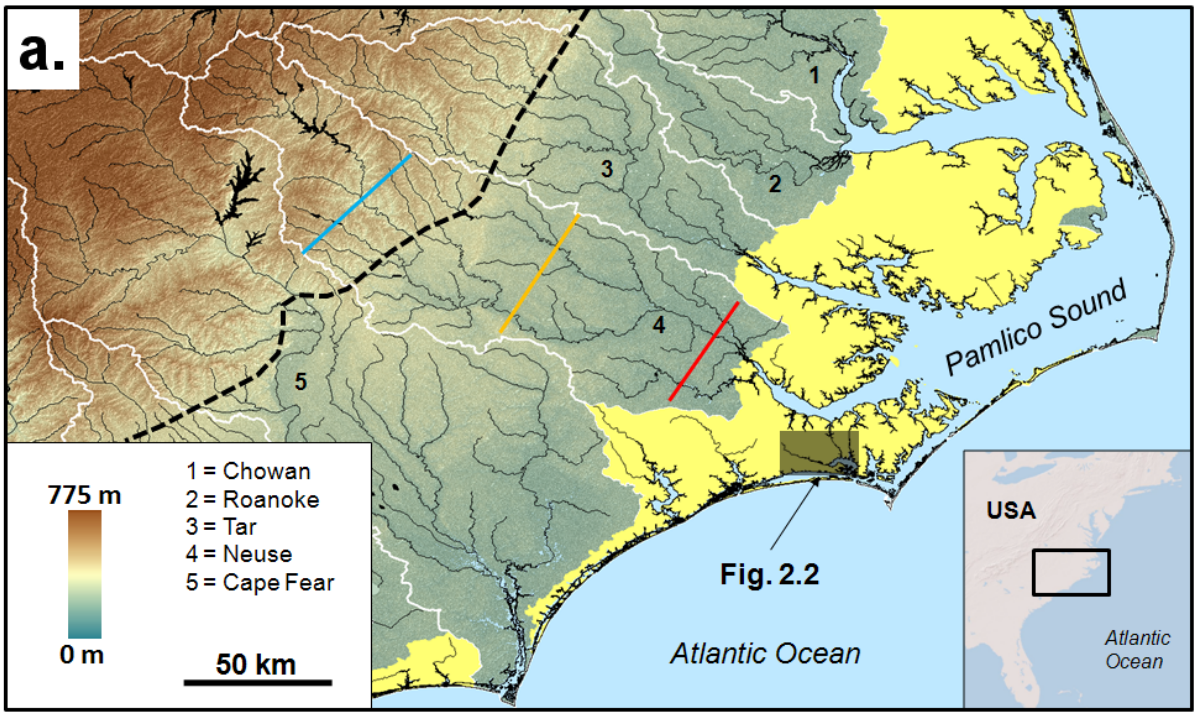

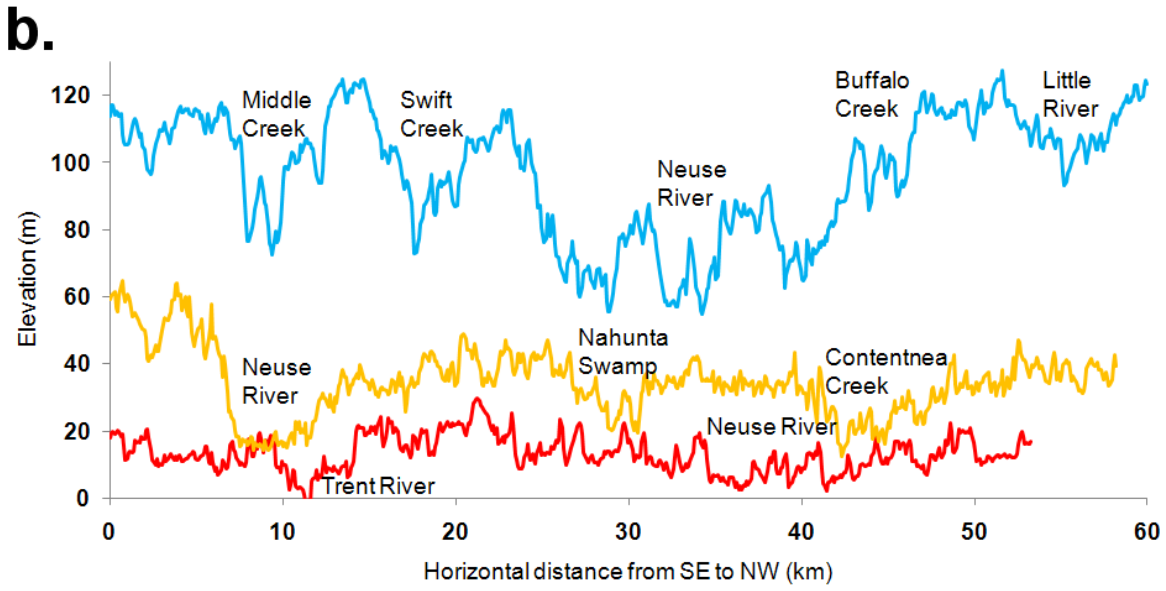

Figure 2.2 - Topography map of coastal North Carolina (a) showing major drainage basins (outlined in white and numbered with legend) and the position of the fall line. Part b shows strike-oriented topographic cross-sections across the Neuse River basin that are 100 km apart along dip from piedmont to lower coastal plain. The profile colors match those of the transect lines on part a. The yellow shading highlights the area of coastal counties that drains into estuaries by small coastal watersheds.

over the past 50 years, which is the timeframe of the study (Figure 2.3a).

2.3. Watershed Modifications and Variations in Delta Morphology

We quantified watershed modifications, including changes in urban, tree farming (silviculture) and agricultural area, and changes in the extent of the bay-head delta shoreline using a time series of digitally mosaicked and georectified aerial photographs (Table 2.1; Figure 2.3a). Based on our analysis of watershed modifications from 7 photos taken at an average interval of 7 years, the areal extent and distribution of agricultural fields were largely unchanged, urbanization steadily increased over time, and the largest change to the watershed was the installment of a silviculture operation (Table 2.2; Figure 2.3a, b). The latter is situated in the middle-lower portion of the watershed at elevations between 1-2 m. Logging records show that initial clear-cutting (of around 3 km^2) began in 1964 and aerial photos taken in January of that year predate the disturbance (Figure 2.3a, b). The maximum extent of the operation had almost been established (~18 km^2; Table 2.2) by 1983 with only minor areas added in the following years. Sun et al. (2001) found that deforestation of low-gradient coastal-plain settings increases surface erosion significantly, albeit not as much as deforestation of high-gradient areas. Silviculture is the most likely land-use modification in the Newport watershed from which a time lag can be measured at the bay-head delta because the operation probably modified river-sediment yield and initiation was abrupt.

The Newport River delta plain and prodelta should be efficient at trapping river sediment because the delta plain is a flat and densely vegetated salt-marsh meadow and an oyster reef partially isolates the upper estuary, limiting sediment transfer offshore through Beaufort Inlet (Johnson, 1959). To determine whether or not the silviculture operation

Vintage	Spatial Coverage	Source	Scale
11/11/58	Newport Delta and Catchment	USDA	1/20000
01/21/64	Newport Delta and Catchment	USDA	1/20000
07/05/67	Newport Delta	NCDOT	1/12000
02/17/71	Newport Delta and Catchment	USDA	1/20000
05/06/75	Newport Delta	NCDOT	1/12000
11/27/79	Newport Delta	NCDOT	1/24000
04/24/82	Newport Delta and Catchment	USDA	1/60000
03/29/83	Newport Catchment	NCDOT	1/60000
10/27/88	Newport Delta and Catchment	USDA	1/40000
03/08/93	Newport Catchment	USGS	3m/pixel
04/19/94	Newport Delta	NCDOT	1/36000
01/25/98	Newport Delta and Catchment	USGS	1m/pixel
05/13/06	Newport Delta	NCDOT	1/9600

Table 2.1. Information on aerial photographs used to quantify changes in land-cover type within the Newport watershed and the position of the deltaic shoreline.

Date	Agriculture (km^2)	Urban (km^2)	Entire Silviculture (km^2)	Bare Silviculture (km^2)	Delta cumulative change since 1958 (m^2)
11/12/58	12.688	1.408	0	0	0
01/21/64	12.72	2.608	0	0	18750
07/05/67	-	-	-	-	115625
02/17/71	10.3968	3.136	3.328	3.328	146875
05/06/75	-	-	-	-	169375
11/27/79	-	-	-	-	247500
09/24/82	-	-	-	-	270625
03/29/83	12.368	6.376	18.176	8.456	-
10/27/88	10.68	7.064	18.736	2.84	378125
04/19/94	10.352	8.56	19.4	3.44	378125
01/25/98	10.72	11.408	19.752	0.896	446875
05/13/06	-	-	-	-	492500

Table 2.2. Changes in the areal extent of urbanized areas, agriculture, silviculture (entire and bare) and the delta as determined from aerial photographs listed in Table 2.1.

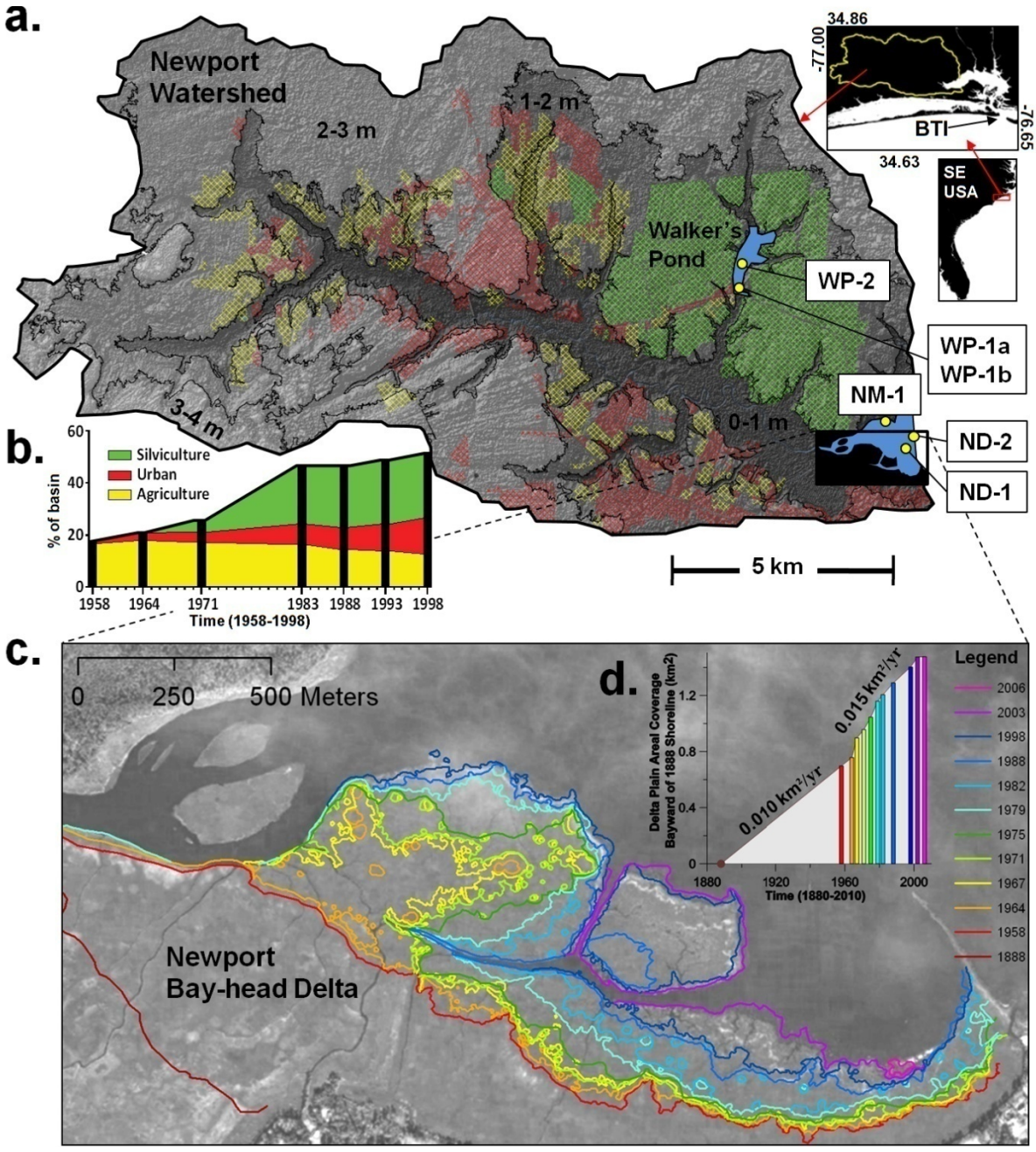

Figure 2.3. Shaded relief map of the Newport Drainage Basin, NC (a), showing 1998 anthropogenic land-surface-cover types and the locations of collected cores (BTI=Beaufort Tidal Inlet; elevation contour interval=1.0 m). The area of land-surface-cover types in the watershed since 1958 (b; excluding supratidal wetlands and forestland) is based on aerial photos and colors correspond to the base map. Aerial photo of the Newport Delta (c) taken 05/2006 shows the broad salt marsh that formed post 1958. Positions of the delta-plain shoreline at 11 times between 1958 and 2006 are superimposed. Respective photographs are shown in Appendix B. The inset histogram (d) displays marsh expansion from the 1888 shoreline (Appendix B) and the colors correspond to the shorelines in c.

impacted sedimentation at the bay-head delta, we measured the delta's shoreline position since 1958 from 11 photos taken at an average interval of 5 years (Figure 2.3a, c). A georectified nautical survey chart published by the United States Coast Survey offers insight into the position of the deltaic shoreline around 1888, predating silviculture by more than 75 years. Our measurements show that the delta prograded into the estuary by as much as 1 km since 1888 and that the associated rate of change in delta-plain area is not constant through time (Figure 2.3a, d). A prominent change in the rate of delta growth is noticed between 1964 and 1967 that distinctly separates two trends. The first trend is defined by 3 data points (1888, 1958, and 1964) that suggest a rate of delta growth of 0.01 km^2/yr pre-dating the onset of silviculture, and the second trend is defined by 9 data points that show an increased rate of 0.015 km^2/yr from 1967 onward (R^2=0.97). The largest resolved increase in the rate of delta growth occurred between 1964 and 1967, which corresponds with the initiation of the silviculture operation. It is not convincing to argue that the rate of delta progradation was entirely uniform prior to the initiation of silviculture because we only have two images of the delta for the 76-year period prior to 1964. To truly assess the connectivity between the upstream and downstream, it is necessary to more precisely compare the timing of increased erosion of the catchment as a result of initial clear-cutting with the increase in sedimentation at the delta.

2.4. Linking Upstream and Downstream Change

Changes in erosion rates of the watershed are difficult to quantify, but sediment in a reservoir located in the middle of the watershed should contain a record of upstream erosion, with an increase in sediment-accumulation rate indicating increased erosion. This is

especially true for small reservoirs with low-gradient shorelines, where sediment-accumulation rates are not impacted by sediment introduced into the basin by shoreline erosion. Walker's Pond (WP) is well suited for recording upstream changes in erosion rates as a result of silviculture because it receives drainage from ~ 25% of the silviculture area, was constructed around AD 1750, and is the only reservoir in the watershed (Figure 2.3a). Comparing the timing of changes in sedimentation rates in WP to changes in sedimentation rates at the Newport Delta directly assesses the connectivity between the catchment basin and the river terminus, which should be an indicator of the buffering capacity of the floodplain. We calculated sedimentation rates for WP and the Newport Delta from measuring the activity of ^{210}Pb and ^{137}Cs in push cores by gamma and/or alpha spectroscopy (Figure 2.4). Core locations are shown in Table 2.3. All cores show little variation in lithology, no bioturbation, and a linear decrease in porosity due to normally-compacting sediment with depth. Based on these observations, we interpret changes in the exponential-decay rate of ^{210}Pb with depth as changes in mass accumulation rate. Core WP-1a is the longest core (0.25 m) we recovered from the deepest part of WP (2.45 m), which is adjacent to the pond's southern shoreline. Based on the exponential decay rate of ^{210}Pb with depth and the peak atmospheric radiocesium fallout between 1964 and 1965 from atmospheric hydrogen bomb testing, a sudden increase in the rate of sediment accumulation exists around 1964 from 0.26 cm/yr to 0.44 cm/yr (Figure 2.4a). Two additional cores, WP-1b (from the southern part of WP (~100 m east from WP-1a) and WP-2 from the center of the pond, were also analyzed, but only for ^{210}Pb activity. Sediment accumulation measured in cores WP-1b and WP-2 shows an increase in rate from 0.26 cm/yr to 0.48 cm/yr and 0.25 cm/yr to 0.43 cm/yr, respectively (Figure 2.4). Given that all three cores show an increase in the rate of sediment

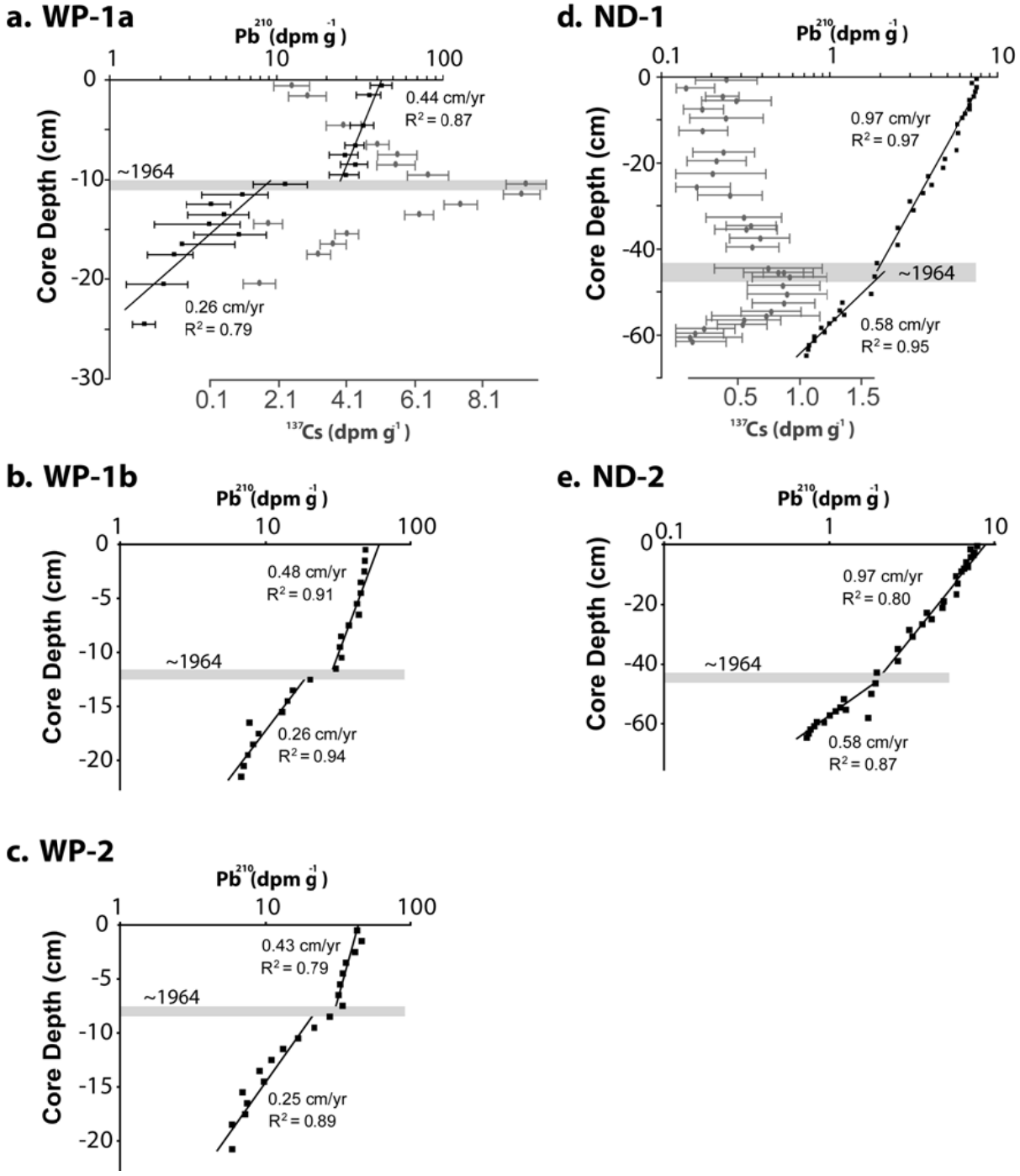

Figure 2.4. Graphs of: a) ^{210}Pb- and ^{137}Cs-profiles from gamma counting for core WP-1a, b) ^{210}Pb- profile for WP-1b, c) ^{210}Pb- profile for WP-2, d) ^{210}Pb- and ^{137}Cs-profiles from alpha and gamma counting, respectively, for core ND-1, and e) ^{210}Pb-profiles for ND-2 (Fig. 1a). Gray boxes highlight depth intervals over which a shift in sedimentation regime occurred and the interval that likely includes 1964 based on the ^{137}Cs profile.

accumulation, calculated from ^{210}Pb activity, at around 10 cm and this depth corresponds to the ^{137}Cs peak in core WP-1a, we infer there to be an increase in the rate of sediment accumulation in WP at 1964. Extrapolating sedimentation rates from 1964 to the surface of the cores indicates that we likely didn't sample the upper ~8.0 cm of pond sediment and field notes that state the top of the core tubes were pushed below the sediment/water interface confirms this. The increase in sedimentation rate coincides with the time of initial deforestation upstream of the pond, signifying that installation of the silviculture operation increased erosion (Figure 2.5a).

Core ND-1 is from the center of the delta front, is 0.65 m long, and based on the ^{210}Pb profile, extends back in time over 75 years, which is well before the aerial-photography record of the delta-plain shoreline. The rate of sediment accumulation in core ND-1 shows an abrupt increase from 0.58 cm/yr to 0.97 cm/yr at ~44.0 cm depth (Figure 2.4d). This depth is close to the ^{137}Cs peak; however, at this delta front location the peak is less defined than what we observed upstream in WP, which is likely due to increased biological mixing. Guinasso and Schink (1975) show that the effect of increasing amounts of mixing on an impulse tracer peak (such as ^{137}Cs) is to shift the peak from the layer at which it occurred to a deeper layer. For core ND-1 this would indicate that 1964 (±3 years) corresponds with the increase in the rate of sediment accumulation and the increase in rate of delta-plain shoreline progradation. An increase in sediment-accumulation rate also exists in the prodelta (core ND-2) from 0.32 cm/yr to 0.50 cm/yr, measured using ^{210}Pb (Figure 2.4e). This change in rate is interpreted to have occurred at 1964, although ^{137}Cs concentrations were not measured to confirm the timing (Figure 2.4e). Additionally, longer vibracores (>2 m) obtained near ND-1 at the margin of the estuary show a change in lithology at 0.40 m below the sediment-

Core	Latitude	Longitude	Coring Date	General Site Description
WP-1a	34.7880	-76.8016	6/27/2008	lower Mills Pond
WP-1b	34.7880	-76.8016	6/27/2008	lower Mills Pond
WP-2	34.7930	-76.8011	6/27/2008	upper Mills Pond
ND-1	34.7533	-76.7554	8/7/2008	delta front
ND-2	34.7562	-76.7530	8/7/2008	prodelta

Table 2.3. Information on collected push cores from the Newport watershed and bay.

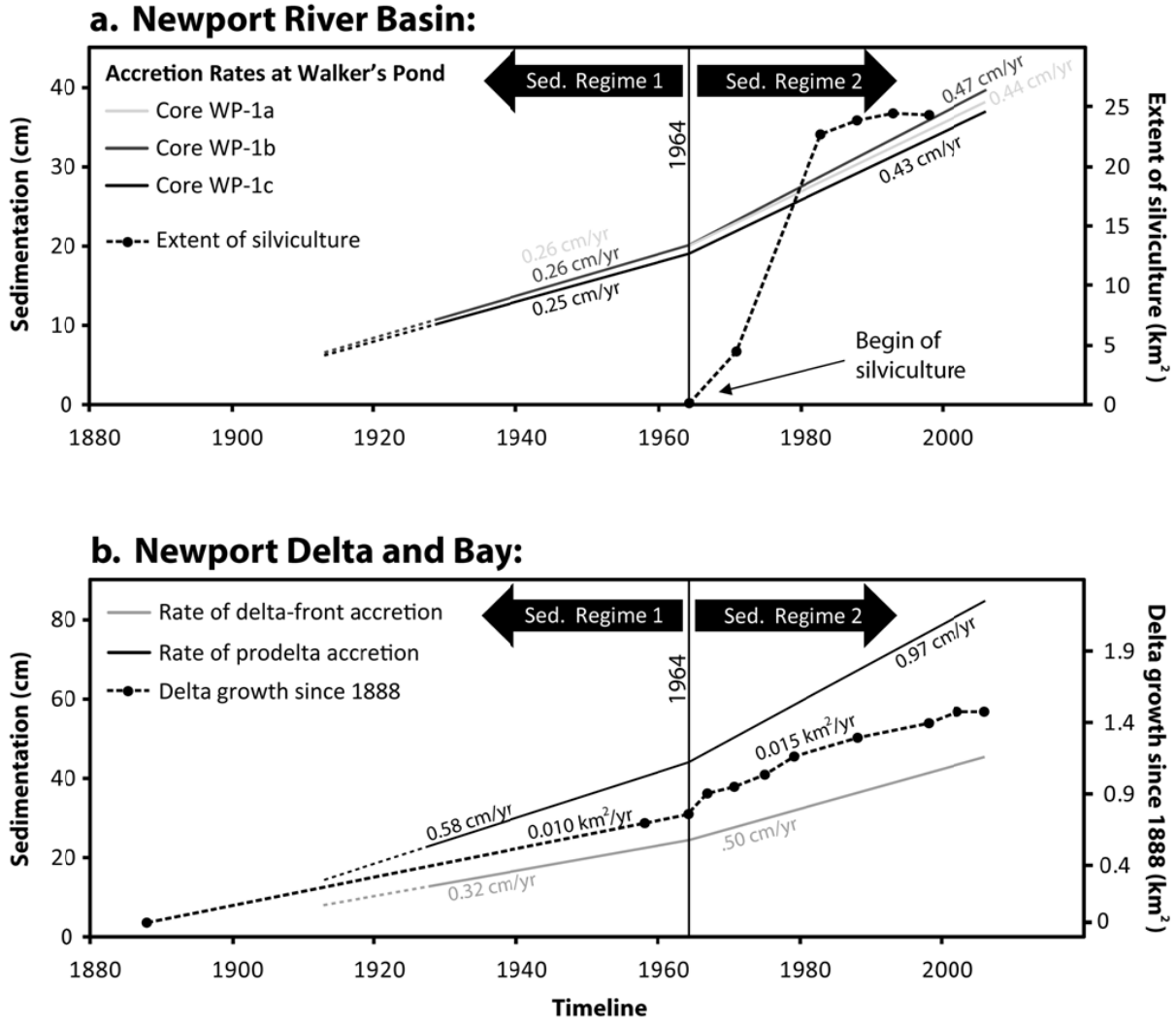

Figure 2.5. Time line, based on the dataset, illustrating that when an abrupt land-use change (silviculture) and associated increase in erosion occurred in the watershed at 1964 (a), the delta plain, delta front, and prodelta responded immediately (b).

water interface from sand-dominated, as mapped by Johnson (1959) at the sediment-water interface, to mud-dominated. This lithologic transition is likely related to the higher post 1964 sediment-accretion rates, measured in core ND-1, filling accommodation at the margins of the estuary.

The time lag between when an increase in erosion occurred upstream, identified by an increase in sediment-accretion rate in WP, and the associated downstream changes in delta and upper estuary sedimentation, in terms of increased rates of sediment accumulation and delta-plain progradation, is within the resolution of the data set (Figure 2.5). The temporal resolution is 3 years, based on the period between when aerial photos of the delta plain were taken and the uncertainty associated with identifying 1964 using the ^{137}Cs peak in core ND-1. The short time lag indicates high connectivity between the watershed and delta and suggests that the buffering capacity of small lower coastal-plain watersheds is low.

The rate of sediment accumulation post 1964 is constant in WP and the Newport delta, suggesting that initiation of the silviculture operation promoted a new regime of higher sediment-accumulation rates throughout the lower Newport watershed and delta (Figure 2.5). Heavy rainfall events (>5 cm) should be important for eroding and transporting sediment from the silviculture area because Slattery et al. (2002 and 2006) and Lecce et al. (2006b) highlight the importance of these events as transport mechanisms for agricultural sediment in low-relief watersheds. The maximum elevation of the silviculture area is only 2 m above sea level, making it likely that during high-precipitation events ground saturation occurs rapidly and sheet flow is dominant, which Amatya et al. (1996) and Lu et al. (2006) show to be efficient at mobilizing sediment. In addition, ditches associated with silviculture development may be important for transporting sediment to tributary creeks during storms,

although Phillips et al. (1999), Slattery et al. (2002), and Lecce et al. (2006b) show them to be significant sediment sinks on the lower coastal plain of North Carolina. Changes in discharge associated with storms are not recognized in the post-1964 sediment-accretion rates at the delta or in WP. At the delta, this is likely due to salt-marsh expansion increasing the buffering capacity of the delta plain due to colonizing vegetation trapping sediment (Morris et al., 2002) and the inability of our sampling interval to resolve sub-annual storm events. No record of high-discharge events exist in WP because of lower sedimentation rates as a result of the pond's relatively small catchment (5 km^2), which further degrades resolution.

2.5. Conclusions

Our study demonstrates that bay-head deltas and upper estuaries of lower coastal-plain river systems are rapidly influenced by upstream changes to the watershed. This implies that the buffering capacity of this river type to changes in sediment yield as a result of changing vegetation cover and/or land-use change in the watershed is low. Because the residence time of particulate material in various reservoirs within a river system strongly influences the fate of micro- and macro-nutrients and organic carbon, the sensitivity of lower coastal-plain river systems to land-use changes is likely to also affect the balance between sequestration and export of geochemically-important constituents. Lower coastal-plain river systems are sensitive to environmental changes (similar to high-elevation and steep river systems commonly found in uplifting settings) and when disturbed, even these small watersheds can deliver significant quantities of sediment to the coastal zone. The upstream portions of lower coastal-plain river systems are directly connected to their termini despite

their low relief because these systems have high gradients and low sediment accommodation in their flood plains and basins (estuaries). In contrast, larger passive-margin river systems that have most of their watershed on the coastal plain and discharge into large estuaries have very low gradients and high sediment accommodation in their extensive floodplains, resulting in the watershed being disconnected from the river outlet due to floodplain buffering (Figure 2.6). The impacts of changes in coastal land-use and likely climate along passive margins will have the most rapid and profound effects on lower coastal-plain river systems and their associated drowned river-mouth estuaries.

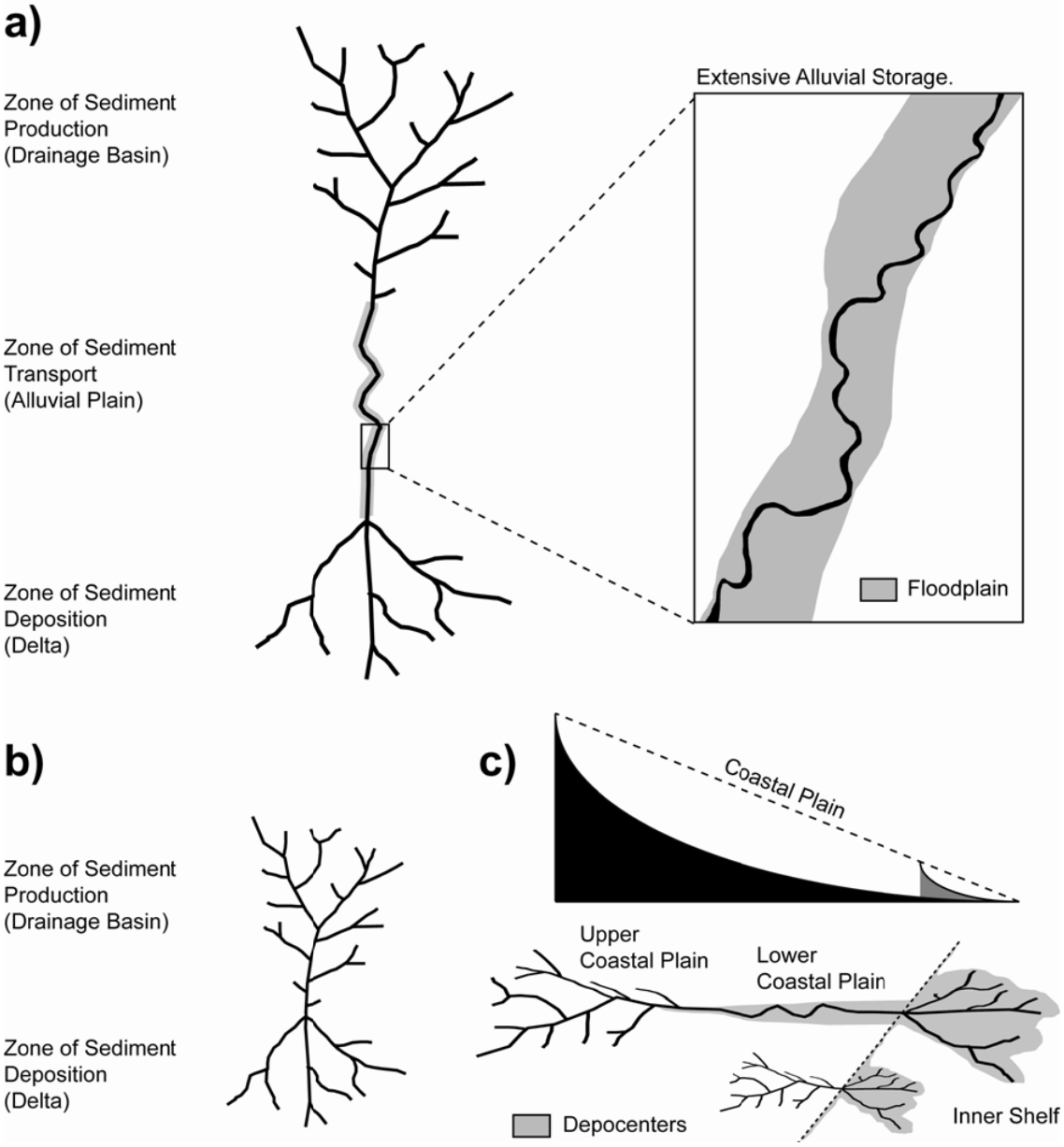

Figure 2.6 - Conceptual diagram depicting the idealilzed fluvial system in its tripartite structure (a), consisting of 1) a higher-gradient zone of sediment production, where the majority of drainage is sequestered, 2) a zone of sediment transport (i.e. alluvial plain), and 3) a zone of sediment deposition (i.e. fluvio-deltaic systems at or near base level). This model applies to large coastal plain systems that have broad floodplains and extensive alluvial storage. Part b shows a modified version of the fluvial system as it applies to systems that lack the zone of transport/storage (i.e. have low alluvial buffering potential), as is the case with high-gradient systems. Part c applies these two models to the coastal plain and suggests that systems of the inner coastal plain are morphologically similar to high-gradient systems in that they have low alluvial buffering capacity and slightly higher gradients than their larger counterparts that extend farther inland.

Chapter 3

Impact of Land-use Change and Hard Structures on the Evolution of Fringing Marsh Shorelines

3.1. Chapter Summary

Fringe marshes, which are common to estuarine shorelines, provide essential ecosystem services to coastal regions, including carbon sequestration and provision of shelter and nursery grounds for aquatic and terrestrial animals. Although the ability of a marsh to sustain itself by vertical accretion is generally limited by inorganic sediment supply, models attempting to forecast marsh response to future sea-level rise do not take land-use changes into account, despite a continuing coastal population boom. Changes in land-use type have the potential to alter sediment sources and modify or disrupt established sediment pathways in coastal settings. This study investigates how landscape modifications can alter nearshore sedimentation regimes and influence marsh-edge evolution. Marshes in this study are located in similar hydrologic and geographic settings and have comparable vegetation densities; however, their respective coastal environments are affected by different land-use modifications. One site is situated within an upper bay environment, whereas the other is located along the estuarine shoreline of a barrier island that is part of the same estuarine system. Marsh-shoreline positions and surface elevations were monitored at the sites over a two-year period using high-resolution terrestrial LIDAR. This data set was supplemented with accretion rates obtained from radioisotope analysis, precipitation records, and information on land-use changes in an effort to develop an understanding of their effect on

marsh evolution. The study region has undergone significant land-use changes, including the introduction of tree farming in the lower reaches of a tributary creek to the upper bay. Widespread deforestation in this watershed led to increased upland erosion and higher sediment-supply rates to the estuary. Radiotracers indicate a very short time lag between upland erosion and appearance of the sediments within the upper bay environments. The sudden increase in sediment load facilitated higher accretion at the upper bay site, promoting marsh colonization and expansion. Distal with respect to the riverine input, the backbarrier site received no contribution from the tree farm, but was modified by the installation of a rock sill and pier, which correlate to increased rates of backbarrier-marsh erosion. Our studied marshes, once similar in terms of nearshore-sediment composition, scarp-shoreline morphology, and shoreline trajectory, started to evolve differently over a short time-period as the result of human-induced changes to the landscape. Coastal development can significantly influence marsh shoreline behavior, which must be taken into account when developing models of coastal response to sea-level rise.

3.2. Introduction and Background

Narrow salt marshes commonly fringe a variety of depositional settings in temperate and high-latitude estuaries from bay-head deltas at their heads to barrier islands at their mouths. These fringing wetland systems are an invaluable asset to coastal and marine environments because they facilitate sedimentation by dampening wave and tidal energies (Knutson et al., 1982; Christiansen et al., 2000; Leonard and Reed, 2002; Möller and Spencer, 2002; Leonard and Croft, 2006) and provide shelter and nursery habitat for a variety of aquatic animal species (Minello et al., 1994; Peterson and Turner, 1994; Shervette and

Gelwick, 2008). Despite their provision of important ecosystem services, little is known about the impacts of land-use changes and the installation of hard structures on sedimentation and morphodynamics at the shorelines of fringing marshes (Bozek and Burdick, 2005; Currin et al. 2008). This is important to address from a coastal management perspective given predictions of future accelerated sea-level rise (Church, 2001) and increased coastal urbanization (McGranahan et al., 2007).

The sedimentary record reveals that, over geologic time (1,000s to 10,000s of years), marshes commonly transgress landward in response to sea-level rise (DeLaune, 1986; Chmura and Aharon, 1995; Gehrels et al., 1996, Gehrels, 1999; Törnqvist et al., 1998, 2002, 2004; Choi et al., 2001; Marsh and Cohen, 2007). However, geologic evidence of marsh retreat provides little insight into the short-term (years to decades) dynamics of marsh-edge evolution, because an overall transgressing marsh shoreline has a low preservation potential. Conceptual models of marsh evolution over the short term define three generalized responses to relative sea-level rise as a function of sediment accumulation (Orson et al., 1985; Allen, 2000) including: 1) Marsh-accretion rates equal the rate of sea-level rise, resulting in marsh-surface aggradation and maintenance; 2) Marsh-accretion rates are higher than rates of sea-level rise, promoting marsh expansion; and 3) Sediment supply and marsh accretion are less than the rate of coastal submergence, leading to marsh drowning.

Marsh accretion is generally regarded as a function of plant-matter accumulation and inorganic sedimentation. These two sediment components are interrelated as inorganic sedimentation promotes vegetative growth (DeLaune et al., 2003) while an increase in the density of plant biomass promotes sediment trapping through flow reduction and turbulence increase (Morris et al., 2002), which is most prominent at the marsh edge (Neumeier and

Ciavola, 2004; Neumeier, 2007). Marsh organic matter may make a substantial contribution to vertical accretion, particularly in high marshes (Turner et al. 2000, Cahoon et al. 2004). , but mineral sedimentation is often found to be the limiting control on marsh accretion and survival during sea-level rise (Hatton et al., 1983; Allen, 1995; Allen, 2000; Temmerman et al., 2004). In these cases, it is important to understand the source of nearshore sediments, because the grain size and concentration of suspended sediment in tidal waters are a direct reflection of respective sediment sources and play a key role in salt-marsh morphodynamics (Voulgaris and Meyers, 2004a). Neubauer (2008) identifies differences in the importance of mineral accumulation depending on coastal setting (tidal freshwater versus saltwater environment), which may coincide with differential plant production and proximity to upland sediment sources.

Shoreline erosion and fluvial input are considered the primary sources of inorganic sediment to fringing marshes (Allen, 2000). Marsh-scarp shorelines are attributed to erosion from tide, wave, and storm-induced currents (Phillips, 1986a, 1986b; Schwimmer, 2001; Wilson and Allison, 2008), but also to differences in the rates of deposition between the rapidly accreting vegetated marsh and the nearshore mudflat (van de Koppel et al., 2005). Although scarped marsh shorelines are evidence of erosion, retreat of the shoreline may only be temporary if sediment supply is high enough to facilitate marsh-grass colonization in the nearshore mudflats. Chauhan (2009) shows that marsh scarps may characterize a brief stage in regressive marsh settings, in which the shoreline is over all advancing bayward. Phillips (1986a and 1986b) and Schwimmer (2001) recognize that the substrates along some marsh shorelines erode more easily than the marsh sediments bound by the root-mat, particularly if the substrate is sandy. This development leads to the formation of an overhanging marsh-

scarp shoreline as wave action undermines the root-mat, ultimately leading to its structural failure (i.e. root-mat toppling; Figure 3.1). Intrinsic sediment eroded from these shorelines may be reworked in the nearshore and transported onto the marsh surface by wave and tidal currents. Despite evidence of sediment recycling, the shoreline trajectory is largely dependent upon extrinsic sediment supply (Chauhan, 2009). Changing river loads and the modification of established sediment-transport pathways to marsh systems are important considerations when investigating marsh-shoreline evolution.

The degree to which anthropogenic landscape modifications can alter nearshore-sedimentation regimes and influence marsh-shoreline erosion and surface deposition necessitates further investigation, as landscape modifications are prevalent in many coastal areas as a result of increasing development (Watzin and Gosselink, 1992). Models that attempt to forecast marsh response to future sea-level rise do not take land-use changes into account (Craft et al., 2007; Kirwan and Temmerman, 2009) despite the continuing global coastal population boom (McGranahan et al., 2007). The modification and/or disruption of sediment sources and established sediment-transfer routes throughout the coastal zone should have varying implications for sediment fluxes to estuarine systems through rivers, creeks, and man-made canals. Additionally, estuarine-shoreline modifications, such as the installation of piers and rock sills, are becoming more abundant in the coastal zone (Corbett et al., 2008). Watershed and shoreline modifications have the potential to dramatically change the evolution of fringing-marsh shorelines. This study explores the impacts of landscape modifications and installation of hard structures on the evolution of fringing-marsh shorelines by investigating two sites that are characterized by similar wave exposure and

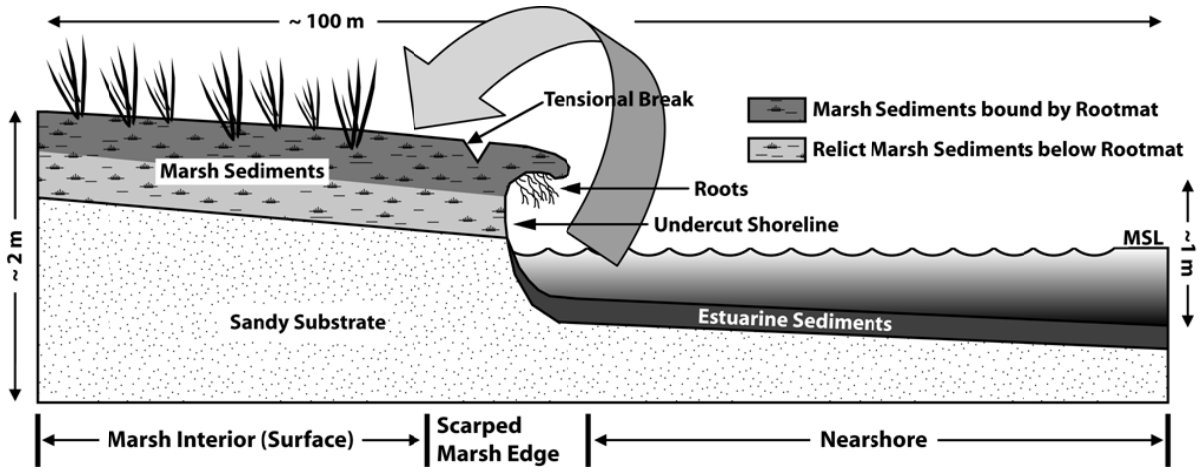

Figure 3.1. Conceptual diagram depicting the stratigraphic relationships between substrate, marsh, and nearshore sediments for a retreating fringe-marsh system. The arrow is indicative of sediment transport from the nearshore, across the scarp, and onto the marsh surface during high-water conditions. The scarp is undercut below the dense rootmat. MSL = mean sea level.

tidal regimes, but are located on opposite ends of the estuary and influenced by different anthropogenic stressors.

3.3. Project Setting

Fringe marshes in North Carolina located along the upper Newport River Estuary (NPR) and Bogue Banks at Pine Knoll Shores (PKS) were chosen for the study because they are positioned proximally and distally to river-sediment sources, respectively (Figure 3.2). The two sites also were likely impacted by the different anthropogenic modifications that are typical of these and other analogous coastal environments. The effects of site-specific anthropogenic stressors are investigated as other control parameters, which otherwise might explain differences in marsh morphology and evolution are held constant, including: substrate lithology, vegetation type and density, wave exposure, and tidal regimes. Both marshes are defined by distinct scarp shorelines (Figures 3.3 and 3.4) and their deposits contain less than 10% organic matter (Currin et al., 2008).

The NPR site represents a river-dominated marsh end-member, situated along the northern shoreline of the upper Newport River Estuary 1.3 km seaward of the river terminus (Figure 3.2). The Newport river basin experienced extensive land-use modifications which have led to an increase in sediment flux to the upper bay. Specifically, the onset of silviculture practices (comprising ~20 % of the river basin), along a major tributary to the delta, changed sediment loads abruptly in 1964, promoting a new regime of higher sedimentation throughout the Newport fluvio-deltaic system (Mattheus et al., 2009).

The PKS site is representative of a marsh that forms in back-barrier settings (Figure 3.2). This location is sediment starved because the wide and high-elevation ridge-and-swale

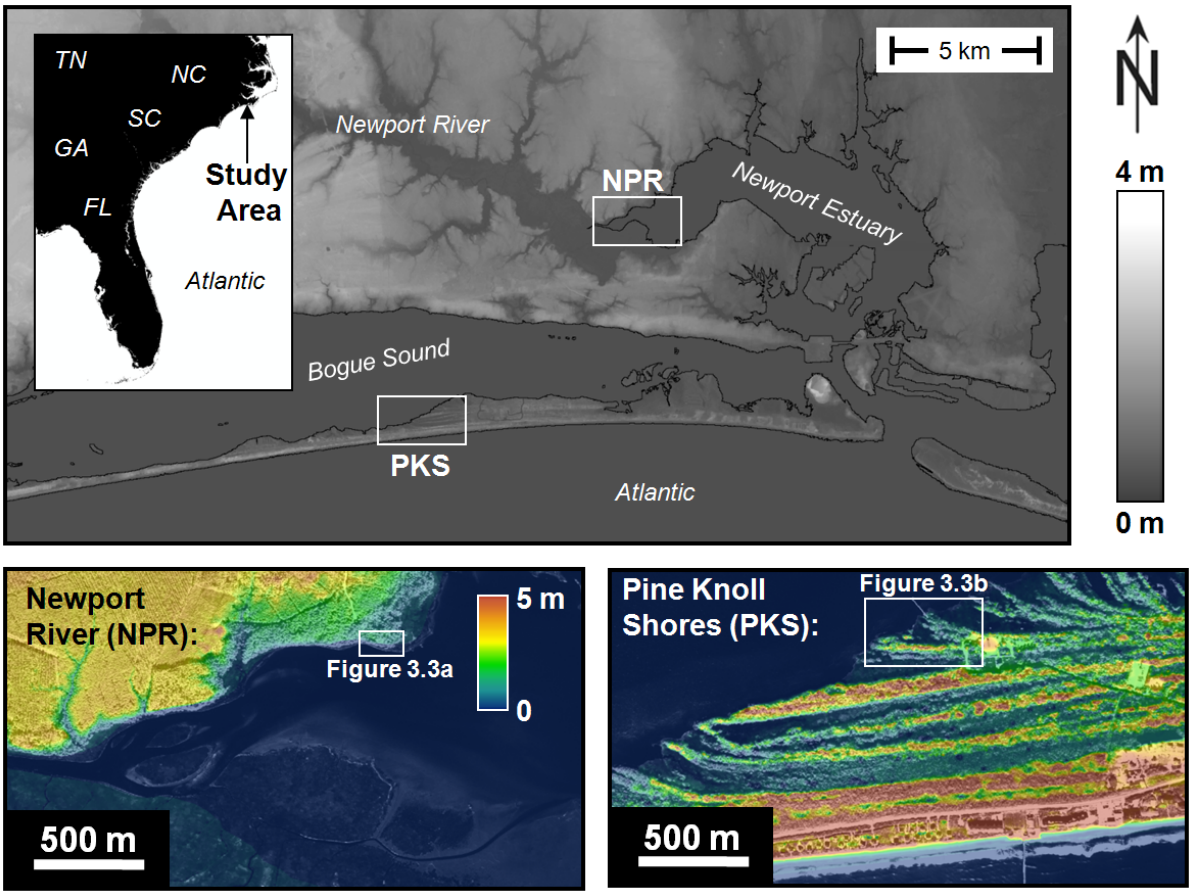

Figure 3.2. Regional topography map showing the general location of the two study sites (above; NPR = Newport River; PKS = Pine Knoll Shores). Aerial photographs reveal the depositional settings of the studied marshes (deltaic versus backbarrier) and exact study locations are outlined, corresponding to the data-distribution maps shown in Figure 3.3.

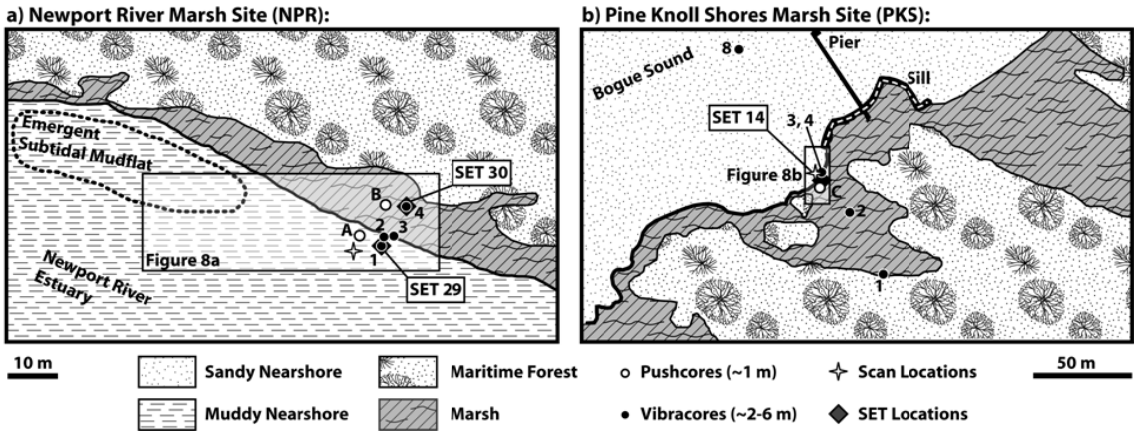

Figure 3.3. Maps of surface cover for each marsh site showing the locations of prominent landforms, structures (pier and rock sill), core-collection sites, SETs, and shoreline-scan positions. The spatial extents of the elevation models shown in Figure 3.8 are outlined and labeled.

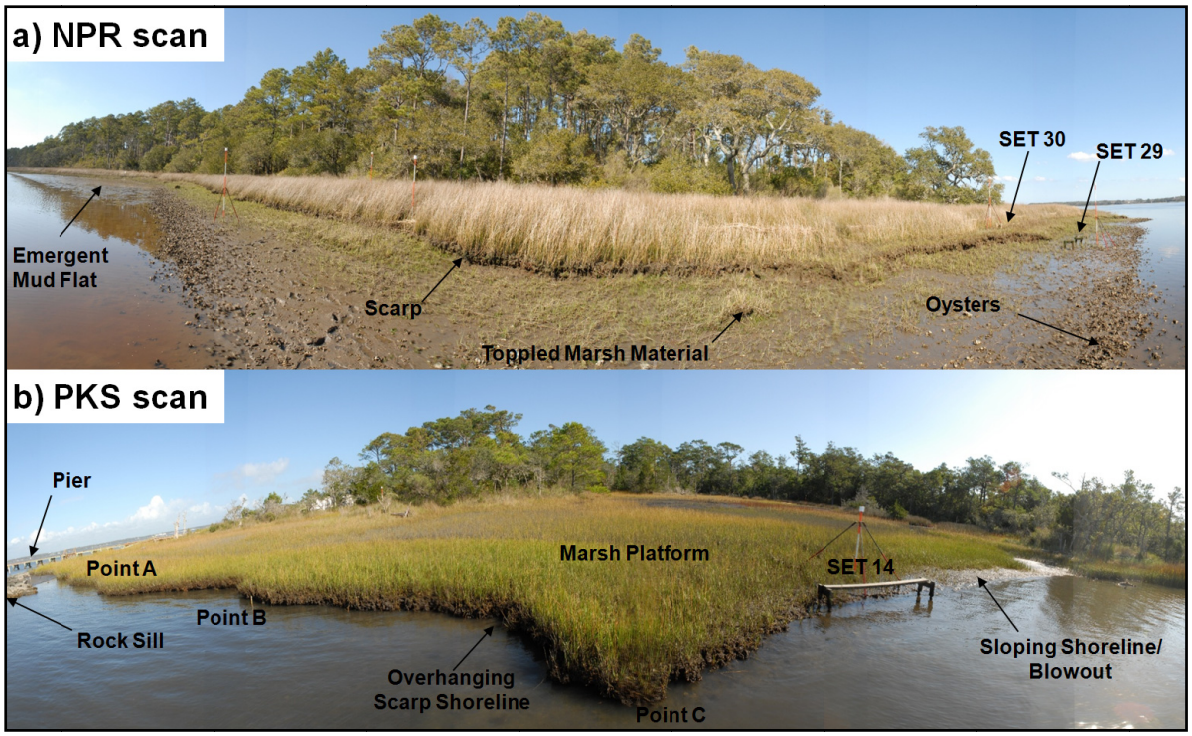

Figure 3.4. Panoramic images taken from the view of the terrestrial LIDAR scanner of the NPR (a) and PKS (b) marsh sites showing SET locations, man-made structures, and key morphologic features.

barrier morphology separating it from the open ocean (Figure 3.2) prevents overwash of beach sediments. Unlike the NPR marsh, this location is removed from direct terrestrial sediment input (i.e. a river outlet), but is not pristine because its nearshore is modified by a pier and a rock sill.

Although the NPR site is South facing and the PKS site is North facing (Figure 3.2), which implies differential influence by weather, the limited fetch across their respective estuarine bodies results in a similarly low wave exposure, as determined by the Wave Exposure Model 3.0 (WEMo 3.0) developed by Malhotra and Fonseca (2007). Additionally, both sites are characterized by similar tidal regimes (~70 cm) and are separated by less than 10 km, which suggests they were impacted by the same rate of relative sea-level rise (Horton et al., 2009), high-energy (i.e. storm) events, and changes in precipitation. Furthermore, the low and high marshes at both sites are dominated by *Spartina alterniflora* and *Juncus patens*, respectively, which are of comparable canopy densities. The scarp at the PKS site is at the marsh edge (i.e. the boundary between marsh and subtidal nearshore). At NPR the marsh scarp is at the boundary between the low and high marsh, which is ~5 m landward of the marsh edge. The transition between low and high marsh at the PKS site varies along shore and is located up to 100 m landward of the marsh scarp. Differences in marsh zonation between the sites are due to lower salinity water and higher gradient at the NPR site.

3.4. Materials and Methods

3.4.1. Lithologic Data

Vibracore transects were collected across the sites from the landward limit of the marsh platform to the nearshore (i.e. several m bayward of the marsh edge; Figure 3.3). Core

locations are listed in Table 3.1 and core descriptions are shown in Appendix A. One transect was collected at the NPR site and two were collected at PKS site to account for potential along-shoreline variability in lithology associated with the ridge-and-swale topography of the area (Figure 3.2). Transects consist of 3-5 cores ranging in length from 150 cm to 550 cm. Core compaction was measured in the field and found to be minimal (<10%). Cores were opened in the lab, photographed (before dehydration and discoloration set in), described, and sampled for grain-size analysis at an interval of 25 cm. Sediment samples were dried, weighed, and hand-sieved for their gravel-sized constituency (> 2 mm mesh size). Total organic carbon was measured using the loss on ignition method outlined in Heiri et al. (2001). Sand- and clay-sized particle percentages were measured using an 1180 CILAS laser particle-size analyzer.

3.4.2. Aerial Photographs

Aerial photographs dating back to 1958 were obtained from the North Carolina Department of Transportation, the United States Department of Agriculture, and the United States Geological Survey to reconstruct decadal-scale shoreline changes at the PKS study site (Figure 3.2). Although an aerial photography record exists for the NPR site, these data were not included in the study because photo resolution is too low. Photograph characteristics vary between the years, the details of which are shown in Table 3.2. Photos were imported into ArcGIS 9.3 for analysis and georectified using pronounced and easily recognizable fixed objects as ground-controls points. Shoreline erosion rates are calculated from the photographs dating to 1958, 1974, 1995, and 2006, as these photos provided suitable timelines for investigating shoreline movements over a 50-year period and were of high-

Site	Core #	Latitude	Longitude	Date	Environment	Core Length (m)
NPR	1	34.759400	76.760460	5/22/2007	nearshore	3.46
NPR	2	34.759420	76.760460	5/22/2007	low marsh	2.67
NPR	3	34.759420	76.760430	5/22/2007	marsh scarp	2.65
NPR	4	34.759480	76.760400	5/22/2007	high marsh	2.17
PKS	1	34.700017	-76.831700	6/5/2006	high marsh	3.31
PKS	2	34.700433	-76.831983	6/5/2006	marsh	2.15
PKS	3	34.700667	-76.831717	6/5/2006	low marsh	2.99
PKS	4	34.700700	-76.832217	6/5/2006	nearshore	3.6
PKS	5	34.701533	-76.832933	6/29/2006	nearshore	3.05

Table 3.1. Information on collected vibracores, including environment, coring date, and core length. Corresponding core descriptions are shown in Appendix A.

Vintage	Source	Resolution (m)	Modifications
11/11/58	USDA	1.4	-
01/21/64	USDA	1.4	-
01/20/68	NCDOT	3.3	-
02/21/73	NCDOT	3.3	-
12/01/74	NCDOT	0.8	-
11/02/80	USDA	2.8	Pier 1
04/24/82	USDA	4.2	Pier 1
03/29/83	NCDOT	4.2	Pier 1
10/27/88	USDA	2.8	Pier 1
03/08/93	USGS	3.0	Pier 1
04/19/94	NCDOT	2.5	Pier 1
11/26/95	NCDOT	0.7	Pier 2
01/25/98	USGS	1.0	Pier 2
06/11/06	NCDOT	0.7	Pier 2 + Sill

Table 3.2. Additional information on the aerial photographs used for evaluating shoreline changes at Pine Knoll Shores and the documented anthropogenic land-use modifications derived. Sources are abbreviated as follows: USDA = United States Department of Agriculture, NCDOT = North Carolina Department of Transportation, and USGS = United States Geological Survey.

enough resolution (<1.0 m for the 1974, 1995, and 2006 sets; Table 3.2) to enable accurate mapping. Additional lower-resolution images of the area surrounding PKS, while unsuitable for spatial analysis, help confirm the timing of anthropogenic landscape modifications (Table 3.2). Volumetric changes are calculated based on the shoreline erosion rates and assume constant ravinement depth at the marsh edge of 1 m, as determined from in-field measurements and cores.

3.4.3. Rates of Sedimentation and Shoreline Retreat

A common problem to marsh research is that variances in accretion and/or erosion are difficult to resolve on a marsh-wide scale. The use of Surface Elevation Tables (SETs; Cahoon et al., 2002a, 2002b) is a frequently used method for quantifying marsh accretion. Data obtained from SETs provide information on surface accretion at specific locations; however, a meaningful representation of the marsh as a whole is not guaranteed since marsh surfaces exhibit microtopographic heterogeneities (Wood and Hine, 2007). Accretion studies using SETs, therefore, commonly show strong temporal and spatial discrepancies (Flessa et al., 1977; Bricker-Urso et al., 1989; Bryant and Chabreck, 1998; Bartholdy et al., 2004).

In this study, short-term changes to the marsh shoreline (in elevation and position) were surveyed over a two-year period using a RTK-GPS and a Riegl LMS-Z210ii terrestrial laser scanner (i.e. terrestrial LIDAR). This method resolves changes of only several mm over a marsh-wide scale. The NPR and PKS marshes (Figure 3.2) were imaged when vegetation cover was lowest in March of 2007 and 2008 (Figure 3.4) to maximize the number of ground returns. Specific scan locations were strategically chosen at each marsh site to maximize the coverage area (with respect to core locations) and minimize data shadows

(Figure 3.3). Scan locations (i.e. where the laser scanner is set up) were re-occupied each survey to ensure overlapping spatial coverage between time steps. Data points, with a ±1 cm spatial error, were imported into Microstation® V8 for processing using the TerraScan (Version 007.015) and TerraModeler (Version 007.007) applications. Ground points (200,000-300,000 points) were isolated from vegetation and other non-ground points and used to create digital elevation models (DEM) of the marsh scarp. These models, covering ~40 m of the NPR and ~30 m of the PKS shorelines (~10 m² and ~50 m² in extent for NPR and PKS, respectively; Figure 3.3), were exported using a 10-cm grid spacing and imported into the contouring and mapping software package Surfer © 8.05 for interpretation and display. The DEM of more recent scans were subtracted from older ones to yield net-accretion/erosion maps for each of the sites. Since parts of the PKS marsh shoreline are characterized by an overhanging scarp (Figure 3.4), the underside of the shoreline (i.e. cliff face) was classified and exported as a separate surface map with a grid spacing of 1.0 cm. This was necessary because an overhang produces two elevations for a given x, y coordinate, i.e. the surface and the underlying overhang. Maps of the marsh surface only include ground points visible from above. Maps of the marsh scarp (the underside of the shoreline) were used to evaluate the amount of scouring below the root-mat.

As part of a longer study, we also installed SETs at the lower edge of *Spartina alterniflora* distribution at the NPR and PKS study sites (Figure 3.3). SETs were established in November of 2004 at PKS and June of 2007 at NPR and sampled approximately every 6 months through March of 2008. At each sampling time, 36 pin positions were measured from each SET to determine change in marsh surface elevation.

In addition to information on marsh-elevation changes obtained from laser scans and SETs, data on long-term marsh-surface sedimentation (over decades) was derived from radiometric analyses of pushcores. Cores, which were collected adjacent to SET locations (Figure 3.3), were subsampled at 1 cm-intervals for ^{210}Pb-analysis to derive sedimentation rates at respective high- and low-marsh locations. The ^{210}Pb method assumes constant atmospheric flux of ^{210}Pb into sediments. Log [excess ^{210}Pb activity] is plotted against core depth for analyzed samples to enable a back-calculation of sedimentation rates from the slopes of corresponding regression lines. Cores were also analyzed for ^{137}Cs to identify the peak fallout from nuclear weapons testing in 1963 and 1964. The spike is used in conjunction with the ^{210}Pb data to provide temporal control when calculating sedimentation rates.

3.5. Results and Interpretations

3.5.1. Substrate Analysis and Marsh Stratigraphy

Core analyses (depicted in Appendix A) show that the substrates at the NPR and PKS marsh sites have similar, lithologies, composed of unconsolidated, fine- and medium-grained sand (Figure 3.5). The substrate sand at PKS is finely laminated and shows signs of cross bedding while at NPR it is massive (i.e. lacks bedding) and contains clay rip-up clasts. These lithologies are interpreted as Holocene beach-ridge and pre-Holocene alluvial deposits, respectively, which are the same depositional environments exposed at the surface of each site landward of the marsh platforms. Marsh deposits are also comparable at the two sites in terms of their low total organic carbon content (5-6%), but marsh sediment at NPR contains a higher clay and silt component and coarser sand than PKS. Nearshore sediment at NPR is

massive and is distinguished from the substrate by its higher clay and silt content (Figure 3.5). The nearshore at PKS is sandy and distinguished from the substrate by bioturbation and a slightly higher percentage of silt (Figure 3.5). The contact between the nearshore and substrate is gradational over an interval of ~10-20 cm at both sites.

The amount of material excavated from marsh shorelines through time is determined by the depth of bay ravinement and the rate of shoreline retreat. Ravinement depth, measured as the vertical distance between the marsh surface at the scarp shoreline and the contact between substrate and nearshore sediment in the most proximal nearshore core (adjacent to the marsh scarp), is approximately 1 m for both marsh sites (Figure 3.6). Ravinement depth is strongly controlled by the wave regime, which is similar between the two sites (Malhotra and Fonseca, 2007). Wilson and Allison (2008) also noticed a high degree of consistency in the ravinement depth of retreating marshes in Louisiana, suggesting equilibration of the marsh-edge morphology to wave power rather than intrinsic sedimentologic variables (grain size, cohesion, etc.). Although the PKS and NPR marshes share comparable substrate lithologies (generally >75% fine grained sand), a similar degree of wave exposure, and a similar ravinement profile (Figure 3.6), they are characterized by different stratigraphic relationships at the edge. Marsh sediment at PKS always overlies the substrate, while at NPR this is only true landward of the scarp. Seaward of the NPR scarp, marsh overlies nearshore sediment, suggesting shoreline regression. A sedimentologic study of the Newport River Estuary undertaken in the late 1950s reveals that the surface sediments around the study area were sandy at this time (Johnson, 1959). Nearshore sediments found immediately overlying the substrate in cores NPR-1 and NPR-2 reflect the sandy substrate composition and contain little silt and clay. The nearshore environment at the NPR

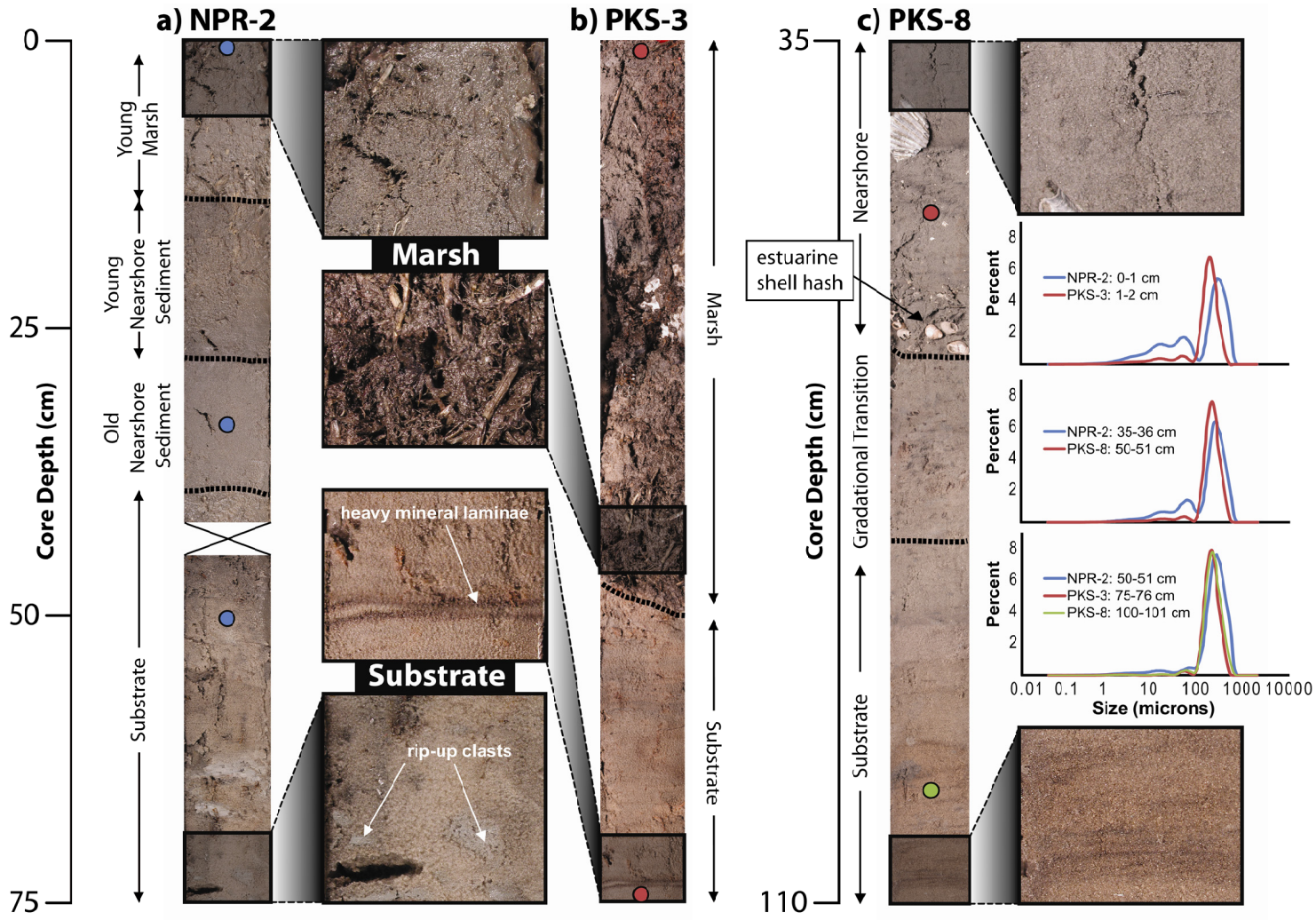

Figure 3.5. Core photographs showing the sedimentological differences between substrate, nearshore, and marsh deposits at the low marsh-nearshore transition for the NPR (a) and PKS (b and c) sites, respectively (Figure 3.3). Grain-size plots to the right of the core photos showing a fining-upward trend at the NPR site and little variability at the PKS site (blue = NPR; red and green = PKS).

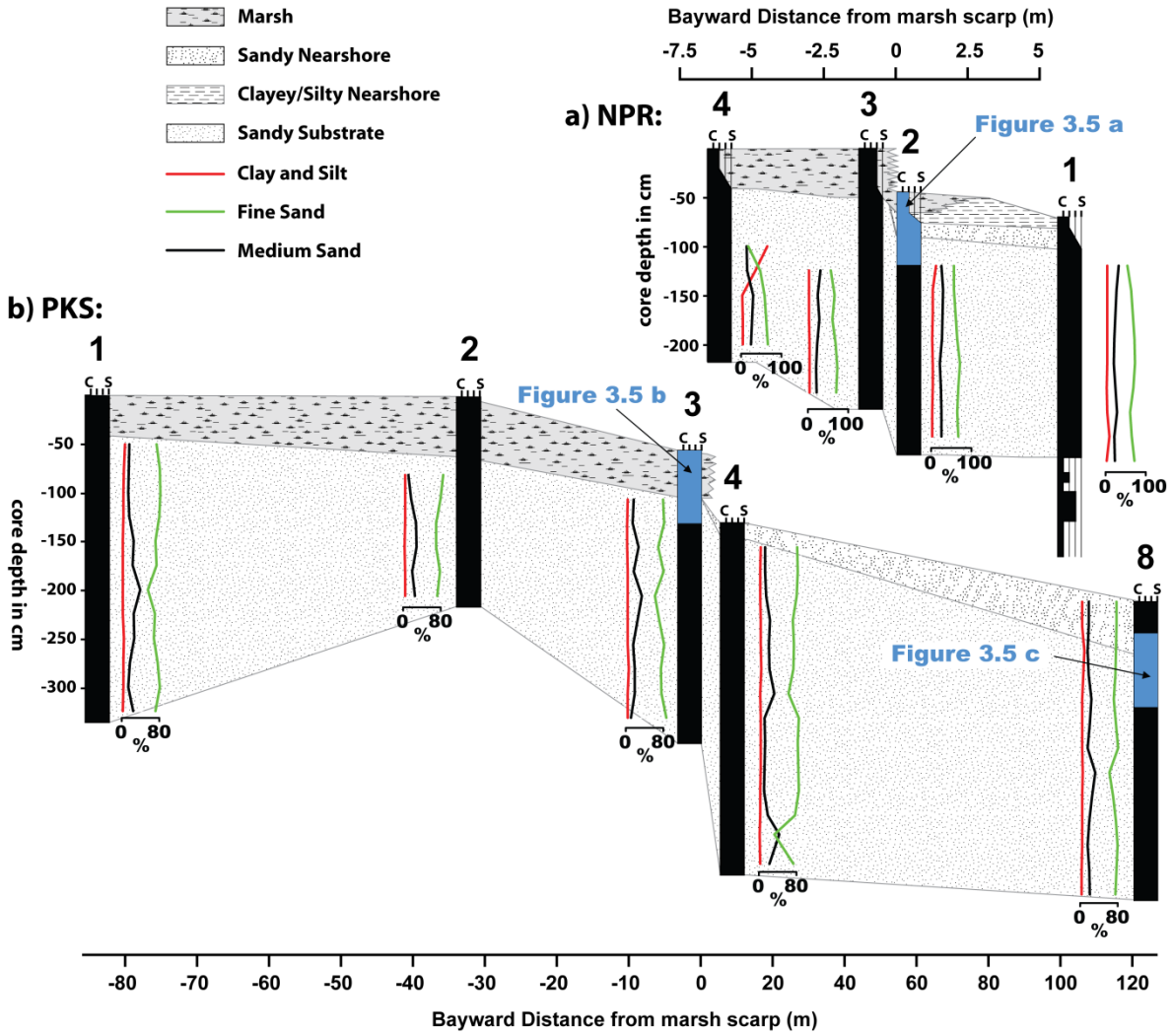

Figure 3.6. Stratigraphic cross sections along the dip-oriented core transects from high marsh to nearshore for the NPR (a) and PKS (b) sites showing grain-size information (color coded) and lithologic interpretations (c = clay, s = sand). Down-core variations in the percent of clay and silt (red) and sand (black and green) are shown adjacent to core logs. Core locations are shown in Figure 3.3. Core descriptions are shown in Appendix A. Depth intervals over which core photos are shown in Figure 3.5 are highlighted in blue and labeled.

resembled that at PKS, with the nearshore being sourced exclusively by shoreline erosion, mirroring its composition (Figure 3.5). Since 1964, an increase in the flux of fine-grained sediment to the nearshore changed its lithology (Mattheus et al., 2009) and facilitated marsh colonization and extension bayward of the shoreline scarp (today's boundary between *Spartina* and *Juncus* marsh), covering the older nearshore deposits. The marsh edge at NPR is situated bayward of the prominent marsh scarp; at PKS, the scarp generally represents the shoreline (Figures 3.4 and 3.6).

3.5.2. Decadal Shoreline Changes

The PKS marsh was impacted by several modifications, including the construction of 2 piers and a rock sill. The first pier, constructed in 1976, extended into the bay by ~50 m in a west-northwesterly direction (as seen in photos from 1980-1994; Table 3.2; Figure 3.7). This structure was replaced between 1994 and 1995 by a longer pier (~75 m) that extended into the bay in a north-northwesterly direction (Figure 3.7). The last major change to the area occurred in 2001/2002, when a rock sill was constructed along the northeastern marsh shoreline where a beach ridge terminates in Bogue Sound forming a point, as seen in the aerial photo of 2006 (Figure 3.7; Table 3.2).

The shoreline at the point (beach-ridge terminus) was eroding rapidly prior to installation of the rock sill, as indicated by photos from 1958, 1974, and 1995 (Figure 3.7). These images were used to measure shoreline retreat by up to 13 m from 1958 to 1974 (~23.25 m^3/yr) and up to 17 m from 1974 to 1995 (~25.90 m^3/yr). Contrary to this trend, the shoreline between the two beach ridges (i.e. along the embayment) was eroding slowly between 1958 and 1974, measured to be ~4 m (~3.90 m^3/yr). This rate of marsh loss in the

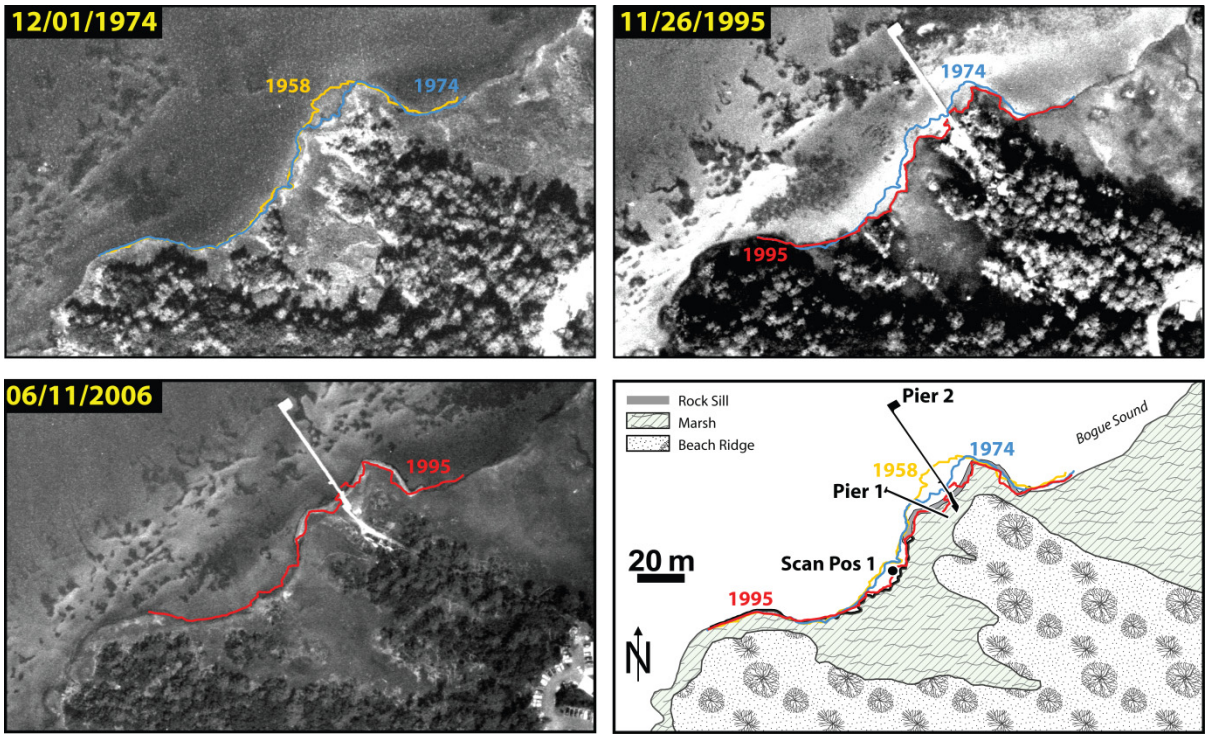

Figure 3.7. Aerial photographs and composite sketch showing the evolution of the PKS shoreline since 1958. Figure 3.3b shows the location of this part of the study area and additional information on the photographs is provided in Table 3.2.

embayment is significantly less than the subsequent periods of 1974-1995 and 1995-2006, which are calculated at ~11.6 m^3/yr and ~14.7 m^3/yr, respectively. Aerial photographs suggest that the installation of the pier accelerated erosion in the embayment and installation of the sill in 2001/2002 further concentrated erosion in the northern part of the embayment (i.e. the area flanking the rock sill). Today, the rapidly eroding stretch of shoreline in the embayment adjacent to the sill is characterized by a scarp overhang. A scarped shoreline makes it difficult to determining the exact rates of retreat and material excavation from the aerial photographs because aerial photographs only image the marsh surface and cannot account for undercutting (Schwimmer, 2001). Nonetheless, the aerial photographs demonstrate that the upper scarp edge in this location has transgressed by a maximum rate of 0.41 m/yr since 1995, well exceeding a pre-sill rate of ~0.24 m/yr (1974-1995) and a pre-pier rate of ~0.25 m/yr (1958-1974). Although construction of the sill helped protect the point, the area to its south (within the embayment) experienced higher rates of shoreline retreat.

3.5.3. Year-to-Year Shoreline Changes

The subtraction map for the PKS embayment, created from the March 2009 and March 2008 DEMs, shows an overall net loss in elevation (Figure 3.8a). This loss is particularly noticeable in the southern portion of the scanned area, where the prominent scarp edge transitions gradually into a ramp-style shoreline, which gently slopes into the sub-tidal nearshore (Figure 3.8a). This gently-sloping shoreline was an average of ~2.5 cm lower in March of 2009 than one year before. Higher values of elevation loss are resolved in the model, but are generally confined to the marsh edge and are the result of the scarp moving landward. The position of the PKS shoreline, defined here as the intersection of 0.0 m

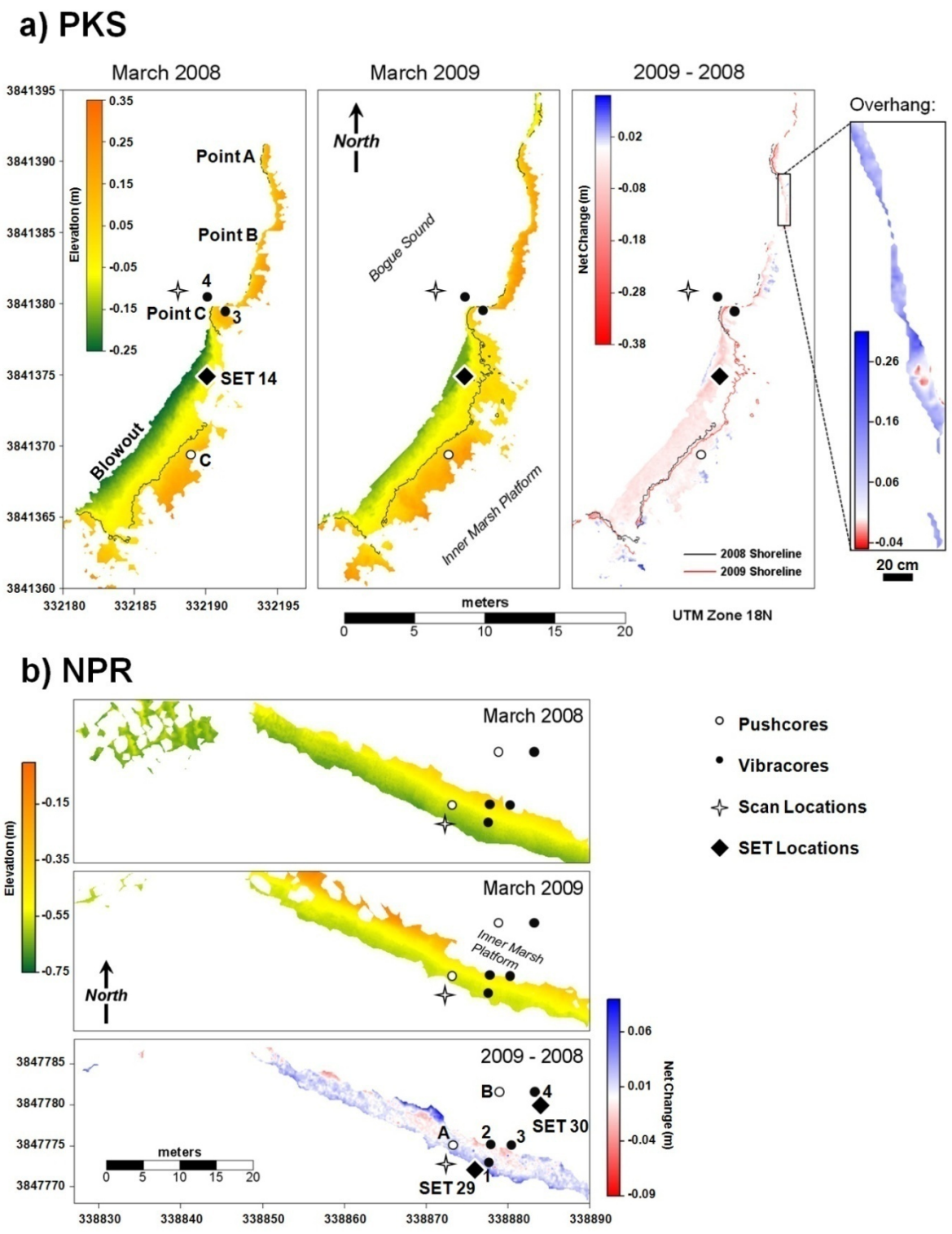

Figure 3.8. DEMs at the NPR (a) and PKS (b) marsh sites for March 2008 and March 2009 along with corresponding subtraction models (2009-2008) showing net-elevation change. Positive values in the overhang subtraction map represent excavation and negative value represents slumping. Maps also depict key morphologic features and the data-collection locations shown in Figures 3.3 and 3.4.

(NAVD 88) in elevation with the modeled marsh surface, is shown to have retreated during this year by up to ~50 cm along the gradually-sloping shoreline. Along the scarp shoreline, evidence of retreat is also recognized by negative elevation changes of ~40 cm in the subtraction model, approximating the height of the (scarp) shoreline (Figure 3.6). Models of the underlying scarp surface show a positive change in elevation from 2008 to 2009, indicating heavy scouring, which reaffirms that marsh materials from underneath the root mat are being excavated (Figure 3.8a). SET 14 (Figure 3.3) recorded a loss in elevation of the lower PKS marsh platform of ~0.56 cm/yr between 2004 and 2008. The entire marsh surface below and immediately around SET 14, which is situated at the transition from scarp shoreline to gently sloping shoreline, was not imaged with the laser scanner because of the dense canopy of *Spartina alterniflora* (Figure 3.4); however, surface elevations around the general area decreased between 0.2 and 0.7 cm/yr. The patchy erosion pattern noticed throughout the marsh from the DEMs attests to the problems associated with making marsh-wide generalizations regarding surface-elevation change; although the average of measured elevation values from the LIDAR data for this general area yields a decrease of ~0.45 cm/yr, which corroborates the SET value.

The NPR marsh scarp was not mapped because the laser could not penetrate the dense *Juncus* canopy; therefore, the DEMs only encompass the low marsh up to the base of the scarp. This low marsh platform is shown to have been overall depositional between March of 2008 and March of 2009 (Figure 3.8b). The coverage area close to the transition to the nearshore, in particular, experienced a uniformly positive net change in elevation of around 2 cm. Several localized pockets of net erosion are measured just seaward of the scarp. Field observations show that these areas are marsh blocks that toppled to the low marsh from the

scarp prior to the 2008 scan and have been redistributed across the low marsh (Figure 3.4). Although LIDAR surveys were not able to image either SET locations at NPR given dense vegetation at SET 30 and inundation of SET 29, erosional and depositional trends from the SETs corroborate the LIDAR data from adjacent areas. SET 30, which is situated on the NPR marsh platform, landward of the scarp (Figure 3.4), recorded a negative change in elevation of ~0.2 cm over the one-year measuring period (March 2008 – March 2009), which is synchronized with the LIDAR surveys. This suggests erosion and vegetation collapse at the scarp edge, where LIDAR measurements also show a negative change in elevation over this period. SET 29, located in the adjacent nearshore (Figures 3.3 and 3.4), measured a positive change in elevation of ~2.8 cm, strengthening the argument that this environment is highly depositional. The amount of elevation change measured using terrestrial LIDAR in surrounding areas is similar (~2.1 cm).

3.5.4. Radioisotope Analyses

Isotope data from the NPR site resolve two distinct sediment regimes over the last 50 years. The ^{210}Pb-excess/core-depth plot in Figure 3.9a shows that the upper 10 cm of Core NPR-A, collected from the proximal nearshore (Figure 3.3), is characterized by a constant sedimentation rate of ~ 0.9 mm/yr (Figure 3.9a). This rate is based on the half life of ^{210} Pb (~22 yrs) and the loss of excess ^{210}Pb with depth. Measurements of excess ^{210}Pb below 10 cm core depth do not yield a net slope, indicating that the prevailing regime may have been erosional and/or excessive biological reworking occurred. This pronounced change in ^{210}Pb–activity coincides with an up-core increase in clay content of the nearshore sediments at -10 cm (Figure 3.6). Measurements of excess ^{210}Pb in core NPR-B also suggest an overall

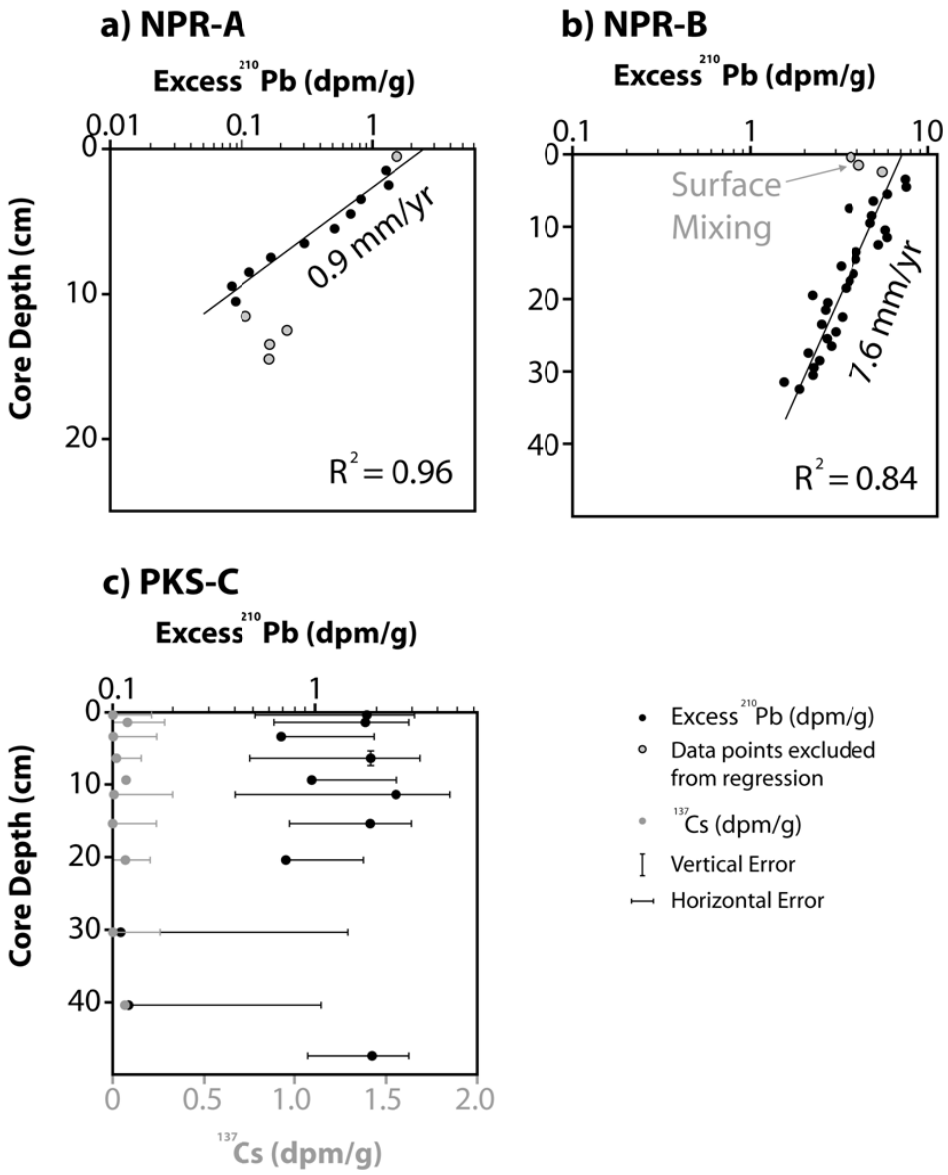

Figure 3.9. Graphs showing ^{210}Pb- profiles from gamma counting for cores NPR-A, NPR-B and PKS-C collected from the marsh-nearshore transition at the Newport River and Pine Knoll Shores marsh sites, respectively. Cores were sampled at a 1.0 cm interval. Core PKS-C was also analyzed for ^{137}Cs-activity, which is plotted along with corresponding ^{210}Pb-activities on a secondary x-axis in the same plot.

constant net sedimentation rate of 0.76 cm/yr with a strong R^2-value of 0.843 (Figure 3.9b). This core is characterized by high excess ^{210}Pb in the upper-most sediments, which is an order of magnitude higher than that in core NPR-A. Distinct wiggles in the excess ^{210}Pb/depth profile may indicate very small (cm-scale on the depth axis) variations in sediment accretion as a result of event-driven (storms and/or wind) deposition.

Short-lived radioisotope analysis of the core from the PKS site is indicative of extremely low net sedimentation over the last 100 years and suggests that little new material is entering the system. PKS-C (Figure 3.3) is depleted in ^{210}Pb and data points yield no net slope, suggesting heavy mixing of old sediments. Evidence of heavy mixing is also presented by the ^{137}Cs-record within this core, which is heavily diluted and displays no clear peak (Figure 3.9c).

3.6. Discussion of Extrinsic versus Intrinsic Sediment Supply

A strong point of contrast between the NPR and PKS sites is the compositions of the nearshore surface sediment. At PKS, nearshore-surface sediment lithology is similar to the substrate and the inorganic constituency of marsh deposits, while the young nearshore and marsh deposits at NPR, unlike the substrate, contain abundant silt and clay (Figure 3.5). Sediment analyses of core data from the two sites show both substrates are characterized by comparable lithologies, comprised exclusively of fine-grained sand (Figures 3.5 and 3.6). Whereas back-barrier shoreline erosion seems to represent the only sediment source to the PKS marsh, as suggested by the similar lithology of nearshore, substrate, and marsh sediments, the NPR site recently received finer-grained sediments from a previously unavailable source. High accretion rates within and around the NPR site (Figures 3.8 and

3.9) are directly attributed to an influx of fine, suspended sediment from the Newport River basin, which shifted the bay-margin depositional regime from one similar to that of PKS to a muddier environment characterized by higher sediment supply. Silviculture practices, which started in the Newport River watershed in 1964 and have endured to today (Mattheus et al., 2009), have introduced a new sediment source to the fringe marshes along the upper bay, promoting higher sedimentation rates through rapid marsh colonization in the proximal nearshore. This process is presented by Fagherazzi et al. (2006), who demonstrate that elevations between tidal flats and salt marshes are inherently unstable and that the transition from nearshore flat to salt marsh is abrupt once it becomes emergent and colonizing vegetation can trap more incoming sediment. The increase in sediment flux to the NPR site is visibly starting to bury the former marsh edge (i.e. scarp shoreline separating *Spartina* and *Juncus* marsh), which is also apparent in the DEMs. What once was likely a shoreline in retreat, as suggested by the presence of a very distinct marsh scarp and sandy nearshore (as at PKS; Figures 3.4 and 3.6), has been transformed into a marsh that is extending bayward by rapid accretion at the nearshore-marsh transition (Figures 3.4, 3.6, and 3.8b).

A similar mechanism of marsh expansion is recognized by Chauhan (2009), who describes initial marsh-scarp formation as being directly linked to differences in accretion rate between recently vegetated surfaces (high accretion rate) and fronting unvegetated tidal flats (low accretion rate), not a morphology exclusive to transgressing marsh shorelines. At NPR, high sedimentation rates in the nearshore led to marsh formation seaward of the marsh shoreline (i.e. the pronounced scarp that separates *Spartina* and *Juncus* marshes). Assuming this high accumulation rate persists in this new low marsh, it is possible that it will accrete to the level of the current marsh scarp, above which deposition may happen more sporadically,

as recorded in the ^{210}Pb-record from core NPR-B (Figure 3.9b) from the inner marsh platform (Figure 3.3). As accretion continues on the lower marsh, a threshold in slope between it and the adjacent nearshore may be overstepped, at which time a new scarp will develop that will help to further distinguish these two sub-environments. The concept of autocyclic marsh growth, as presented by Chauhan (2009), highlights the importance of marsh- and nearshore-surface accretion in facilitating intrinsic geomorphic processes at the marsh shoreline. In the Newport example, landscape changes have induced this high-sediment supply scenario, causing expansion of a marsh that had previously shown no signs of regression.

Unlike the present NPR marsh, our data from PKS indicate that this back-barrier marsh is sediment-starved. Shoreline erosion seems to be a more important process in providing sediment to the marsh platform and evidence suggests that newly installed hard structures influenced erosion patterns on a marsh-wide scale. The embayed marsh shoreline at PKS lost substantially more material after construction of two piers and a rock sill on the adjacent headland (Figure 3.7; Table 3.2). The 1960s and 1990s were exceptionally stormy with 4 major hurricanes affecting the area between 1962 and 1968 and 5 between 1996 and 2005. Although the increased storm activity in the late 1990s and early 2000s coincides with higher rates of shoreline erosion in the embayment, the relatively low rate of erosion in the embayment during the very stormy 1960s, and constant erosion rates observed at the point through stormy and quiescent times, suggests that storm climate had little to do with the variations in erosion rates. Most of the pre-1974 erosion occurred at the headland (Figure 3.7), presumably because it is exposed to more incoming wave and current energies than the embayment. This headland was subsequently modified by the installation of several piers

(Table 3.2), which coincided with increased erosion along the adjacent embayment (Figure 3.7). The construction of a rock sill in the early 1990s protected the pier by stabilizing the headland from which it extends from (Figure 3.7); however, since its construction, marsh-shoreline erosion concentrated on the area immediately adjacent to it (Figure 3.7). This stretch of marsh shoreline adjacent to the rock sill is also characterized by significant undercutting, as observed in the field and resolved in the DEMs (Figure 3.8). The installation of hard structures at this back-barrier site shifted the locations of shoreline erosional "hotspots", yet the marsh shoreline as a whole has historically and presumably always will be sediment starved and in retreat.

3.7. Conclusions

The NPR and PKS marshes, once very similar in terms of nearshore sediment composition, marsh substrate, shoreline morphology, and likely shoreline trajectory, are now evolving dissimilarly in response to different human influences, which are typical to their respective locations. The history of the NPR site shows that upland land-use changes can alter sediment yields of small coastal rivers, providing an increase in flux of inorganic materials to marshes in the upper estuary, which promotes accretion and expansion. The introduction of finer-grained sediment from upstream promotes additional growth of marsh grasses, because clayey/silty sediments are more nutrient-rich than sandy sediments, (Day, 1989). The threshold-driven formation of new marsh in recently emergent nearshore tidal flats increases sedimentation by more effective trapping. Agricultural land-use changes and urbanization are generally associated with increased suspended-sediment loads, creating the potential for nutrient-rich sediment transport to upper estuarine environments. Marshes such

as the one studied at NPR will presumably have an increased chance of maintaining a favorable elevation with respect to future sea-level rise as a result of the land-used change.

Unlike marshes located in the upper estuary, back-barrier marshes, such as the one at PKS, are disconnected from terrestrial (i.e. fluvial) sediment sources and therefore limited with respect to fine-grained sediment and the corresponding additional nutrients. The homogeneity in sediment composition between substrate, nearshore, and marsh samples from the PKS site (Figure 3.5) and the ^{210}Pb-record are indicative of heavy sediment reworking and suggest that little extrinsic sediment is entering the system. Receiving inorganic sediment only from the immediate nearshore, these marsh systems are less likely to keep up with accelerated sea-level rise. Even if a marsh platform can keep up with the level of the sea through accumulation of plant matter, sedimentation in the nearshore from an extrinsic source is required to fill accommodation space seaward of the scarp and promote marsh-edge regression. The marsh edge at PKS had a long history of retreat, which was made worse by the installment of sills and other hard structures that preserve and promote marsh accretion locally (behind the hard structure), but increase erosion to their sides due to disruption of the along-shore sediment transport and/or wave refraction. The construction of several piers and a rock sill at PKS seem to have redirected nearshore energy regimes, shifting hotspots of erosion. Understanding marsh response to different human influences is important for addressing marsh sustainability along rapidly urbanizing coastlines that are likely to experience increased rates of relative sea-level rise.

Appendix A – Core Descriptions

Core descriptions depicted in this appendix are constructed from notes and descriptions made immediately after opening and photographing the cores. Information on grain size should is an initial, raw assessment since these observations were based on the simple study of sediments using a hand-lens during the sediment-description process. The legend for the core descriptions is shown below.

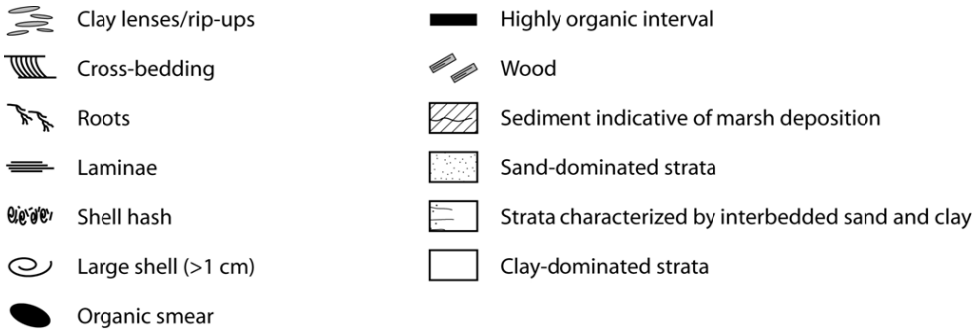

NPJ-07-1

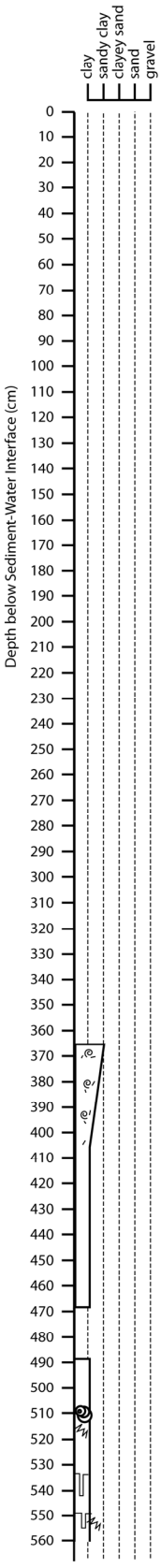

366-406 cm:
greenish black (5G 2/1) silty clay; few small, isolated shell fragments;

406-477 cm:
greenish black (5G 2/1) homogenous, soft clay;

488-570 cm:
greenish black (5G 2/1) clay to silty clay; downcore increase in silt content;

508-509 cm:
gastropod shell; woody material;

515 cm:
woody material;

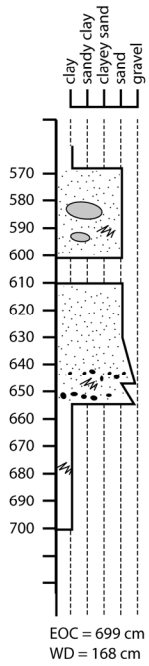

515-516 cm:
woody material;

528 cm:
shell fragment (~1 cm length);

551 cm:
woody material;

528-558 cm:
series of sand-filled burrows (vertical);

538-568 cm:
occurence of small specks of woody material;

570 cm:
sharp contact;

571-599 cm:
light olive gray (5Y 6/1) fine-grained sand;

580 cm:
woody smear;

583 cm:
greenish black (5G 2/1) clay lense;

591 cm:
woody material;

594-596 cm:
greenish black (5G 2/1) clay lense;

610-653 cm:
light olive gray (5Y 6/1) fine grained sand transitioning gradually downcore to light olive gray (5Y 6/1) coarse-grained sand;

637-640 cm:
discoloration to brownish gray (5YR 4/1);

646 cm:
woody material;

653 cm:
sharp lithologic contact;

653-699 cm:
dark greenish gray (5GY 4/1) to greenish gray (5GY 6/1) slightly mottled, very stiff clay;

660 c,:
woody material;

678 cm:
woody material;

WOJ-07-1

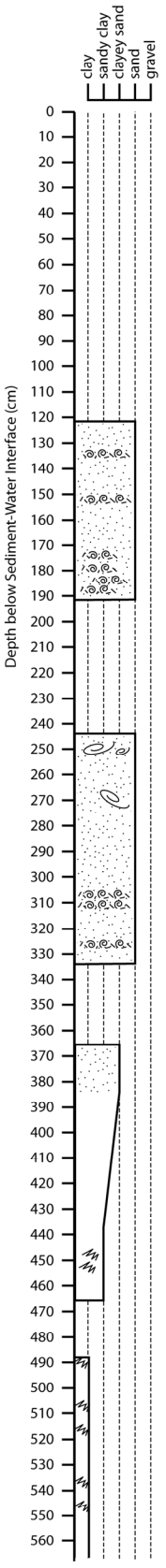

122-192 cm:
olive gray (5Y 4/1) medium-grained sand and shell hash;

132-137 cm:
increase in shell content;

143 cm:
large shell fragment (~1 cm);

149-158 cm:
large shell fragments (~ 1 cm); concentrated layer of shell debris;

172-192 cm:
concentrated layer of shell debris;

244-294 cm:
olive gray (5Y 4/1) clayey sand intermixed with sand and shell hash;

244-259 cm:
increase in shell content; inclusion of oyster valves;

266-269 cm:
oyster valve;

294 cm-334 cm:
olive gray (5Y 4/1) sand and shell hash;

304-314 cm:
increase in shell content; large oyster-shell fragments;

324-326 cm:
increase in shell content; large oyster-shell fragments;

366-416 cm:
olive gray (5Y 4/1) clayey sand with few scattered shell fragments;

416-466 cm:
olive gray (5Y 4/1) silty-sandy clay;

446 cm:
woody debris;

453-454 cm:
woody debris;

456 cm:
shell fragment;

466 cm:
shell fragment;

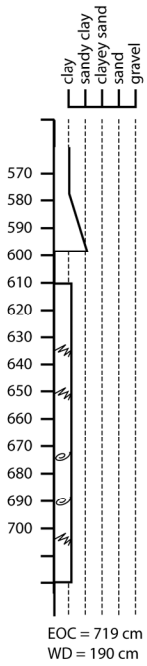

488-598 cm:
greenish black (5G 2/1) clay containing woody material throughout;

490 cm:
wood fragment;

510 cm:
woody fragment;

518 cm:
wood fragment;

537 cm:
woody material;

544-545 cm:
woody material;

578-598 cm:
downcore increase in mean grain size from clay to sandy clay;

585-593 cm:
shell material;

610-719 cm:
greenish black (5G 2/1) clay with woody material and some silt in upper few cm;

638 cm:
wood fragment;

650 cm:
woody fragment;

674 cm:
shell material;

691 cm:
shell material;

703 cm:
woody material;

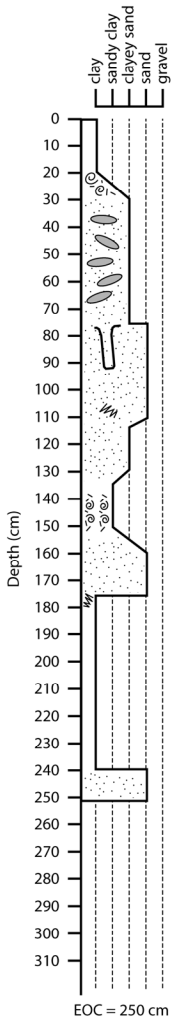

NR-07-1

0-25 cm:
grayish black (N2) organic-rich, very soft clay;

25-70 cm:
olive gray (5Y 4/1) sandy clay to clayey sand (fU-mL); inclusion of grayish black (N2) clay lenses;

25-31 cm:
presence of shell hash;

45-50 cm:
few shell fragments;

72-110 cm:
olive gray (5Y 4/1) fine-grained sand;

75-90 cm:
vertical burrow filled with medium light gray (N6) sand;

110 cm:
gradational contact;

110-135 cm:
olive black (5Y 2/1) sandy clay with small wood fragments throughout;

135-155 cm:
olive black (5Y 2/1) sandy clay;

140-150 cm:
inclusion of shell hash;

155-175 cm:
light olive gray (5Y 6/1) medium-grained sand;

155-157 cm:
inclusion of some olive black (5Y 2/1) clay;

175 cm:
sharp contact;

175-240 cm:
grayish black (N2) clay;

178-179 cm:
wood fragment;

178-180 cm:
3 cm-long vertical burrow filled with light olive gray (5Y 6/1) sand;

233-235 cm:
small wood fragments;

190-191 cm:
woody material;

240 cm:
sharp contact;

240-250 cm:
medium- to coarse-grained olive gray (5Y 4/1) sand;

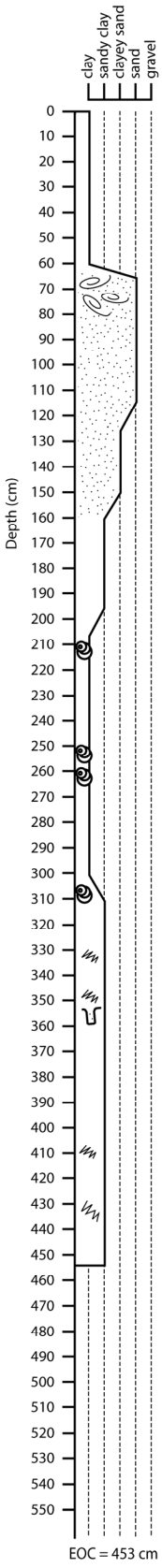

NR-07-2

0-60 cm:
dark greenish gray (5GY 4/1) homogenous soft clay;

60-70 cm:
transition to dark greenish gray (5GY 4/1), medium-grained sand to clayey sand;

57-59 cm:
oyster valve,

60-65 cm:
oyster valve;

65-70 cm:
oyster valve;

77-81 cm:
oyster fragments;

70-110 cm:
greenish black (5G 2/1) medium-grained sand;

110 cm:
gradational contact;

110-151 cm:
brownish black (5YR 2/1) medium-grained sand to clayey sand;; downcore increase in clay content;

151-195 cm:
brownish black (5YR 2/1) sandy clay; downcore decrease in sand content;

195 cm:
gradational contact;

195-302 cm:
olive gray (5Y 4/1) clay;

208 cm:
gastropod shell;

252 cm:
gastropod shell;

262-263 cm:
gastropod shell;

302-303 cm:
dark greenish gray (5GY 4/1) to olive gray (5Y 4/1) clay to slightly sandy clay;

303-453 cm:
olive gray (5Y 4/1) sandy clay; downcore increase in sand content;

305-310 cm:
gastropod shells;

333-335 cm:
wood fragment;

347 cm:
wood fragment;

355 cm:
sand-filled burrow;

407-411 cm:
wood fragments;

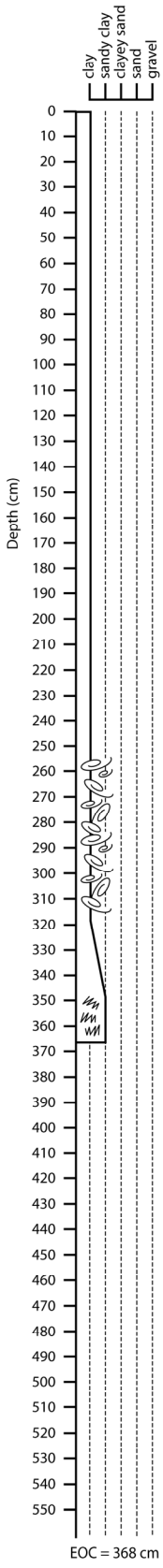

NR-07-3

0-150 cm:
greenish black (5G 2/1) soft homogenous clay;

150-225 cm:
dark greenish gray (5GY 4/1) homogenous soft clay;

225cm:
sharp contact;

225-295 cm:
dark greenish gray (5GY 4/1) clay containing oyster hash and whole oyster vlaves;

255-295 cm:
oyster valves;

295-322 cm:
olive gray (5Y 4/1) soft clay containing oyster valves and shell fragments;

322 cm:
gradational contact;

322-368 cm:
brownish black (5YR 2/1) sandy clay containing woody material;

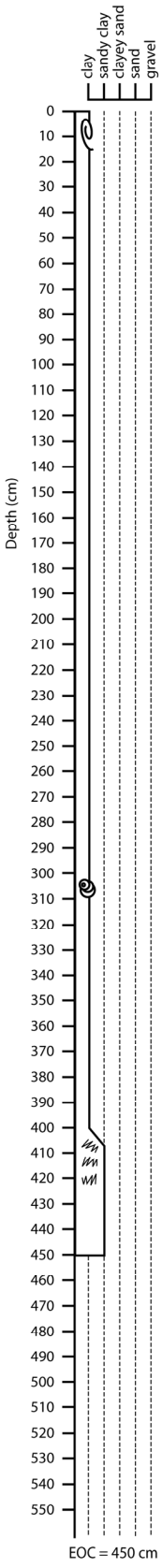

NR-07-4

0-154 cm:
olive black (5Y 2/1) to dark greenish gray (5GY 4/1) homogenous, soft clay; downcore increase in clay stiffness;

3-14 cm:
bivalve;

154-298 cm:
dark greenish gray (5GY 4/1) homogenous, soft clay;

193cm:
shell fragments;

233 cm:
shell fragments;

236 cm:
shell fragments;

298-355 cm:
dark greenish gray (5GY 4/1) clay including small shell fragments;

305 cm:
gastropod shell;

355 cm:
sharp contact;

355-395 cm:
brownish black (5YR 2/1) woody clay; organic fibers are found throughout;

395 cm:
gradational contact;

395-450 cm:
brownish black (5YR 2/1) to black (N1) organic-rich sandy clay containing plant materials;

420-422 cm:
wood fragments;

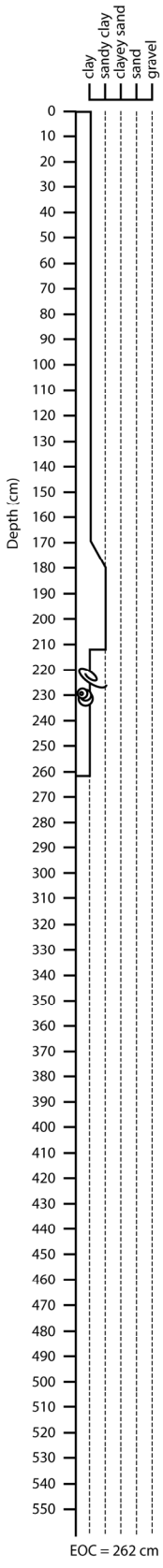

NR-07-5

0-148 cm:
dark greenish gray (5GY 4/1) homogenous soft clay;

148-170 cm:
olive gray (5GY 4/1) homogenous soft clay;

170 cm:
gradational contact;

170-211 cm:
olive black (5Y 2/1) homogenous soft clay to sandy clay; downcore increase in stiffness;

211-262 cm:
dark greenish gray (5GY 4/1) homogenous soft clay containing shell fragments;

225 cm:
bivalve;

231-234 cm:
gastropod shell (~ 1 cm in length);

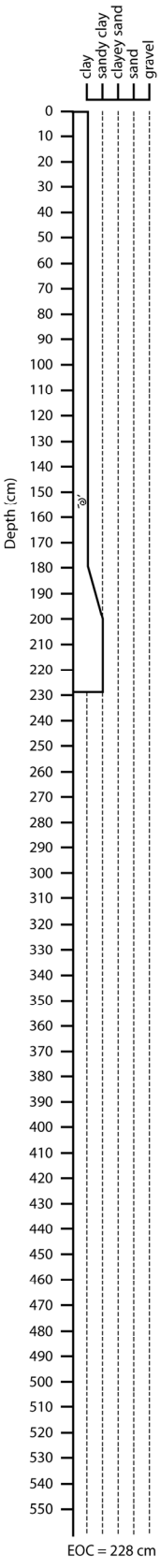

NR-07-6

0-195 cm:
medium dark gray (N4) homogenous soft clay;

150-153 cm:
shell hash;

195 cm:
gradational contact;

195-228 cm:
olive black (5Y 2/1) sandy clay; downcore increase in sand content;

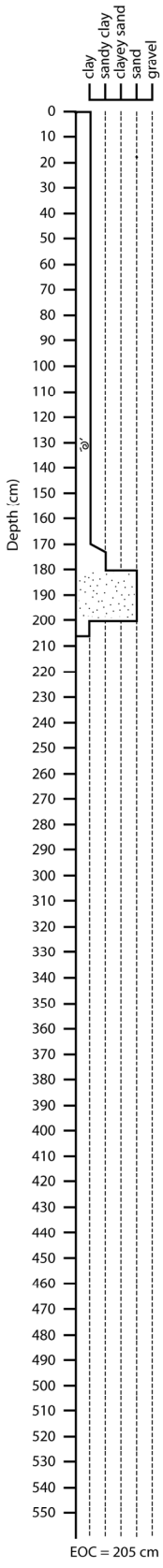

NR-07-7

0-166 cm:
greenish black (5G 2/1) homogenous soft clay;

130 cm:
shell fragments;

166-181 cm:
greenish black (5G 2/1) soft clay and silt;

181 cm:
sharp contact;

181-200 cm:
olive gray (5Y 4/1) fine- to medium-grained sand;

200 cm:
sharp contact;

200-205 cm:
greenish black (5G 2/1) soft clay;

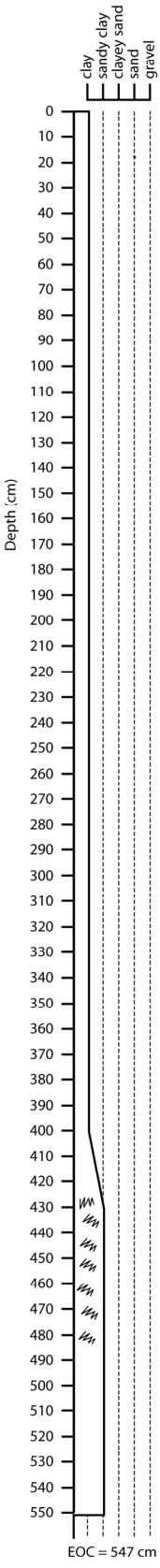

NR-07-9

0-400 cm:
dark greenish gray (5GY 4/1) homogenous soft clay;

185 cm:
shell fragment;

190-195 cm:
small shell fragments;

240-245 cm:
small shell fragments;

297 cm:
small shell fragment;

316-317 cm:
small shell fragments;

325 cm:
small shell fragment;

364 cm:
small shell fragment;

400 cm:
gradational contact;

400-488 cm:
brownish black (5YR 2/1) organic-rich clay and woody debrix; downcore decrease in amount of wood material;

430-435 cm:
large wood fragments;

488-496 cm:
brownish black (5YR 2/1) clay;

496 cm:
sharp contact;

496-518 cm:
olive gray (5Y 4/1) clay;

518 cm:
gradational contact;

518-543 cm:
dusky yellowish brown (10YR 2/2) clayey sand to sandy clay;

543 cm:
sharp contact;

543-550 cm:
brownish black (5YR 2/1) clay to silty clay;

NR-07-8

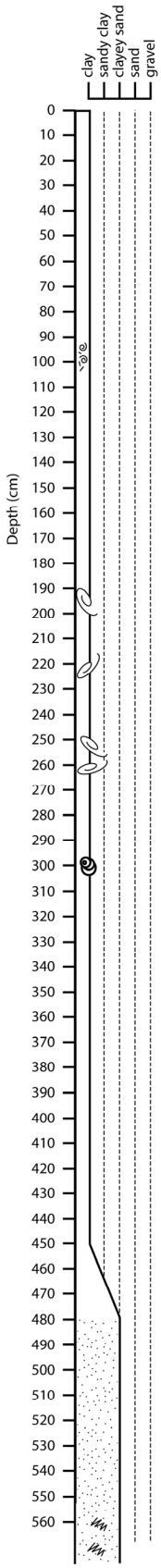

0-152 cm:
greensih black (5G 2/1) soft clay; downcore increase in stiffness;

90-105 cm:
shell hash composed of oyster shells and fragments around 2 cm in size;

152-170 cm:
greenish black (5G 2/1) homogenous soft clay;

170 cm:
gradational contact;

170-305 cm:
olive gray (5Y 4/1) soft clay containing oyster valves;

190-195 cm:
oyster valves;

218-227 cm:
oyster valves;

250-265 cm:
oyster valves;

299 cm:
gastropod shell;

305-457 cm:
greenish black (5GY 2/1) homogenous soft clay;

319 cm:
shell fragment;

457-465 cm:
olive black (5Y 2/1) sandy clay;

465 cm:
gradational contact;

465-610 cm:
olive black (5Y 2/1) clayey sand; downcore increase in sand content;

560 cm:
woody material;

568 cm:
woody material;

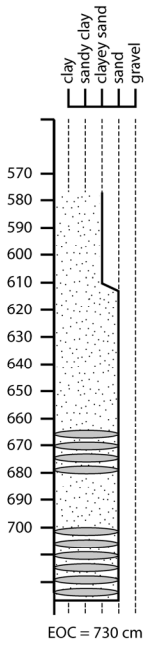

610-735 cm:
light olive gray (5Y 6/1) clean, fine-grained sand;

665-680 cm:
light olive gray (5Y 6/1) fine-grained sand interbedded with olive gray (5Y 4/1) clayey sand;

700-730 cm:
light olive gray (5Y 6/1) fine-grained sand interbedded witholive gray (5Y 4/1) clayey sand;

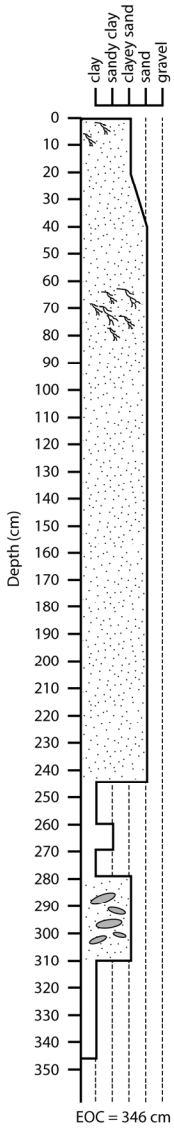

NP-1

0-30 cm:
olive gray (5Y 2/1) to dark gray (N3) fine- to medium-grained sand and silt; rich in organic matter (roots, etc.);

30 cm:
gradational contact;

30-152 cm:
light olive gray (5Y 6/1) fine- to medium-grained sand; few root remnants;

65-80 cm:
root remains;

152-210 cm:
light olive gray (5Y 6/1) fine- medium-grained sand;

210-245 cm:
moderate yellowish brown (10YR 5/4) staining;

245-250 cm:
dark yellowish brown (10YR 4/2) clay rip-up clast;

250-260 cm:
dark yellowish brown (10YR 4/2) stiff clay;

260-270 cm:
light olive gray (5Y 5/2) sandy clay;

270-280 cm:
moderate yellowish brown (10YR 5/4) stiff clay;

280-310 cm:
dark gray (N3) clay to clayey sand;
presence of rip-up clasts;

310-346 cm:
dark gray (N3) stiff clay;

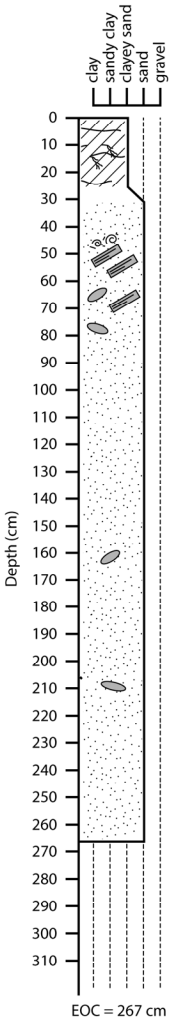

NP-2

0-50 cm:
olive black (5Y 2/1) to grayish black (N2) fine-grained sand, silt, and clay with root material;

0-25 cm:
roots;

45 cm:
shell fragments;

48 cm:
wood fragments;

50 cm:
gradational contact;

50-75 cm:
light olive gray (5Y 6/1) fine- to medium-grained sand;

55 cm:
wood fragment;

65-70 cm:
wood fragments;

65 cm:
light blue-gray (5B 7/1) clay lense;

67cm:
light blue-gray (5B 7/1) clay lense;

75-76 cm:
light blue-gray (5B 7/1) clay lense;

75:
gradational contact;

75-90 cm:
dusky yellow (5Y 6/4) sand;

90 cm:
gradational contact;

90-153 cm:
light olive gray (5Y 5/2) sand;

155-267 cm:
light olive gray (5Y 6/1) fine- to medium-grained sand;

163 cm:
light olive gray (5Y 6/1) clay rip-up;

210 cm:
light olive gray (5Y 6/1) clay rip-up;

245-267 cm:
color change to dark yellowish orange (10YR 6/6);

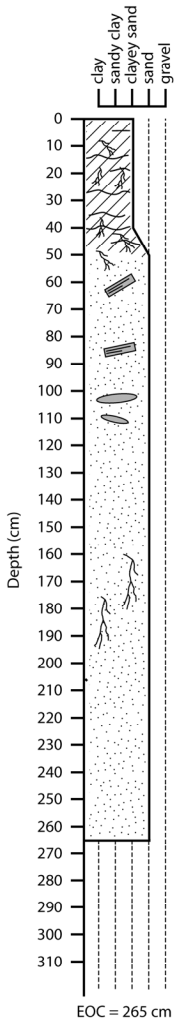

NP-3

0-95 cm:
dusky yellowish brown (10YR 2/2) to olive gray (5Y 3/2) to dark gray (N3) organic-rich clay, silt, and sand;

0-50 cm:
high % of organic matter (roots, ect.);

50-95 cm:
increase in sand %;

61 cm:
plant remains;

84 cm:
woody material;

95 cm:
sharp contact;

95-102 cm:
light olive gray (5Y 6/1) fine- to medium-grained sand with light gray (N7) clay lenses;

102-155 cm:
light olive gray (5Y 6/1) medium-grained sand;

110-115 cm:
medium light gray (N6) clay lenses;

160-195 cm:
root remnants;

155-265 cm:
light olive gray (5Y 6/1) medium-grained sand;

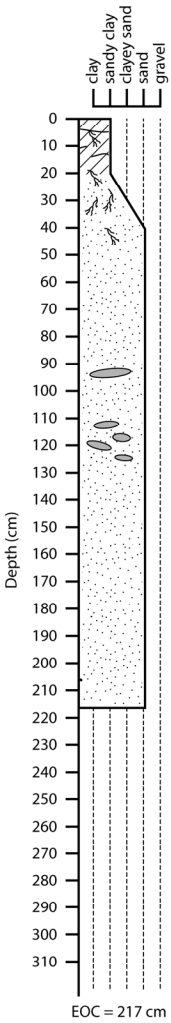

NP-4

0-20 cm:
brownish black (5YR 2/1) organic-rich clay to silty clay, roots, and plant debris;

20 cm:
gradational contact;

20-85 cm:
olive gray (5Y 4/1) organic-rich sand (medium-grained);

85 cm:
gradational contact;

85-154 cm:
light olive gray (5Y 6/2) to yellowish gray (5Y 7/2) fine- to medium-grained sand;

90-135 cm:
light blue-gray (5B 7/1) clay lenses/rip-ups;

135-142 cm:
sand discolored (oxidized) to moderate yellowish brown (10YR 5/4);

154-217 cm:
light olive gray (5Y 6/1) medium-grained sand;

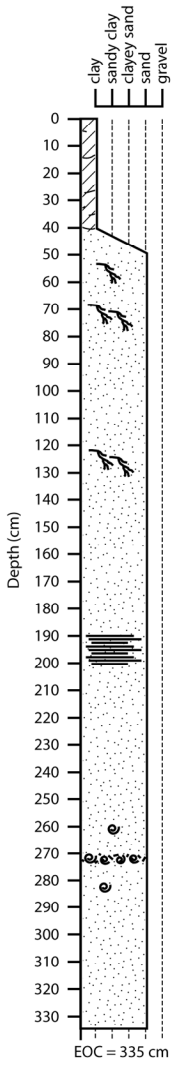

PKS-06-1

0-45 cm:
Black (N1) clay and organic material (roots);

~ 45 cm:
gradational contact between clay and sand;

45-50 cm:
pale yellowish brown (10YR 6/2) to dark yellowish brown (10YR 4/2) fine-grained sand;

50-60cm:
gradiational color change to medium yellowish brown (10YR 5/4) sand;

55cm:
root

70-75 cm:
roots;

120-125 cm:
roots;

60-152 cm:
laminated, fine-grained sand displaying color changes from medium yellowish brown (10YR 5/4) to dark yellowish brown (10YR 4/2) to pale yellowish brown (10 YR 6/2);

190-200 cm:
grayish black (N2) laminations;

262 cm:
shell valve;

270 cm:
shell layer;

282 cm:
oyster valve;

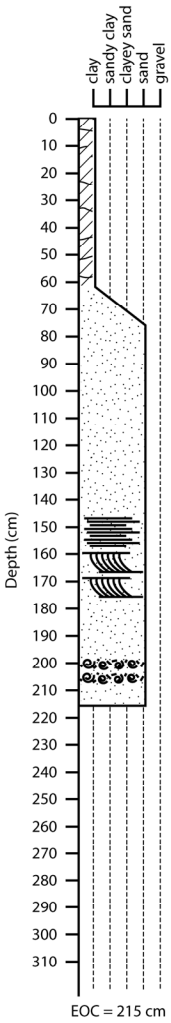

PKS-06-2

0-65 cm:
brownish black (5YR 2/1) to black (N1) clay and organic material (roots, etc.);

22 cm:
large root;

60-75 cm:
gradational contact between marshy sediments and underlying sand;

75-110 cm:
pale yellowish brown (10YR 6/2) sand;

100-102 cm:
large root;

110-140 cm:
gradual color transition to medium light gray (N6) and medium gray (N5);

140-215 cm:
medium light gray (N6) to medium gray (N5) sand;

140-180 cm:
grayish black cross-beds (N2);

195-215 cm:
inclusion of small shell fragments;

200-205 cm:
two fine layers of shell hash;

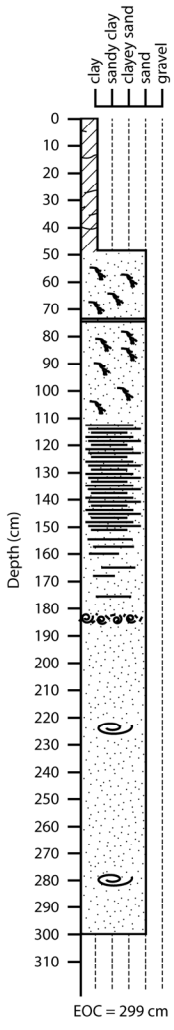

PKS-06-3

0-48 cm:
brownish black (5YR 2/1) to black (N1) clay and organic material (roots, etc.);

0-10 cm:
large root;

40-48 cm:
high concentration of roots;

48-49 cm:
sharp lithologic contact;

49-100 cm:
dark yellowish brown (10YR 4/2) to pale yellowish brown (10YR 6/2) fine-grained sand; gradational color change downcore;

73 cm:
black (N1) organic laminations;

100-153 cm:
medium gray (N5) to medium dark gray (N4) fine-grained and parallel laminated sand;

153-299 cm:
medium gray (N5) to medium dark gray (N4) fine-grained sand;

153-187 cm:
fine grayish black (N2) to black (N1) parallel laminations;

187-299 cm:
homogeneity;

225 cm:
oyster-valve fragment;

280 cm:
oyster-valve fragment;

280-299 cm:
increase in shell material (gravel-sized fraction);

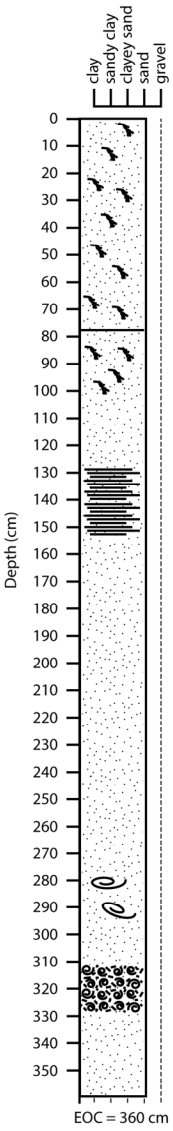

PKS-06-4

0-13 cm:
medium gray (N5) to medium dark gray (N4) fine-grained sand; gradational color change downcore;

13-25 cm:
pale yellowish brown (10YR 6/2) sand; gradational color change;

25-45 cm:
grayish brown (5YR 3/2) to dusky brown (5YR 2/2) sand; gradational color change;

45-74 cm:
pale yellowish brown (10YR 6/2) to dark yellowish brown (10YR 4/2) sand; gradational color change;

74-153 cm:
olive gray (5Y 4/1) to olive black (5Y 2/1) to brownish black (5YR 2/1) fine-grained sand;

76 cm:
dusky brown (5YR 2/2) organic layer of ~ 1 cm thickness;

130-153 cm:
very fine laminations;

153-220 cm:
dark gray (N3) to olive gray (5Y 4/1) fine-grained, thinly laminated sand; gradational color change;

220-360 cm:
medium gray (N5) to medium light gray (N6) sand; absence of laminae; downcore increase in shell material;

280 cm:
large oyster valve;

290 cm:
large oyster valve;

310-330 cm:
shell hash including large oyster valves;

PKS-06-8

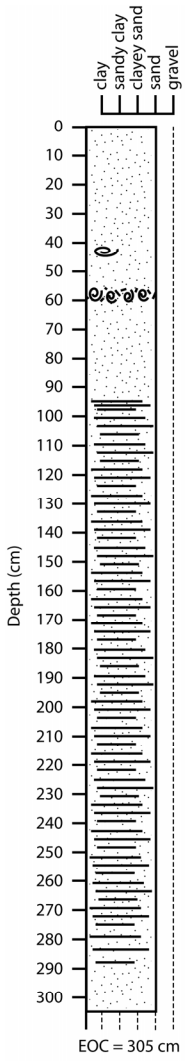

0-40 cm:
medium dark gray (N4) sand;

40-45 cm:
large shell fragment (scallop);

40-62 cm:
transition from medium dark gray (N4) sand to olive gray (5Y 4/1) sand with traces of organic matter;

55-61 cm:
shell hash;

62-90 cm:
olive gray (5Y 4/1) sand;

90-95 cm:
gradational transition;

95-130 cm:
olive gray (5Y 4/1) to brownish gray (5YR 4/1) sand with brownish black (5 YR 2/1) laminations;

130 cm:
gradational transition to medium dark gray (N4) sand with fine grayish black (N2) to black (N1) laminations;

130-290 cm:
finely laminated medium dark gray (N4) sand;

290-305 cm:
medim dark gray (N4) unlaminated sand;

APPENDIX B – AERIAL PHOTOGRAPHS

This appendix shows an 1888 map of the upper Newport bay area compiled by the United States Coast and Geodetic Survey along with aerial images of the Newport delta dating back to 1958. The survey map was obtained from the University of North Carolina's digital map library and shows the location of the aerial photographs. Photograph characteristics, including source, exact date of collection, and resolution are listed in Table 2.1. Photographs are labeled by year and data source.

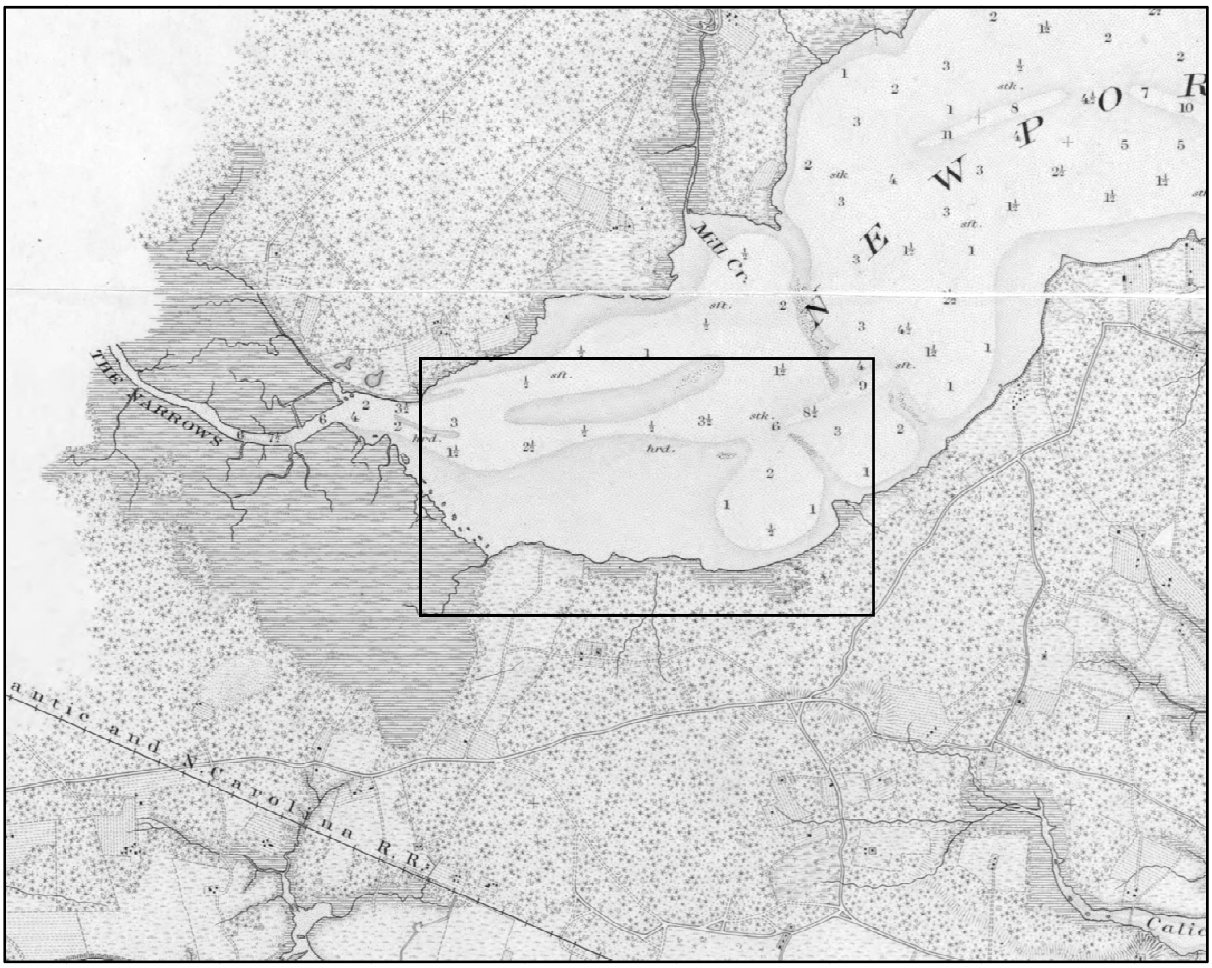


11/11/1958 - USDA


01/21/1964 - USDA


07/05/1967 - NCDOT

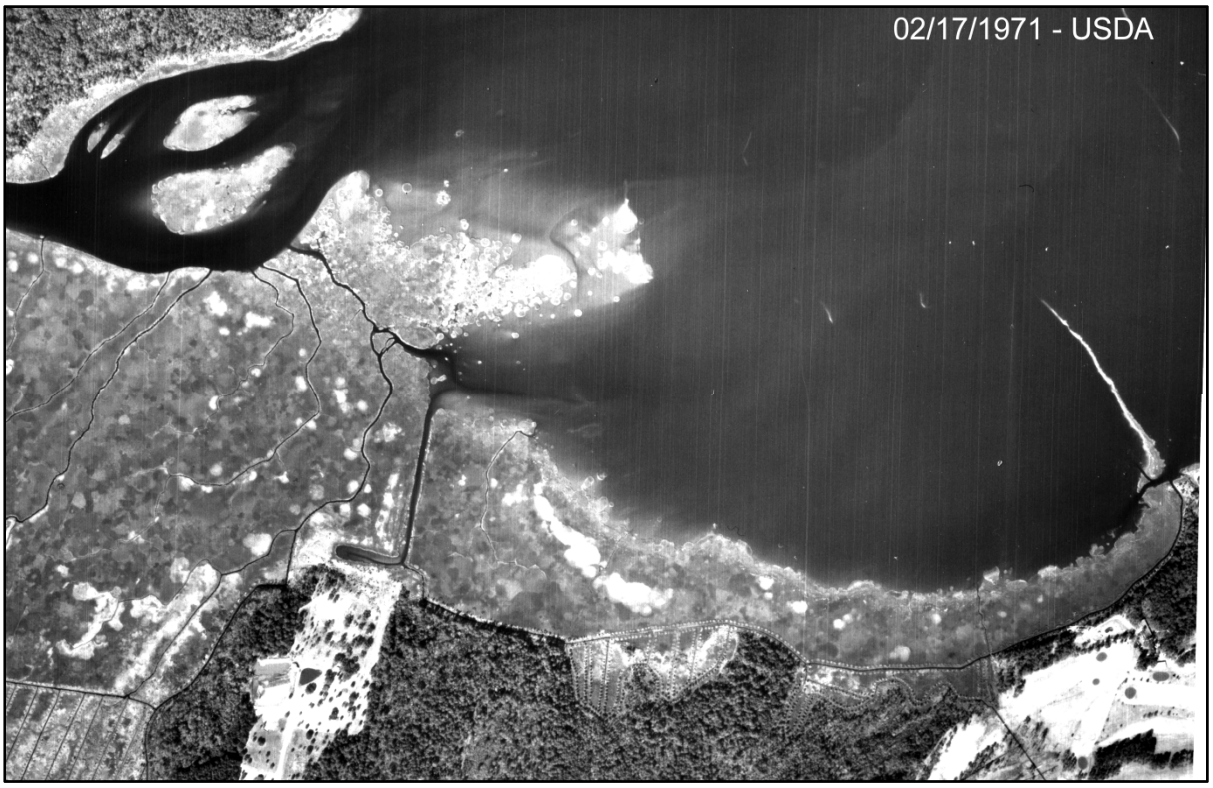
02/17/1971 - USDA

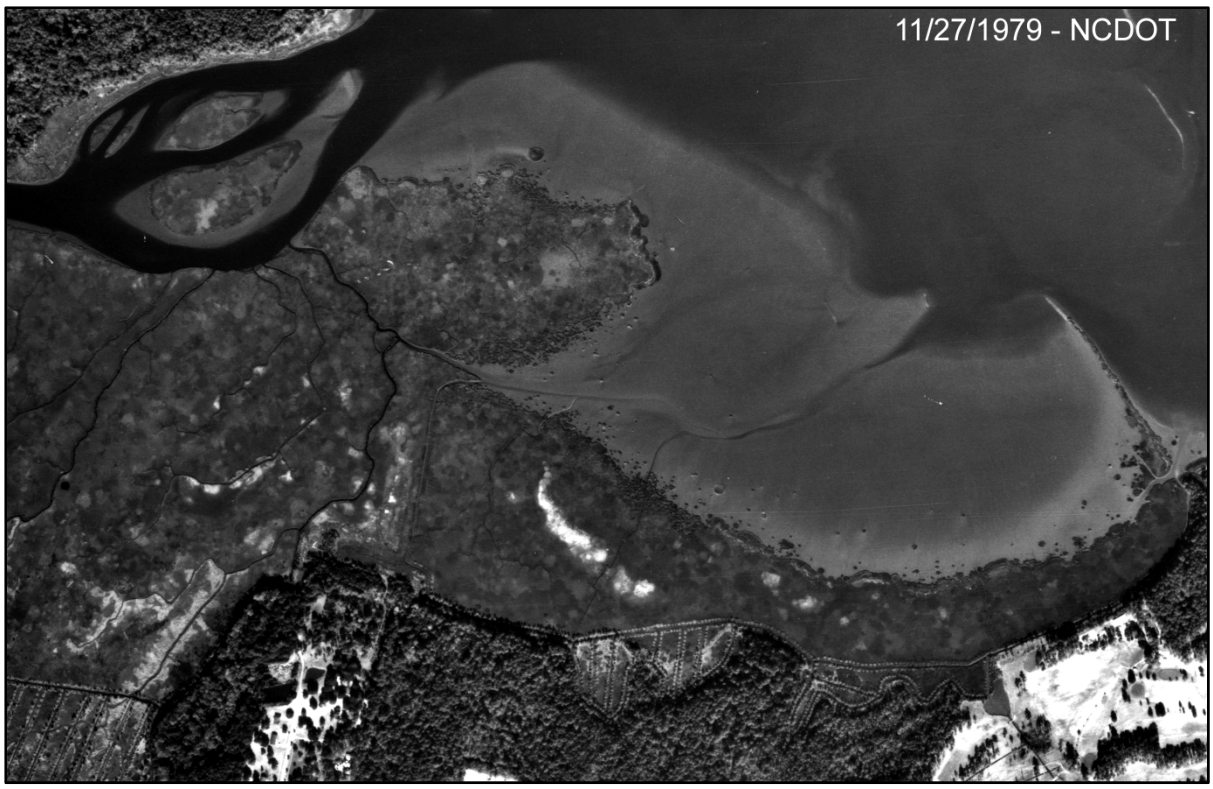
11/27/1979 - NCDOT


04/24/1982 - USDA


10/27/1988 - USDA


01/25/1998 - USGS


05/23/2003 - Google


05/13/2006 - NCDOT

REFERENCES

Adams, J.M. and Faure, H. 1997. Preliminary vegetation maps of the world since the Last Glacial Maximum: an aid to archaeological understanding. *Journal of Archaeological Science*, **24**: 623-647.

Ainsworth, R.B. and Walker, R.G. 1994. Control of Estuarine Valley-Fill Deposition by Fluctuations of Relative Sea-Level, Cretaceous Bearpaw-Horseshoe Canyon Transition, Drumheller, Alberta, Canada. *Incised-valley Systems: Origin and Sedimentary Sequence. SEPM Special Publication* (Ed R.W. Dalrymple, Boyd, R., Zaitlin, B.A.), **51**: 159-173.

Allen, J.R.L. 1995. Salt-marsh growth and fluctuating sea level: implications of a simulation model for Flandrian coastal stratigraphy and peat-based sea-level curves. *Sedimentary Geology*, **100**: 21-45.

Allen, J.R.L. 2000. Morphodynamics of Holocene salt marshes: a review sketch from the Atlantic and southern North Sea coasts of Europe. *Quaternary Science Reviews*, **19**: 1155-1231.

Allen, P.A. 2008. From landscapes into geological history. *Nature*, **451**: 274-276.

Amatya, D.M., Skaggs, R.W., and Gregory, J.D. 1996. Effects of controlled drainage on the hydrology of drainage pine plantations in the North Carolina coastal plain. *Journal of Hydrology*, **181**: 211-232.

Anderson, J.B., Rodriguez, A., Abdulah, K.C., Fillon, R.H., Banfield, L.A., McKeown, H.A. and Wellner, J.S. 2004. Late Quaternary stratigraphic evolution of the northern Gulf of Mexico margin: a synthesis. In: *Late Quaternary stratigraphic evolution of the northern Gulf of Mexico margin: a synthesis. SEPM Special Publication* (Ed J.B. Anderson and Fillon, R.H.), **79**, pp. 1-23.

Ardies, G.W., Dalrymple, R.W., and Zaitlin, B.A. 2002. Controls on the Geometry of Incised Valleys in the Basal Quartz Unit (Lower Cretaceous), Western Canada Sedimentary Basin. *Journal of Sedimentary Research*, **72**: 602-618.

Bard, E., Hamelin, B., Fairbanks, R.G., and Zindler, A. 1990. U-Th ages obtained by mass spectrometry in corals from Barbados: sea level during the past 13,000 years. *Nature*, **346**: 456-458.

Bartholdy, J., Christiansen, C., and Kunzendorf, H. 2004. Long term variations in backbarrier salt marsh deposition on the Skallingen peninsula - the Danish Wadden Sea. *Marine Geology*, **203**: 1-21.

Belk, D.R. and Phillips, J.D. 1993. Hydrologic recovery of artificially-drained wetlands in coastal North Carolina. *Coastal Zone '93* (Ed O.T. Magoon)*, American Society of Civil Engineers,* 3254-3268.

Belknap, D.F., Kraft, J.C., and Dunn, R. 1994. Transgressive valley-fill lithosomes: Delaware and Maine. *Incised Valley Fill Systems: Origin and Sedimentary Sequences. SEPM Special Publication* (Ed R.W. Dalrymple, Boyd, R., Zaitlin, B.A.), **51**: 341-354.

Belknap, D.F. and Kraft, J.C. 1981. Preservation potential of transgressive coastal lithosomes on the U.S. Atlantic shelf. *Marine Geology*, **42**: 429-442.

Bernard, H.A. and LeBlanc, R.J. 1965. Resume of the Quaternary geology of the northwestern Gulf of Mexico province. In: *The Quaternary of the United States* (Ed H.E. Wright and D.G. Frey), pp. 137-185. Princeton University Press, Princeton.

Binkley, D. and Brown, T.C. 1993. Forest practices as nonpoint sources of pollution in North America. *Water Resources Bulletin*, **29**: 729-740.

Blum, M.D. 1994. Genesis and Architecture of Incised Valley Fill Sequences: A Late Quaternary Example from the Colorado River, Gulf Coastal Plain of Texas. *Siliciclastic Sequence Stratigraphy: Recent Developments and Applications. American Association of Petroleum Geologists Memoir* (Ed P. Weimer and Posamentier, H.W.), **58**: 259-283.

Blum, M.D., Sivers, A.E., Zayac, T. and Goble, R. 2003. Middle Holocene sea-level and the evolution of the Gulf of Mexico coast. *Gulf Coast Association of Geological Societies, Transactions*, **53**: 64-77.

Blum, M.D., Toomey III, R.S., and Valastro, S. Jr. 1994. Fluvial response to Late Quaternary climatic and environmental change, Edwards Plateau, Texas. *Paleogeography, Paleoclimatology, Paleoecology*, **108**: 1-21.

Blum, M.D. and Törnqvist, T.E. 2000. Fluvial responses to climate and sea-level change: a review and look forward. *Sedimentology*, **47**: 2-48.

Boyles, R.P. and Raman, S. 2003. Analysis of climate trends in North Carolina (1949-1998). *Environment International*, **29**: 263-275.

Bozek, C.M. and Burdick, D.M. 2005. Impacts of seawalls on saltmarsh plant communities in the Great Bay Estuary, New Hampshire USA. *Wetlands Ecology and Management*, **13**: 553-568.

Bricker-Urso, S., Nixon, S.W., Cochran, J.K., Hirschberg, D.J., and Hunt, C. 1989. Accretion Rates and Sediment Accumulation in Rhode Island Salt Marshes. *Estuaries*, **12**: 300-317.

Brierley, G., Fryirs, K., and Jain, V. 2006. Landscape connectivity: the geographic basis of geomorphic applications. *Area*, **38.2**: 165-174.

Brill, A.L. 1996. *The Suffolk Scarp: A Pleistocene Barrier Island in Beaufort and Pamlico Counties*. Masters, Duke University, 137 pp.

Bryant, J.C. and Chabreck, R.H. 1998. Effects of Impoundment on Vertical Accretion of Coastal Marsh. *Estuaries*, **21**: 416-422.

Cahoon, D.R., Lynch, J.C., Hensel, P.F., Boumans, R.M., Perez, B.C., Segura, B., and Day, J.W. 2002a. High precision measurement of wetland sediment elevation: I. recent improvements to the sedimentation-erosion table. *Journal of Sedimentary Research*, **72**: 730-733.

Cahoon, D.R., Lynch, J.C., Perez, B.C., Segura, B., Holland, R., Stelly, C., Spephenson, G., and Hensel, P.F. 2002b. High precision measurement of wetland sediment elevation: II. the rod surface elevation table. *Journal of Sedimentary Research*, **72**: 734-739.

Cahoon, D.R., Ford, M.A. and Hensel, P.F. 2004. Ecogemorphology of Spartina patens–dominated tidal marshes: soil organic matter accumulation, marsh elevation dynamics, and disturbance. In: *The Ecogeomorphology of Tidal Marshes* (Eds S. Fagherazzi, M. Marani and L.K. Blum), **Coastal and Estuarine Studies 59**, pp. 247–266. American Geophysical Union, Washington, D.C.

Cecil, C.B., Dulong, F.T., Harris, R.A., Cobb, J.A., Gluskoter, H.G. and Nugroho, H. 2003. Observations on climate and sediment discharge in selected tropical rivers, Indonesia. In: *Climate Controls on Stratigraphy* (Eds C.B. Cecil and N.T. Edgar), **77**, pp. 29-50. SEPM Special Publication.

Chappell, J. and Skackleton, N.J. 1986. Oxygen Isotopes and Sea Level. *Nature*, **324**: 137-140.

Chauhan, P.P.S. 2009. Autocyclic erosion in tidal marshes. *Geomorphology*, **110**: 45-57.

Chmura, G.L. and Aharon, P. 1995. Stable carbon isotope signatures of sedimentary carbon in coastal wetlands as indicators of salinity regime. *Journal of Coastal Research*, **11**: 124-135.

Choi, Y., Wang, Y., Hsieh, Y.-P., and Robinson, L. 2001. Vegetation succession and carbon sequestration in a coastal wetland in northwest Florida: Evidence from carbon isotopes. *Global Biogeochemical Cycles*, **15**: 311-319.

Christiansen, T., Wiberg, P.L., and Milligan, T.G. 2000. Flow and sediment transport on a tidal salt marsh surface. *Estuarine, Coastal and Shelf Science*, **50**: 315-331.

Church, J.A. 2001. How fast are sea levels rising? *Science*, **294**: 802-803.

Clifton, H.E. 1994. Preservation of Transgressive and Highstand Late Pleistocene Valley-Fill/Estuary Deposits, Willipa Bay, Washington. *Incised-valley Systems: Origin and Sedimentary Sequence. SEPM Special Publication* (Ed R.W. Dalrymple, Boyd, R., Zaitlin, B.A.), **51**: 322-333.

Corbett, D.R., Walsh, J.P., Cowart, L., Riggs, S.R., Ames, D.V. and Culver, S.J. 2008. Shoreline Change within the Albemarle-Pamlico Estuarine System, North Carolina, East Carolina University in-house report, pp. 10.

Couper, P. 2003. Effects of silt-clay content on the susceptibility of river banks to subaerial erosion. *Geomorphology*, **56**: 95-108.

Craft, C. 2007. Freshwater input structures soil properties, vertical accretion, and nutrient accumulation of Georgia and U.S. tidal marshes. *Limnology and Oceanography*, **52**: 1220-1230.

Currin, C.A., Delano, P.C. and Valdes-Weaver, L.M. 2008. Utilization of a citizen monitoring protocol to assess the structure and function of natural and stabilized fringing salt marshes in North Carolina. *Wetlands Ecology and Management*, **16**: 97-118.

Dabrio, C.J., Zazo, C., Goy, J.L., Sierro, F.J., Borja, F., Lario, J., González, J.A., and Flores, J.A. 2000. Depositional history of esturaine infill during the last postglacial transgression (Gulf of Cadiz, Southern Spain). *Marine Geology*, **162**: 381-404.

Dalrymple, R.W., Zaitlin, B.A., and Boyd, R. 1992. Estuarine Facies Models: Conceptual Basis and Stratigraphic Implications. *Journal of Sedimentary Petrology*, **62**: 1130-1146.

Davidson, S.K. and North, C.P. 2009. Geomorphological Regional Curves for Prediction of Drainage Area and Screening Modern Analogues for Rivers in the Rock Record. *Journal of Sedimentary Research*, **79**: 773-792.

Day, J.W. 1989. Estuarine Ecology. *Wiley-Interscience Publication, New York,* 558.

de Vente, J., Poesen, J., Arabkhedri, M., and Verstraeten, G. 2007. The sediment delivery problem revisited. *Progress in Physical Geography*, **31**: 155-178.

DeLaune, R.D. 1986. The use of delta^{13}C signature of C-3 and C-4 plants in determining past depositional environments in rapidly accreting marshes of the Mississippi River deltaic plain, Louisiana, USA. *Chemical Geology*, **59**: 315-320.

DeLaune, R.D., Jugsujinda, A., Peterson, G.W., and Patrick, W.H. Jr. 2003. Impact of Mississippi River freshwater reintroduction on enhancing marsh accretionary processes in a Louisiana estuary. *Estuarine, Coastal and Shelf Science*, **58**: 653-662.

Delcourt, P.A. 1981. Vegetation maps for eastern North America: 40,000 yr B.P. to the Present. *In: Romans, R.C. Editor, "Geobotany II", New York*123-165.

Doyle, M.W. and Harbor, J.M. 2003. Modelling the Effect of Form and Profile Adjustment on Channel Equilibrium Timescales. *Earth Surface Processes and Landforms*, **28**: 1271-1287.

Ethridge, F.G., Germanoski, D., Schumm, S.A., and Wood, L.J. 2005. The morphological and stratigraphical effects of base-level change: a review of experimental studies. *Special Publication of the International Association of Sedimentologists*, **35**: 213-241.

Fagherazzi, S., Carniello, L., d'Alpaos, L., and Defina, A. 2006. Critical bifurcation of shallow microtidal landforms in tidal flats and salt marshes. *PNAS*, **103**: 8337-8341.

Fairbanks, R.G. 1989. A 17,000-year glacio-esutatic sea level record: influence of glacial melting rates on the Younger Dryas event and deep-ocean circulation. *Nature*, **342**: 637-642.

Finnegan, N.J., Roe, G., Montgomery, D.R., and Hallet, B. 2005. Controls on the channel width of rivers: Implications for modeling fluvial incision of bedrock. *Geology*, **33**: 229-232.

Flessa, K.W., Constantine, K.J., and Cushman, M.K. 1977. Sedimentation Rates in a Coastal Marsh Determined From Historical Records. *Chesapeake Science*, **18**: 172-176.

Foyle, A.M. and Oertel, G.F. 1997. Transgressive systems tract development and incised-valley fills within a Quaternary estuary-shelf system: Virginia inner shelf, USA. *Marine Geology*, **137**: 227-249.

Fryirs, K.A., Brierley, G.J., Preston, N.J., and Kasai, M. 2007. Buffers, barriers and blankets: The (dis)connectivity of catchment-scale sediment cascades. *Catena*, **70**: 49-67.

Galloway, W.E., Ganey-Curry, P.E., Li, X., and Buffler, R.T. 2000. Cenozoic depositional history of the Gulf of Mexico basin. *AAPG Bulletin*, **84**: 1743-1774.

Gehrels, W.R. 1999. Middle and Late Holocene Sea-Level Changes in Eastern Maine Reconstructed from Foraminiferal Saltmarsh Stratigraphy and AMS ^{14}C Dates on Basal Peat. *Quaternary Research*, **52**: 350-359.

Gehrels, W.R., Belknap, D.F., and Kelley, J.T. 1996. Integrated high-precision analyses of Holocene sea-level changes: Lessons from the coast of Maine. *Geological Society of America Bulletin*, **108**: 1073-1088.

Gibling, M.R. 2006. Width and Thickness of Fluvial Channel Bodies and Valley Fills in the Geological Record: A Literature Compilation and Classification. *Journal of Sedimentary Research*, **76**: 731-770.

Greene, D.L.J., Rodriguez, A.B., and Anderson, J.B. 2007. Seaward-Branching Coastal-Plain and Piedmont Incised-Valley Systems through Multiple Sea-Level Cycles: Late Quaternary Examples from Mobile Bay and Mississippi Sound, U.S.A. *Journal of Sedimentary Research*, **77**: 139-158.

Guinasso, N.L., Jr. and Schink, D.R. 1975. Quantitative Estimates of Biological Mixing Rates in Abyssal Sediments. *Journal of Geophysical Research*, **80**: 3032-3043.

Harvey, A.M. 2002. Effective timescales of coupling within fluvial systems. *Geomorphology*, **44**: 175-201.

Hassan, M.A. and Klein, M. 2002. Fluvial adjustment of the Lower Jordan River to a drop in the Dead Sea level. *Geomorphology*, **45**: 21-33.

Hatton, R.S., DeLaune, R.D., and Patrick, W.H. Jr. 1983. Sedimentation, accretion, and subsidence in marshes of Barataria Basin, Louisiana. *Limnology and Oceanography*, **28**: 494-502.

Heap, A.D. and Nichol, S.L. 1997. The influence of limited accommodation space on the stratigraphy of an incised-valley succession: Weiti River estuary, New Zealand. *Marine Geology*, **144**: 229-252.

Heiri, O., Lotter, A.F., and Lemcke, G. 2001. Loss-on-ignition as a method for estimating organic and carbonate content in sediments: reproducibility and comparability of results. *Journal of Paleolimnology*, **25**: 101-110.

Helland-Hansen, W. and Martinsen, O.J. 1996. Shoreline Trajectories and Sequences: Description of Variable Depositional-Dip Scenarios. *Journal of Sedimentary Research*, **66**: 670-688.

Hine, A.C. and Snyder, S.W. 1985. Coastal lithosome preservation: evidence from the shoreface and inner continental shelf off Bogue Banks, North Carolina. *Marine Geology*, **63**: 307-330.

Horton, B.P., Peltier, W.R., Culver, S.J., Drummond, R., Engelhart, S.E., Kemp, A.C., Mallinson, D., Thieler, E.R., Riggs, S.R., Ames, D.V. and Thomson, K.H. 2009. Holocene sea-level changes along the North Carolina Coastline and their implications for glacial isostatic adjustment models. *Quaternary Science Reviews*, **28**: 1725-1736.

Jackson, S.T., Web, R.S., Anderson, K.H., Overpeck, J.T., Webb III, T., Williams, J.W., and Hansen, B.C.S. 2000. Vegetation and environment in Eastern North America during the Last Glacial Maximum. *Quaternary Science Reviews*, **19**: 489-508.

Johnson, F.K. 1959. The Sediments of the Newport River Estuary, Morehead City, North Carolina. *University of North Carolina at Chapel Hill*, 36.

Kirwan, M. and Temmerman, S. 2009. Coastal marsh response to historical and future sea-level acceleration. *Quaternary Science Reviews*, **28**: 1801-1808.

Knighton, D. 1998. *Fluvial forms and processes*. John Wiley & Sons Inc., New York, 400.

Knutson, P.L., Brochu, R.A., Seelig, W.N., and Inskeep, M. 1982. Wave damping in *Spartina alterniflora* marshes. *Wetlands*, **2**: 87-104.

Koss, J.E., Ethridge, F.G., and Schumm, S.A. 1994. An Experimental Study of the Effects of Base-Level Change on Fluvial, Coastal Plain and Shelf Systems. *Journal of Sedimentary Research*, **B64**: 90-98.

Lacey, G. 1930. Stable channels in alluvium. In: *Proceedings of the Institute of Civil Engineers*, London.

Lecce, S.A., Gares, P.A., and Pease, P.P. 2006a. Drainage ditches as sediment sinks on the coastal plain of North Carolina. *Physical Geography*, **27**: 447-463.

Lecce, S.A., Pease, P.P., Gares, P.A., and Wang, J. 2006b. Seasonal controls on sediment delivery in a small coastal plain watershed, North Carolina, USA. *Geomorphology*, **73**: 246-260.

LeGrand, H.E. 1961. Summary of geology of Atlantic Coastal Plain. *Bulletin of the American Association of Petroleum Geologists*, **45**: 1557-1571.

Leigh, D.S. and Feeney, T.P. 1995. Paleochannels indicating wet climate and lack of response to lower sea level, southeast Georgia. *Geology*, **23**: 687-690.

Leigh, D.S., Srivastana, P., and Brook, G.A. 2004. Late Pleistocene braided rivers of the Atlantic Coastal Plain, USA. *Quaternary Science Reviews*, **23**: 65-84.

Leonard, L.A. and Reed, D.J. 2002. Hydrodynamics and sediment transport through tidal marsh canopies. *Journal of Coastal Research*, **Special Issue 36**: 459-469.

Leonard, L.A. and Croft, A.L. 2006. The effect of standing biomass on flow velocity and turbulence in *Spartina alterniflora* canopies. *Estuarine, Coastal and Shelf Science*, **69**: 325-336.

Leonard, L.A. and Luther, M.E. 1995. Flow hydrodynamics in tidal marsh canopies. *Limnology and Oceanography*, **40**: 1474-1484.

Leopold, L.B. and Maddock, T., Jr. 1953. The hydraulic geometry of stream channels and some physiographic implications. *US Geological Survey Professional Paper*, **252**.

Leopold, L.B., Wolman, M.G. and Miller, J.P. 1964. *Fluvial Processes in Geomorphology*. W.H. Freeman and Company, San Francisco: 535.

Lu, S., Sun, G., Amatya, D.M., Harder, S.V., and McNulty, S.G. 2006. Understanding the Hydrologic Repsonse of a Coastal Plain Watershed to Forest Management and Climate Change in South Carolina, U.S.A. *American Society of Agricultural and Biological Engineers, Proceedings of the International Conferenc:* 231-239.

Malhotra, A. and Fonseca, M.S. 2007. WEMo (Wave Exposure Model): Formulation Procedures and Validation. *NOAA Technical Memorandum NOS NCCOS*, **65**: 28.

Mallinson, D., Riggs, S., Culver, S., Thieler, R., Foster, D. Corbett, D., Farrell, K., and Wehmiller, J., 2005. Late Neogene and Quaternary evolution of the northern Albemarle Embayment (Mid-Atlantic Continental Margin, USA). *Marine Geology*, **217**: 97-117.

Marsh, P.E. and Cohen, A.D. 2007. Identifying high-level salt marshes using a palynomorphic fingerprint with potential implications for tracking sea level change. *Review of Palaeobotany and Palynology*, **148**: 60-69.

Mattheus, C.R., Rodriguez, A.B., Greene, D.L.Jr, Simms, A.R., and Anderson, J.B. 2007. Control of Upstream Variables on Incised-Valley Dimension. *Journal of Sedimentary Research*, **77**: 213-224.

Mattheus, C.R., Rodriguez, A.B., and McKee, B. 2009. Direct Connectivity between Upstream and Downstream Promotes Rapid Response of Lower Coastal-plain Rivers to Land-use Change. *Journal of Geophysical Research*, **36**: L20401.

McGranahan, G., Balk, D., and Anderson, B. 2007. The rising tide: assessing the risks of climate change and human settlements in low elevation coastal zones. *Environment and Urbanization*, **19**: 17-37.

Milliman, J.D. and Syvitski, J.P.M. 1992. Geomorphic/Tectonic control of sediment discharge to the ocean: the importance of small mountaineous rivers. *The Journal of Geology*, **100**: 525-544.

Minello, T.J., Zimmerman, R.J., and Medina, R. 1994. The importance of edge for natant macrofauna in a created salt marsh. *Wetlands*, **14**: 184-198.

Mitchum, R.M., Jr., Vail, P.R., and Thompson, S. III 1977. Seismic Stratigraphy and Global Changes of Sea Level, Part 2: The Depositional Sequence as a Basic Unit for Stratigraphic Analysis. *AAPG Memoir*, **26**: 53-62.

Möller, I. and Spencer, T. 2002. Wave dissipation over macro-tidal saltmarshes: Effects of marsh edge typology and vegetation change. *Journal of Coastal Research*, **36**: 506-521.

Morris, J.T., Sundareshwar, P.V., Nietch, C.T., Kjerfve, B., and Cahoon, D.R. 2002. Responses of coastal wetlands to rising sea level. *Ecology*, **83**: 2869-2877.

Morton, R.A., Blum, M.D., and White, W.A. 1996. Valley Fills of Incised Coastal Plain Rivers, Southeastern Texas. *Transactions of the Gulf Coast Association of Geological Societies*, **46**: 321-331.

Murphy, S. and Voulgaris, G. 2006. Identifying the role of tides, rainfall and seasonality in marsh sedimentation using long-term suspended sediment concentration data. *Marine Geology*, **227**: 31-50.

Musgrove, M.L., Banner, J.L., Combs, L.E., James, E.W., Cheng, H., and Edwards, R.L. 2001. Geochronology of late Pleistocene to Holocene speleothems from central Texas: implications for regional paleoclimate. *GSA Bulletin*, **113**: 1532-1543.

Nelson, E.J. and Booth, D.B. 2002. Sediment sources in an urbanizing, mixed land-use watershed. *Journal of Hydrology*, **264**: 51-68.

Neubauer, S.C. 2008. Contributions of mineral and organic components to tidal freshwater marsh accretion. *Estuarine, Coastal and Shelf Science*, **78**: 78-88.

Neumeier, U. 2007. Velocity and turbulence variations at the edge of saltmarshes. *Continental Shelf Research*, **27**: 1046-1059.

Neumeier, U. and Ciavola, P. 2004. Flow resistance and associated sedimentary processes in a *Spartina maritima* salt-marsh. *Journal of Coastal Research*, **20**: 435-447.

Noe, G. B. and Hupp, C.R. 2009. Retention of Riverine Sediment and Nutrient Loads by Coastal Plain Floodplains. *Ecosystems,* **12**: 728-746.

Nichol, S.L., Boyd, R., and Penland, S. 1996. Sequence Stratigraphy of a Coastal-Plain Incised Valley Estuary: Lake Calcasieu, Louisiana. *Journal of Sedimentary Research*,**66**: 847-857.

Orson, R., Panageotou, W., and Leatherman, S.P. 1985. Response of tidal salt marshes to rising sea levels along the U.S. Atlantic and Gulf coasts. *Journal of Coastal Research*, **1**: 29-37.

Osterkamp, W.R. 1980. Sediment-morphology relations of alluvial channels. In: *Proceedings of the Symposium on Watershed Management, American Society of Civil Engineers*, pp. 188-199, Boise.

Otvos, E.G. 1991. Houston Ridge, SW Louisiana - end link in the Late Pleistocene Ingleside barrier chain? Prarie Formation newly defined. *Southeastern Geology*, **31**: 235-249.

Otvos, E.G. and Howat, W.E. 1992. Late Quaternary coastal units and marine cycles: correlations between northern Gulf sectors. *Gulf Coast Association of Geological Societies, Transactions*, **42**: 571-585.

Paola, C., Heller, P.L., and Angevine, C.L. 1992. The large-scale dynamics of grain-size variation in alluvial basins, 1: Theory. *Basin Research*, **4**: 73-90.

Peterson, G.W. and Turner, R.E. 1994. The Value of Salt Marsh Edge vs. Interior as a Habitat for Fish and Decapod Crustaceans in a Louisiana Tidal Marsh. *Estuaries*, **17**: 235-262.

Phillips, J.D. 1986a. Coastal Submergence and Marsh Fringe Erosion. *Journal of Coastal Research*, **2**: 427-436.

Phillips, J.D. 1986b. Spatial Analysis of Shoreline Erosion, Delaware Bay, New Jersey. *Annals of the Assocation of American Geographers*, **76**: 50-62.

Phillips, J.D. 1992. Delivery of Upper-Basin Sediment to the Lower Neuse River, North Carolina, U.S.A. *Earth Surface Processes and Landforms*, **17**: 699-709.

Phillips, J.D. 1997b. A Short History of a Flat Place: Three Centuries of Geomorphic Change in the Croatan National Forest. *Annals of the Association of American Geographers*, **87**: 197-216.

Phillips, J.D., Slattery, M.C. and P.A., G. 1999. Truncation and accretion of soil profiles on coastal plain croplands: implications for sediment redistribution. *Geomorphology*, **28**: 119-140.

Plint, A.G. and Wadsworth, J.A. 2003. Sedimentology and paleogeomorphology of four large valley systems incising delta plains, western Canada Foreland Basin: implications for mid-Cretaceous sea-level changes. *Sedimentology*, **50**: 1147-1186.

Posamentier, H.W. 2001. Lowstand alluvial bypass systems: Incised vs. unincised. *AAPG Bulletin*, **85**: 1771-1793.

Posamentier, H.W. and Allen, G.P. 1999. Siliciclastic sequence stratigraphy: concepts and applications. In: *SEPM Concepts in Sedimentology and Paleontology*, **7**: 210.

Prentice, C., Bartlein, P.J., and Webb III, T. 1991. Vegetation and climate change in eastern North America since the Last Glacial Maximum. *Ecology*, **72**: 2038-2056.

Ray, N. and Adams, M. 2001. A GIS-based vegetation map of the world at the Last Glacial Maximum (25,000-15,000 BP). *Internet Archaeology*, **11**: 1-44.

Richard, G.A. 1978. Seasonal and Environmental Variations in Sediment Accretion in a Long Island Salt Marsh. *Estuaries*, **1**: 29-35.

Richards, H.G. 1967. Stratigraphy of Atlantic Coastal Plain between Long Island and Georgia; review. *AAPG Bulletin*, **51**: 2400-2429.

Riggs, S., Cleary, W.J., and Snyder, S.W. 1995. Influence of inherited geologic framework on barrier shoreface morphology and dynamics. *Marine Geology*, **126**: 213-234.

Riggs, S.R. and Ames, D.V. 2003. Drowning of the North Carolina Coast: Sea-Level Rise and Estuarine Dynamics. *North Carolina Sea Grant Publication:* 152.

Riggs, S.R., Snyder, S.W., Hine, A.C., and Mearns, D.L. 1996. Hardbottom Morphology and Relationship to the Geologic Framework: Mid-Atlantic Continental Shelf. *Journal of Sedimentary Research*, **66**: 830-846.

Ritter, D.F., Kochel, R.C., and Miller, J.R. 1978. Process Geomorphology. *McGraw-Hill, New York*: 545.

Rodriguez, A.B., Anderson, J.B., and Simms, A.R. 2005. Terrace Inundation as an Autocyclic Mechanism for Parasequence Formation: Galveston Estuary, Texas, U.S.A. *Journal of Sedimentary Research*, **75**: 606-618.

Ruddiman, W.F. and Glover, L.K. 1972. Vertical mixing of ice-rafted volcanic ash in North Atlantic Sediments. *Geological Society of America Bulletin*, **83**: 2817-2836.

Sager, E.D. and Riggs, S.R. 1998. Models for the Holocene Valley-Fill History of Albemarle Sound, North Carolina, USA. *Tidalites: Processes and Products, SEPM Special Publication* (Ed C.R. Alexander, Davis, R.A., and Henry, V.J.), **61**: 119-127.

Schumm, S.A. 1960. The shape of alluvial channels in relation to sediment type. In: *US Geological Survey Professional Paper*, **352B**, pp. 17-30.

Schumm, S.A. 1968. River adjustment to altered hydrologic regimen, Murrumbigbee River and paleochannels, Australia. In: *US Geological Survey Professional Paper*, **598**.

Schumm, S.A. 1977. The Fluvial System, Wiley: 338.

Schumm, S.A. 1993. River response to baselevel change: implications for sequence stratigraphy. *Journal of Geology*, **101**: 279-294.

Schumm, S.A. and Brackenridge, S.A. 1987. River response. In: *North America and adjacent oceans during the last deglaciation*, *Geological Society of America* (Ed W.F. Ruddiman, and Wright, H.E., Jr.), **K-3**, pp. 221-240.

Schumm, S.A. and Ethridge, F.G. 1994. Origin, evolution and morphology of fluvial valleys. In: *Incised-valley Systems: Origin and Sedimentary Sequence. SEPM Special Publication* (Ed R.W. Dalrymple, Boyd, R., Zaitlin, B.A.), **51**, pp. 10-27.

Schumm, S.A., Harvey, M.D. and Watson, C.C. 1984. *Incised channels: morphology, dynamics and control*. Water Resources Publication, Chelsea, Michigan: 200.

Schwimmer, R.A. 2001. Rates and Processes of Marsh Shoreline Erosion in Rehoboth Bay, Delaware, U.S.A. *Journal of Coastal Research*, **17**: 672-683.

Schwimmer, R.A. and Pizzuto, J.E. 2000. A model for the evolution of marsh shorelines. *Journal of Sedimentary Research*, **70**: 1026-1035.

Shervette, V.R. and Gelwick, F. 2008. Relative nursery function of oyster, vegetated marsh edge, and nonvegetated bottom habitats for juvenile white shrimp *Litopenaeus setiferus*. *Wetlands Ecology and Management*, **16**: 405-419.

Simms, A.R., Lambeck, K., Purcell, A., Anderson, J.B. and Rodriguez, A.B. 2007. Sea-level history of the Gulf of Mexico since the Last Glacial Maximum with implications for the melting history of the Laurentide Ice Sheet. *Quaternary Science Reviews*, **26**: 920-940.

Slattery, M.C., Gares, P.A., and Phillips, J.D. 2002. Slope-Channel Linkage and Sediment Delivery on North Carolina Coastal Plain Cropland. *Earth Surface Processes and Landforms*, **27**: 1377-1387.

Slattery, M.C., Gares, P.A., and Phillips, J.D. 2006. Multiple modes of storm runoff generation in a North Carolina coastal plain watershed. *Hydrological Processes*, **20**: 2953-2969.

Small, C. and Cohen, J. 2004. Continental Physiography, Climate and the Global Distribution of Human Population. *Current Anthropology*, **45**: 269-277.

Smyth, W.C. 1991. Seismic Facies Analysis and Depositional History of an Incised-Valley System, Galveston Bay Area, Texas. 170.

Strong, N. and Paola, C. 2006. Fluvial landscapes and stratigraphy in a flume. *The Sedimentary Record*, **June 2006**: 4-8.

Strong, N. and Paola, C. 2008. Valleys that never were: Time surfaces versus stratigraphic surfaces. *Journal of Sedimentary Research*, **78**: 579-593.

Sun, G., McNulty, S.G., Shepard, J.P., Amatya, D.M., Riekerk, H., Comerford, N.B., Skaggs, W., and Swift, L. Jr. 2001. Effects of timber management on the hydrology of wetland forests in the southern United States. *Forest Ecology and Management*, **143**: 227-236.

Swiechovicz, J. 2002. The influence of plant cover and land use on slope-channel decoupling in a foothill catchment: a case study from the Carpathian foothills, southern Poland. *Earth Surface Processes and Landforms*, **27**: 463-479.

Talling, P.J. 1998. How and where do incised valleys form if sea level remains above the shelf edge? *Geology*, **26**: 87-90.

Temmerman, S., Govers, G., Wartel, S., and Meire, P. 2004. Modelling estuarine variations in tidal marsh sedimentation: response to changing sea level and suspended sediment concentrations. *Marine Geology*, **212**: 1-19.

Thomas, M.A. and Anderson, J.B. 1994. Sea-level control on the facies architecture of the Trinity/Sabine incised-valley system, Texas continental shelf. In: *Incised-valley Systems: Origin and Sedimentary Sequences* (Eds R.W. Dalrymple, R. Boyd and B.A. Zaitlin), **51**, pp. 63-82. SEPM Special Publication.

Thornthwaite, C.W. 1948. An approach toward a rational classification of climate. *Geographical Review*, **38**: 55-94.

Tooth, S., Brandt, D., Hancox, P.J., and McCarthy, T.S. 2004. Geological controls on alluvial river behaviour: a comparative study of three rivers on the South African Highveld. *Journal of African Earth Sciences*, **38**: 79-97.

Törnqvist, T.E., González, J.L., Newsom, L.A., Van der Borg, K., and De Jong, A.F.M. 2002. Reconstructing "background" rates of sea-level rise as a tool for forecasting coastal wetland loss, Mississippi Delta. *Eos*, **83**: 530-531.

Törnqvist, T.E., González, J.L., Newsom, L.A., Van der Borg, K., and De Jong, A.F.M., and Kurnik, C.W. 2004. Deciphering Holocene sea-level history on the U.S. Gulf Coast: A high-resolution record from the Mississippi Delta. *Geological Society ofAmerica Bulletin*, **116**: 1026-1039.

Törnqvist , T.E., van Ree, M.H.M., van't Veer, R., and van Geel, B. 1998. Improving Methodology for High-Resolution Reconstruction of Sea-Level Rise and Neotectonics by Paleoecological Analysis and AMS14C Dating of Basal Peats. *Quaternary Research*, **49**: 72-85.

Törnqvist, T.E., Wallinga, J., Murray, A.S., de Wolf, H., Cleveringa, P., and de Gans, W. 2000. Response of the Rhine-Meuse system (west-central Netherlands) to the last Quaternary glacio-eustatic cycles: a first assessment. *Global and Planetary Change*, **27**: 89-111.

Törnqvist, T.E., Wortman, S.R., Mateo, Z.R., Milne, G.A., and Swenson, J.B. 2006. Did the last sea level lowstand lead to cross-shelf valley formation and source-to-sink sediment flux? *Journal of Geophysical Research*, **111**: F04002.

Trimble, S.W. 1983. A Sediment Budget for Coon Creek Basin in the Driftless Area, Wisconsin, 1853-1977. *American Journal of Science*, **283**: 454-474.

Turner, R.E., Swenson, E.M., and Milan, C.S. 2000. Organic and inorganic contribution to vertical accretion in salt marsh sediments. In: *Concepts and Controversies in Tidal Marsh Ecology* (Ed M.P.a.K. Weinstein, D.A.), pp. 583-595. Kluwer Academic Publishers, Boston.

van de Koppel, J., van der Wal, D., Bakker, J.P., and Herman, P.M.J. 2005. Self-Organization and Vegetation Collapse in Salt Marsh Ecosystems. *The American Naturalist*, **165**: E1-E12.

van Heijst, M.W.I.M., Postma, G., Meijer, X.D. Snow, J.N., and Anderson, J.B. 2001. Quantitative analogue flume-model study of river-shelf systems: principles and verification exemplified by the late Quaternary Colorado river-delta evolution. *Basin Research*, **13**: 243-268.

van Heijst, M.W.I.M. and Postma, G. 2001. Fluvial response to sea-level changes: a quantitative analogue, experimental approach. *Basin Research*, **13**: 269-292.

van Proosdij, D., Davidson-Arnott, R.G.D., Ollerhead, J. 2006a. Controls on spatial patterns of sediment deposition across a macro-tidal salt marsh surface over single tidal cycles. *Estuarine, Coastal and Shelf Science*, **69**: 64-86.

van Proosdij, D., Ollerhead, J., Davidson-Arnott, R.G.D. 2006b. Seasonal and annual variations in the volumetric sediment balance of a macro-tidal salt marsh. *Marine Geology*, **225**: 103-127.

Van Wagoner, J.C., Mitchum, R.M., Campion, K.m., and Rahmanian, V.D. 1990. Siliciclastic Sequence Stratigraphy in Well Logs, Core, and Outcrops: Concepts for High-resolution Correlation of Time and Facies. In: *American Association of Petroleum Geologists, Methods in Exploration Series*, pp. 55.

Van Wagoner, J.C., Posamentier, H.W., Mitchum, R.M., Vail, P.R., Sarg, J.F., Loutit, T.S., and Hardenbol, J. 1988. An overview of sequence stratigraphy and key definitions. In: *Sea-level Changes: An Integrated Approach* (Ed C.K. Wilgus, Hastings, B.S., Kendall, C.G.St.C., Posamentier, H.W., Ross, C.A., and Van Wagoner, J.C.), **42**, pp. 39-45. SEPM Special Publication.

Vandenberghe, J. 1995. Timescales, Climate, and River Development. *Quaternary Science Reviews*, **14**: 631-638.

vanEerdt, M. 1985. The influence of vegetation on erosion and accretion in salt marshes of the Oosterschelde, the Netherlands. *Vegetatio*, **62**: 367-373.

Voulgaris, G. and Meyers, S.T. 2004a. Temporal variability of hydrodynamics, sediment concentration and sediment settling velocity in a tidal creek. *Continental Shelf Research*, **24**: 1659-1683.

Voulgaris, G. and Meyers, S.T. 2004b. Net effect of rainfall activity on salt-marsh sediment distribution. *Marine Geology*, **207**: 115-129.

Walling, D.E. 1983. The Sediment Delivery Problem. *Journal of Hydrology*, **65**: 209-237.

Walling, D.E., Russell, M.A., Hodgkinson, R.A., and Zhang, Y. 2002. Establishing sediment budgets for two small lowland agricultural catchments in the UK. *Catena*, **47**: 323-353.

Watzin, M.C. and Gosselink, J.G. 1992. The fragile fringe: coastal wetlands of the continental United States. *Lousiana Sea Grand College Program, Lousiana State University, Baton Rouge, **LA*16**.

Webb III, T., Anderson, K.H., Bartlein, P.J., and Webb, R.S. 1998. Late Quaternary climate change in eastern North America: a comparison of pollen-derived estimates with climate model results. *Quaternary Science Reviews*, **17**: 587-606.

Wells, J.T. and Kim, S.-Y. 1989. Sedimentation in the Albemarle-Pamlico Lagoonal System: Synthesis and Hypotheses. *Marine Geology*, **88**: 263-284.

Wilkinson, B.H. and Byrne, J.R. 1977. Lavaca Bay-Transgressive deltaic sedimentation in central Texas estuary. *American Association of Petroleum Geologists Bulletin*, **61**: 527-545.

Williams 2002. Variations in tree cover in North America since the last glacial maximum. *Global and Planetary Change*, **35**: 1-23.

Williams, J.W., Shuman, B.N., Web III, T., Bartlein, P.J., and Leduc, P.L. 2004. Late-Quaternary vegetation dynamics in North America: Scaling from Taxa to Biomes. *Ecological Monographs*, **74**: 309-334.

Wilson, C.A. and Allison, M.A. 2008. An equilibrium profile model for retreating marsh shorelines in southeast Louisiana. *Estuarine, Coastal and Shelf Science*, **80**: 483-494.

Winker, C.D. and Howard, J.D. 1977. Correlation of tectonically deformed shorelines on the southern Atlantic Coastal Plain. *Geology*, **5**: 123-127.

Wohl, E. and Achyuthan, H. 2002. Substrate Influences on Incised-Channel Morphology. *Journal of Geology*, **110**: 115-120.

Wolanski, E. and Spagnol, S. 2000. Environmental degradation by mud in tropical estuaries. *Regional Environmental Change*, **1**: 152-162.

Wood, L.J., Ethridge, F.G. and Schumm, S.A. 1993. An experimental study of the influence of subaqueous shelf angles on coastal-plain and shelf deposits. In: *Siliciclastic sequence stratigraphy - recent developments and applications* (Eds P. Weimer and H.W. Posamentier), pp. 381-391. American Association of Petroleum Geologists.

Wood, L.J., Ethridge, F.G., and Schumm, S.A. 1994. An Experimental Study of the Influence of Subaqueous Shelf Angles on Coastal Plain and Shelf Deposits. *Recent Advances in and Applications of Siliciclastic Sequence Stratigraphy: American Association of Petroleum Geologists Memoir*, **58**: 381-391.

Wood, N. and Hine, A.C. 2007. Spatial Trends in Marsh Sediment Deposition Within a Microtidal Creek System, Waccasassa Bay, Florida. *Journal of Coastal Research*, **23**: 823-833.

Yeager, K.M., Santschi, P.H., Phillips, J.D., and Herbert, B.E. 2005. Suspended sediment sources and tributary effects in the lower reaches of a coastal plain stream as indicated by radionuclides, Loco Bayou, Texas. *Environmental Geology*, **47**: 382-395.

York, L.L., Thieler, E.R., Brill, A.L., Riggs, S.R. and Wehmiller, J.F. 2000. Aminostratigraphic age estimate for the Suffolk Scarp, North Carolina coastal plain. In: *Geological Society of America, Southeastern Section, 49th annual meeting*, **32**, pp. 85.

Yu, B. and Wolman, M.G. 1987. Some dynamic aspects of river geometry. *Water Resources Research*, **23**: 501-509.

Zaitlin, B.A., Dalrymple, R.W. and Boyd, R. 1994. The stratigraphic organization of incised-valley systems associated with relative sea-level change. In: *Incised-Valley Systems: Origin and Sedimentary Sequences* (Ed R.W. Dalrymple, Boyd, R., Zaitlin, B.A.), pp. 45-60. Soc. Econ. Paleont. Miner.